Université Paris-René Descartes

Ecole Doctorale bioSPC

THESE

En vue d'obtenir le grade de

Docteur de l'université Paris-Descartes

Spécialité: Biologie Cellulaire et Physiopathologie

Role of vascular plasticity in muscle remodeling in the child

Présentée et soutenue publiquement le 27 mars 2015

Cyril Gitiaux

Jury

Dr Alain-Pierre Gadeau, Rapporteur
Pr François Rivier, Rapporteur
Pr Romain Gherardi, Examinateur
Pr Pierre Quartier-dit-Maire, Examinateur
Dr Bénédicte Chazaud, Directeur de Thèse
Pr Isabelle Desguerre, Directeur de Thèse

Je remercie,

Isabelle Desguerre de m'avoir convaincu de débuter le long parcours, parfois épineux, de la thèse de science et de m'avoir fait découvrir le monde passionnant des maladies neuromusculaires.

Bénedicte Chazaud d'avoir accepté la codirection de ma thèse et de m'avoir initié à la recherche fondamentale.

Romain Gherardi de m'avoir soutenu depuis de nombreuses années et pour les nombreuses heures passées ensemble lors de discussions scientifiques.

Fabrice Chrétien pour m'avoir accueilli dans son laboratoire à l'institut Pasteur.

Tous les fameux (ex) membres de la « muscle team » de l'Institut Cochin : Rémi Mounier, Mélanie Magnan, Sylvain Cuvellier, Marine Théret, Marielle Saclier, Emmeran Le Moal et Claire Latroche, ma comparse de thèse qui ont chaleureusement accueilli un pédiatre en leur sein.

Francois Rivier et Pierre-Alain Gadeau d'avoir accepté d'être les rapporteurs de ma thèse.

Pierre Quartier d'avoir accepté d'être examinateur de ma thèse.

Mes parents pour leur présence et leur soutien.

Marie, Antonin et Anna, mes amours, pour leur soutien sans faille.

Summary

Abbreviations:

ALP: Alkaline Phosphatase
Ang1/Ang2: Angiopoietin 1/2
bFGF/FGF-2: basic Fibroblast Growth Factor / Fibroblast Growth Factor 2
CCL: CC Chemokine Ligand
CCR: CC Chemokine Receptor
CD: Capillary Density
C/F: Capillary/Fiber
CD31/PECAM: Cluster of Differentiation 31 / Platelet Endothelial Cell Adhesion Molecule
CD56/NCAM: Cluster of Differentiation 56 / Neural Cell Adhesion Molecule
CM: Conditioned Media
CMAS: Childhood Myositis Assessment Scale
CPK: Creatine Phosphokinase
CXCL: Chemokine Ligand
CXCR: Chemokine Receptor
(J)DM: (Juvenile) Dermatomyositis
DMD: Duchenne Muscular Dystrophy
DGC: Dystrophin Glycoprotein Complex
DNA: Deoxyribonucleic acid
DWI: Diffusion Weighted Imaging
ECs: Endothelial Cells
ECM: Extracellular Matrix
EDL: Extensor Digitorum Longus
EGF: Epidermal Growth Factor
eNOS: endothelial Nitric Oxide Synthase
ERK: Extracellular signal-regulated kinases
ERRα: Estrogen-related receptor alpha
FACS: Fluorescence-activated cell sorting
FGF: Fibroblast Growth Factor
GFP: Green Fluorescent Protein
GO: Gene Ontology
GRMD: Golden Retriever Muscular Dystrophy
HE: Hematoxylin and Eosin
HGF: Hepatocyte Growth Factor
Hh: Hedgehog
HIF: Hypoxia Inducible Factor
HLA: Human Leukocyte Antigen
HSC: Hematopoietic Stem Cell
ICAM: InterCellular Adhesion Molecule
IFN: Interferon
IGF-1: Insulin Growth Factor 1
IL: Interleukin
iNOS: inducible Nitric Oxide Synthase
MAC: Membrane Attack Complex
MAPK: Mitogen-activated Protein Kinase
MCP-1: Macrophage Chemoattractant Protein 1
M-CSF: Macrophage Colony Stimulating Factor
Anti-MDA5: anti-Melanoma Differentiation Associated gene 5

Mdx: X chromosome-linked muscular dystrophy
MMP: Metalloproteinase
MMT: Manual Muscle Testing
MO/MP : Monocytes/Macrophages
MPCs: Myogenic Precursor Cells
MRI: Magnetic Resonance Imaging
MRP: Myeloid Related Protein
MSAs: Myositis Specific Autoantibodies
MVU: Microvascular unit
NF-κB: Nuclear Factor kappa B
NG2: Nerve/Glial antigen 2
NGF: Nerve Growth Factor
NO: Nitric Oxide
NSC: Neural Stem Cells
Anti-NXP2: Anti-Nuclear Matrix Protein 2
Pax: Paired box gene
PDCs: Plasmocytoid Dendric Cells
PDGF: Platelet-derived Growth Factor
PDGFR: PDGF Receptor
PECAM : Platelet Endothelial Cell Adhesion Molecule
PGC-1α: Peroxisome proliferator-activated receptor gamma coactivator 1-alpha
RNA: Ribonucleic acid
SPP1: Secreted Phosphoprotein 1
SV2: Synaptic Vesicle glycoprotein 2
TA: Tibialis Anterior
TGF: Transforming Growth Factor β
TIF1γ: anti-transcriptional intermediary factor 1γ
TIMP: Tissue Inhibitors of Metalloproteinases
TLR: Toll Like Receptor
Tie: Tyrosine kinase with immunoglobulin and EGF homology domains
TNF: Tumor Necrosis Factor
TNF: Tumor Necrosis Factor
VECAM: Vascular Cell Adhesion Molecule
VEGF: Vascular Endothelial Growth Factor
VEGFR: VEGF Receptor

List of figures:

INTRODUCTION

Introduction

In vertebrates, there are three types of muscles: the striated skeletal muscle, the smooth muscle and the striated cardiac muscle. Skeletal muscle represents 40% of the body mass. Muscles provide motility to an organism through muscle fiber contraction/relaxation events. In order to obtain these contraction/relaxation cycles, muscles need to be vascularized and innervated. Skeletal muscle is one of the most vascularized tissues. The importance of vessels in providing oxygen and nutriments has been known for a long time, illustrated by the highly adaptive behavior of microvessels depending on the muscle demand (rest *vs.* activity, acute *vs.* endurance exercise…). However, more recent studies have shown that vessels, and particularly microvessels, fully participate to skeletal muscle homeostasis through the development of specific interactions with neighboring cells including myofibers and satellite cells. Moreover, peri-endothelial cells and perivascular cells have been shown to possess myogenic stem cell properties. The present introduction aims at giving an overview of the interactions developed between vessels and muscle cells, at the tissue, cell and molecular levels. It also provides a description of two myopathies in the child, which may be used as opposite paradigmatic models of vessel plasticity during human muscle regeneration: Juvenile Dermatomyositis (JDM) and Duchenne muscular dystrophy (DMD).

1. Adult skeletal muscle anatomy

The contractile unit of human skeletal muscle is the muscle fiber, which is a long cylindrical cell measuring up to several cm long and 10 to 100 µm of diameter. The muscle fibers are multinucleated cells, containing several hundreds of nuclei in peripheral position. Each muscle fiber is surrounded by a basement membrane, while a thin layer of connective tissue filling the intercellular space is the endomysium (Figure 1). Approximately 20–100 of these

muscle fibers are grouped together in a parallel arrangement called a muscle fascicle that is encapsulated by a perimysium connective tissue. Finally, several muscle fascicles form the muscle, surrounded by connective tissue called epimysium wrapping the whole muscle (Engel and Franzini-Armstrong, 2004; Gillies and Lieber, 2011).

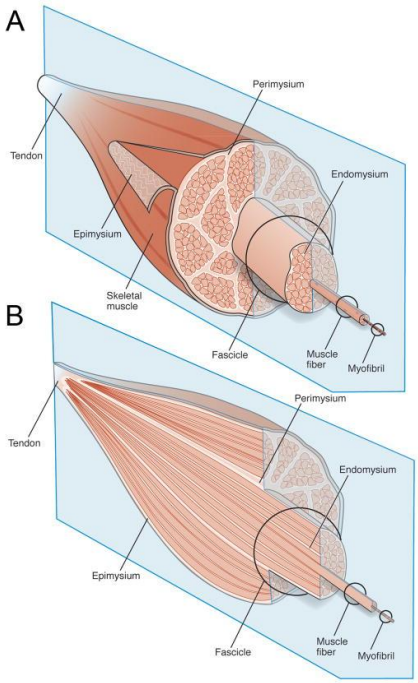

Figure 1: Schematic diagram of the general organization of muscle tissue and muscle extracellular matrix (ECM)-tendon organization. (A) Muscle ECM can be categorized as epimysium (surrounding the muscle), perimysium (surrounding muscle fascicles), and endomysium (surrounding muscle fibers). (B) Cross-section of muscle tissue indicating that the perimysium may be continuous with the tendon, whereas endomysium is contained within muscle fascicles (adapted from Gillies et al., 2011).

Skeletal muscle is composed of an heterogeneous collection of muscle fiber type classified using by their histochemical (myosin ATPase immunolabeling), biochemical (aerobic/oxidative or anaerobic/glycolytic enzymes) and morphological (size) characteristics. As compared with type fast contractile II fibers, slow-twitch or type I fibers are generally thinner, invested by a denser capillary network, and appear red owing to the presence of a large amount of the oxygen-binding protein myoglobin. These type I fibers are resistant to

fatigue, relying on oxidative metabolism for energy, and thus exhibit high mitochondrial and oxidative enzyme content, and low glycogen levels and glycolytic enzyme activity (Engel and Franzini-Armstrong, 2004).

The muscle fiber contraction, and consequently the entire muscle contraction, is provided by myofibrils. The myofibrils consist of chaining sarcomeres. The sarcomere is the smallest contractile entity measuring 1.5-2.5 μm long. It is made up of regions presenting different structures, which explains the striated look of myofibrils in optical microscopy. This aspect is due to the combination of two types of myofilaments: actin thin myofilaments (5-7 nm diameter) and myosin thick myofilaments (14-16 nm diameter). During muscle contraction, the sarcomere decreases its length. This is due to a bigger overlap between thin and thick filaments. During the muscle relaxation, this overlap decreases and the sarcomere increases its length (Engel and Franzini-Armstrong, 2004).

2. Microvasculature structure in skeletal muscle

Skeletal muscle is one of the most vascularized tissues. Beyond oxygen and nutriment supply, new functions for vessels have been recently identified. Vessels, and particularly microvessels, fully participate to skeletal muscle homeostasis through the development of specific interactions with neighboring cells, particularly with muscle stem cells, the satellite cells. Satellite cells are found in close proximity and interact with endothelial cells for their expansion and differentiation. Thus, vessels participate to the control of muscle homeostasis. Thanks to these interactions, vessel cells play a central role in the tissue remodeling after an injury.

2-1. The concept of microvascular unit (MVU)

Mammal skeletal muscle is highly vascularized. The role of microcirculation is to support muscle contractile activity that depends on an active consumption of energy substrates and requires a continuous replenishment of their pools and the removal of end products of energetic metabolism. These functional characteristics are based on intimate anatomical interrelations between muscle cells and vessels. Knowledge on skeletal muscle microvascularization exclusively comes from historic studies performed in small animals (*e.g.* rats, hamsters or cats). Most studies were performed on muscles which could be transilluminated *in vivo* such as *cremaster* and *spinotrapezius* in rat, *tenuissimus* in cat and rabbit, or *gluteus* in mice (Myrhage and Eriksson, 1980; Skalak and Schmid-Schönbein, 1986)**.** Muscle vessels are embedded in the extracellular matrix (ECM). Muscle arterioles are classified according to both their location in the ECM and their diameter (~20 to ~50 µm). In most muscles, microcirculation branches from one or more feed arteries in the epimysium into a network of interconnected arcade arterioles in the perimysium (Engelson et al., 1985; Snyder, 1988) (Figure 2). These interconnections allow for compensation if blood flow is compromised by occlusion of one arcade arteriole. At regular intervals, arcades give rise to transverse arterioles which penetrate into the endomysium and divide asymmetrically to yield terminal arterioles which, in turn, give rise to capillary networks. Blood returns to collecting venules which merge to form larger venules, arranged in a similar manner to arterioles and veins (Engelson et al., 1985, 1986; Eriksson and Myrhage, 1972; Hudlicka, 2011; Saltzman et al., 1992; Schmid-Schönbein et al., 1987).

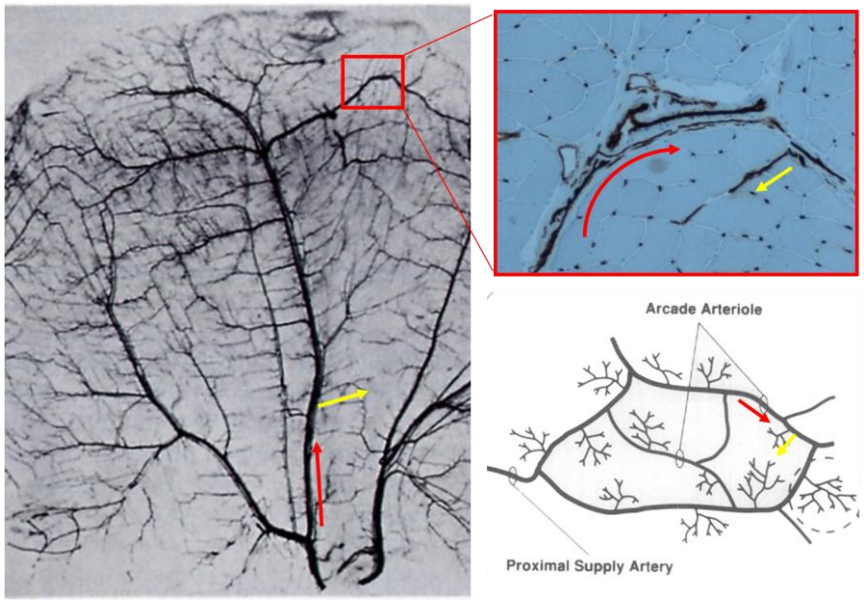

Figure 2: Microanatomic organization of the muscle arterioles: Arcade (red arrow) and transverse arterioles (yellow arrow) are illustrated in rodent transilluminated vascular bed (left panel), in human deltoid biopsy immunostained for CD31 and in a schematic drawing recapitulating the different type of arterioles (right panel).

Capillaries embedded in the endomysium run parallel to the muscle fibers to collect into venules, which merge to form larger venules. All capillaries perfused by one terminal arteriole and collected by one venule define the muscle microvascular unit (MVU), which represents the smallest functional unit for blood flow regulation in skeletal muscle. One MVU irrigates a cylinder of muscle tissue of 500-1000 µm in length in all animals studied. In rat and in other small mammals, it comprises 5-10 capillaries located in-between 3-4 adjacent myofibers (Bloch and Iberall, 1982; Cheung, 1996; Lo et al., 2003; Skalak and Schmid-Schönbein, 1986).

Techniques used to study muscle microvasculature in small animals (based on intravascular ink injection) cannot apply to human muscle biopsy explaining that the literature is scarce in Human. A human post-mortem study of the temporal muscle microvascularization has shown an arteriole-to-venule distance of about 900 µm but did not provide data on the MVU size (Cheung, 1996). We confirmed, using optic stacks and serial sectioning of alkaline

phosphatase-treated human muscle biopsies, that the overall vascular organization is strikingly similar to those observed in small animals (Gitiaux et al., 2013) (Figure 3). Interspecies conservation of the microcirculation structure stresses a major role of capillary-muscle interactions in physiological and pathological conditions.

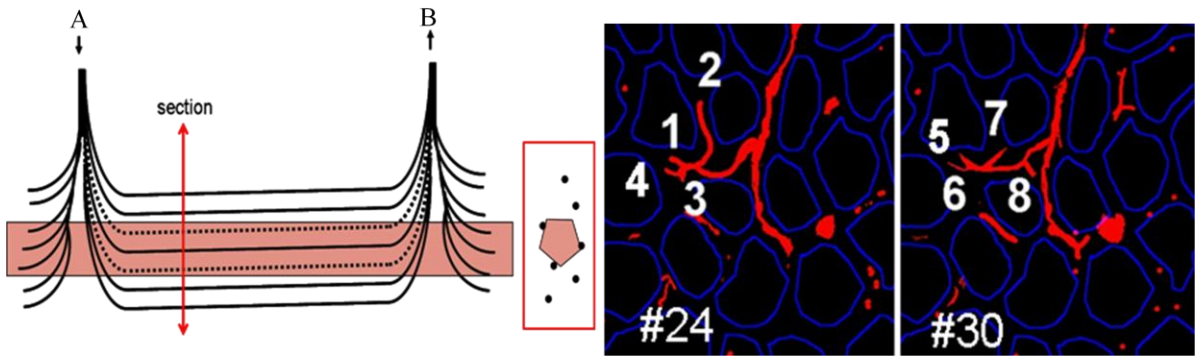

Figure 3: Microvascular unit of the normal deltoid muscle vasculature: On the left, schematic representation of the normal human muscle MVU and its spatial relationship with a myofiber (A: terminal arteriole; V: postcapillary venule), on the right, two optic sections allowing visualization of the 8 capillaries of the MVU issued from one of the two endings of the terminal arteriole (Alkaline phosphatase histoenzymatic reaction with DAPI, x 160) (adapted from Gitiaux et al., 2013).

2-2. Muscle capillarization

Muscle capillarization is related to aerobic functions because it represents the exchange of respiratory gases and metabolites between the muscle fiber and its vascular supply. Historically, the microscopic anatomy of capillaries in muscle tissue has been investigated in relation to their functional role in oxygen transport. Krogh et al. originally proposed that capillaries are the primary site of oxygen exchange between blood and muscle and developed a mathematical model of oxygen transport (Krogh, 1919). Since these pioneering publications, a number of *variations on the theme* of this model have been proposed but it is

still considered as a unifying principle in the study of oxygen transport (Lo et al., 2003; Pittman, 2011). Capillaries are not only uniform static semi-permeable tubes that act as a passive barrier delineating the blood/tissue interface but are now considered as dynamic structures involved in gas exchanges. It was demonstrated that these gas exchanges and the corresponding difference in oxygen partial pressure gradient from capillary to tissue required to maintain adequate oxygen supply are correlated with the capillarity (Hepple et al., 1997; McCall et al., 1996). As a result, the capillary–muscle interface is viewed as a critical determinant of maximal O2 flux capacity in skeletal muscle function. To determine the capillary supply, morphometric indexes are measured from histochemical or immunocytochemical stainings of transverse muscle sections. The indexes used to quantify capillarity include "global indexes": capillary density (CD), capillary/fiber ratio (C/F). Although CD is one of the most commonly reported global indexes of capillarity, it has drawbacks related to tissue swelling or shrinking and does not account for fiber size or fiber type. The C/F attempts to account for some of these factors and therefore provides a better mean to compare results obtained from different studies. Both parameters are easily used particularly for human muscle capillarity description and provide a global aspect of muscle blood supply (McCall et al., 1996; Qu et al., 1997). However, the use of CD and C/F indices: i) assumes a regular distribution of capillaries in the whole muscle and gives no information on the intramuscular heterogeneity in capillary distribution, ii) does not take into account the fiber size and the fiber type. Thus, "local indexes" allowing the evaluation of capillarity at the level of the individual muscle fiber were introduced: capillaries contact to fiber (CC), fiber area *per* capillary (FA/C), fiber perimeter *per* capillary (FP/C) and capillary-to-fiber perimeter exchange index (the CFPE index) derived as the quotient of the individual capillary-to-fiber ratio (*i.e.*, the capillary-to-fiber ratio calculated individually for each fiber) on the fiber

perimeter (Harris, 2005; Hepple and Mathieu-Costello, 2001; Mathieu-Costello et al., 1991; Porter et al., 2002a).

Table1: Morphometric indexes used to describe the capillarization of skeletal muscle (adapted from Harris, 2005 and Porter et al., 2002a)

Global indexes		
Capillary density (CD)	Number of capillaries per unit area	Little information on capillary supply to individual fibers. Dependent on fiber size and sensitive to fiber size changes.
Fiber density (FD)	Number of fibers per unit area	
Capillaries per fiber ratio (C/F)	Ratio of capillary density to fiber density	Little information on capillary supply to individual fibers. Not effected by fiber size changes, but dependent on capillary : muscle fiber geometry.
Stereology (three-dimensional modelling)		Information on longitudinal capillary geometry. Little information on capillary supply to individual fibers.
Individual fibers indexes		
Capillary contacts (CC)	Number of capillaries in contact with each fiber	No information on the effects of fiber type size.
Fiber area per capillary (FA/C) and Fiber perimeter per capillary (FP/C)	Fiber area and perimeter supplied by each capillary	Reflects changes in fiber dimensions and proportions, and potential effects of diffusion.
Capillary to Fiber Perimeter Exchange (CFPE) Index	Capillary to individual fiber ratio divided by fiber perimeter	Does not account for capillary geometry.

These “local indexes” provide a more direct depiction of capillarity specific to fiber size and fiber type. However, results obtained from different studies are difficult to compare due to the wide range of type of muscles studied and the different capillary indices chosen. Skeletal muscle is composed of an heterogeneous collection of muscle fiber type and the proportion of each fiber type varies among the different muscles and among the different species (Brooke and Kaiser, 1970; Schroeder et al., 2014). It has been shown that type II fibers have generally lower level of capillary supply than type I fibers (Buckley and Bossen, 2013; Sjøgaard, 1982). For example, in human *tibialis anterior* muscle, although type II fibers have higher numbers of capillary in contact (CC) compared with type I fibers, the fact that type II fibers are larger than type I fibers for both men and women results in a higher FA/C and FP/C for type II fibers as compared with type I fibers. This indicates that larger area is being supplied by each

capillary, and this reflects the lower level of capillarization of type II fibers (Porter et al., 2002a, 2002b). Capillary supply of skeletal muscle indicates the potential exchange capacity between the vascular system and the muscle fibers and therefore reflects the muscle fiber composition in steady state conditions. Although the evaluation of capillary supply remains a useful tool for the understanding of muscle-vessel interactions, the comparison between different pathological and physiological conditions must be interpreted with cautious depending on which morphometric parameter is used. Furthermore, due to physiological variations of capillarization during post-natal muscle development, patient age is an important parameter to consider when assessing capillarity in children (Kottlors and Kirschner, 2010; Sallum et al., 2013).

2-3. Cellular mechanisms of angiogenesis

Angiogenesis, the growth of blood vessels, is a major biological process that controls embryonic development and is also involved in numerous human diseases. New blood vessels are formed by various mechanisms, including assembly by mesodermal endothelial progenitor cells or angioblasts (vasculogenesis, *i.e.* differentiation of hemangioblast-derived cells into endothelial cells), longitudinal splitting of existing vessels (intussusceptions, *i.e.* splitting angiogenesis) and enlargement of the vasculature through sprouting, proliferation and remodeling processes (sprouting angiogenesis) (Figure 4). Splitting or sprouting angiogenesis occurs depending on the mechanical stimulus operating from either the luminal or the extravascular side of the vessels. Splitting angiogenesis is defined by the division of the lumen by endothelial protrusion and vessel splitting without breakdown of the basement membrane. In contrast, sprouting angiogenesis is characterized by the migration and proliferation endothelial cells towards an extravascular angiogenic stimulus (Egginton, 2011; Egginton et al., 2001; Hansen-Smith et al., 1996; Hudlicka, 1998; Hudlicka and Brown,

2009). Splitting and sprouting angiogenesis differently involve pericytes, which are the perivascular cells located in close proximity to endothelial cells in capillaries and in post-capillaries venules beneath a common basement membrane (Egginton et al., 1996). Pericytes are generally considered to stabilize the vessel wall, controlling endothelial cell proliferation and thereby the growth of new capillaries. In addition, they are believed to participate in the regulation of microvascular blood flow *via* a contractile mechanism (Ribatti et al., 2011). Splitting angiogenesis is a mostly pericyte independent process whereas sprouting angiogenesis requires the release of growth factors into the local environment and migration and activation of pericytes (Bloor, 2005; Lindahl et al., 1997). Under certain controlled experimental conditions, such as chronic muscle stretching and vasodilatation, angiogenesis has been shown to proceed in the two distinct modes: by abluminal lateral sprouting and intraluminal splitting (Egginton, 2011; Egginton et al., 2001). Under other conditions both types of angiogenesis may occur. Whereas sprouting angiogenesis appears to be a major process involved in the formation of the majority of blood vessels during tissue repair or diseases (Flamme et al., 1997; Herbert and Stainier, 2011) physiological angiogenesis during exercise in skeletal muscle likely does not occur by sprouting angiogenesis (*i.e.* tip-cell formation) but rather via intussusception, a process that remains poorly understood due to the paucity of appropriate experimental model (Brown et al., 2003; Gianni-Barrera et al., 2013, 2014).

Figure 4: Early morphogenic events during sprouting and splitting (intussusception): In sprouting, specialized endothelial tip cells (white) are first selected (**A**), which then migrate and eventually connect with each other, whereas trailing stalk cells proliferate to form the new vascular trunk (**B**). In intussusception, at first,

pre-existing vessels enlarge by circumferential growth (**C**) and subsequently endothelial processes invaginate from opposing vascular walls to form transluminal pillars, leading to the splitting into two new vessels (**D**) (adapted from Gianni-Barrera ., et al 2011).

Blood vessel formation by sprouting angiogenesis is a multistep process that requires the tight control and coordination of endothelial cell behavior. It is generally assumed that common sequence of events is initiated by the proteolytic breakage of the basement membrane surrounding capillaries. In quiescent vasculature, endothelial cells form a cobblestone monolayer of quiescent cells that covers the luminal surface of the vessels. Upon angiogenic cues, endothelial cells lose their cell to cell junctions, activate matrix metalloproteases that degrade the surrounding basement membrane and, in turn, become mobile, invasive and initiate sprouting from the basal surface of the blood vessels. Several types of specialized endothelial cells required to build a new functional vessel have been identified. Tip cells located at the distal end of each sprout extend numerous filopodia, respond to attractive or repulsive guidance signals (*e.g.* vascular endothelial growth factor (VEGF) gradient) within their immediate environment and proliferate minimally. Tip cells are trailed by endothelial stalk cells which maintain the connectivity with the parental vessels, are less mobile and more proliferative and initiate the formation of the new vessel lumen (De Smet et al., 2009). Sprouting angiogenesis is mainly controlled by the secreted VEGF tyrosine kinase receptor-2 (also known as Flk1). Tie-2 and Notch signalings are also key pathways in sprouting angiogenesis. Ang-Tie signaling controls vessel quiescence in adults and also regulates the later steps of the angiogenic cascade that are related to vessel maturation (Augustin et al., 2009; Carmeliet and Jain, 2011). Although the understanding of the anastomotic process remains limited, it is clear that other cell types may also influence vessel fusion. In particular, the recruitment of other cells is a critical factor in the subsequent maturation of the nascent vasculature. Factors such as platelet-derived growth factor B (PDGFB) secreted by

endothelial cells recruit mural cells (pericytes and vascular smooth muscle cells) to the developing vasculature, which stabilizes vessel walls (Naylor et al., 2014).

2-4. Development of the muscle microvasculature

Muscle vasculogenesis is mainly confined to the formation of the first primitive vasculature in the embryo. Both myogenic and endothelial cells share a common embryonic origin. Myogenic progenitor cells derive from the dorsal somite, the dermomyotome, which also gives rise to derma, to endothelial and smooth muscle cells of blood vessels (Buckingham and Vincent, 2009). Multipotent Pax3-positive (Pax3+) cells in the somites give rise to skeletal muscle and to cells of the vasculature. FoxC2, a member of the Forkhead box transcription factors family is also expressed in the somite, and mutual repression between FoxC2 and Pax3/7 has been shown to determine myogenic (high Pax3/7:FoxC2 ratio) or vascular (low Pax3/7:Foxc2 ratio) fates in the murine dermomyotome (Lagha et al., 2009). The Notch pathway affects the Pax3:FoxC2 balance and promotes the endothelial *versus* myogenic cell fate in the somite, before migration to the limb (Mayeuf-Louchart et al., 2014).

At the tissue level, the muscle development of the chick wing consists of an initial migration phase of somatic cells and organization into dorsal and ventral premuscle masses. During the second phase, theses masses undergo a series of splits thus giving rise to all the muscles of the wing. The timing of vascular invasion of the limb occurs at a later stage, just prior the establishment of the final muscle pattern, suggesting that myogenic differentiation is not oxygen or nutrient dependent (Murray and Wilson, 1997). Furthermore, in mouse Extensor Digitorum Longus, at early stage (12 days in utero) the developing muscle consists of primary myotubes surrounded by a pleomorphic population of mononucleated cells devoid of myofilaments. At this stage, blood vessels and nerves are found in the periphery but not within the developing muscle mass. By 14 days in utero, small blood vessels and

unmyelinated nerve bundles are found throughout the developing muscle in parallel with maturation of myotubes leading from 18 days in utero to the polygonal shape fascicular arrangement and ultrastructure characteristic of more mature myofibers (Ontell and Kozeka, 1984). Vessels and nerves progressively penetrate into the developing muscle with a clear temporal pattern and progressively separate the various muscle masses producing the individual muscles (Schroeter and Tosney, 1991).

At the cell level, during chick and mouse limb development, angioblasts colonize the limb regions before muscle precursors cells and organize correctly in space, even in the absence of muscle progenitors (in $Pax3^{-/-}$ mice). In addition, anarchic ectopic blood vessels, induced by overexpression of VEGF, inhibit muscle formation while the absence of vessel formation, induced by soluble form of VEGF receptor 1 (VEGF1/Flt1), leads to muscle fusion, preventing the splitting into distinct limb muscles. At the molecular level, PDGBB secreted by endothelial cells crossing the muscle mass may act as a paracrine signal. PDGFB may increase locally the production of connective tissue by promoting connective tissue cell migration and accumulation at the future sites of cleavage, excluding myogenic cells and forcing them to split at these sites, and finally allowing the formation of separate muscles of the limb (Tozer et al., 2007) (Figure 5).

Figure 5: Model for the effect of the vasculature on muscle development. (**A**) The endothelial cells (blue) delineate the future cleavage site in the muscle mass, which is composed of myogenic cells (red) and muscle connective tissue cells (green). (**B**) At a later stage, the muscle masses are separated. (**C**) The PDGFB secreted by the endothelial cells acts in a paracrine manner on muscle connective tissue cells, which express PDGF receptor. In response to PDGFB, connective tissue cells increase the secretion of extracellular matrix by producing collagen I allowing muscle mass separation. (adapted from Tozer et al., 2007).

After birth, an intensive construction takes place, which is correlated with the gradual morphological and functional maturation of the muscle tissue (Oertel, 1988; Ontell and Dunn, 1978). In mouse, while the number of myofibers remains constant after birth, post-natal growth is characterized by an extensive hypertrophy of the muscle fibers. This hypertrophy is initially supported until day 21 (P21) by a rapid increase in the number of myonuclei, as satellite cells proliferate to generate fusion-competent myoblasts for muscle growth (White et al., 2010). It was shown in human deltoid muscle a 5-fold increase in fiber diameter (25 fold increase in cross sectional area) from 10 µm at birth up to 50 µm at 15-20 years (Oertel, 1988) associated with a progressive increase of satellite cells per myofiber and a decrease of satellite cells per square millimeter (Sallum et al., 2013; Verdijk et al., 2014; White et al., 2010). At birth, muscle vascularization is rudimentary, most growing myofibers being unconnected to capillaries during early post-natal development. The postnatal maturation of muscle fibers is supported by an architectural rearrangement of the microvascular bed (Stingl and Rhodin, 1994). The architecture of the terminal vessels develops gradually from an immature shape to its final feature. In rat, the average length of terminal arterioles increases progressively and the capillary network consisting initially of numerous small meshes, very irregular in size and shape, gradually develops into a characteristic pattern of long meshes, parallel to the course of muscle fibers (Snyder and Coelho, 1989; Stingl and Rhodin, 1994). Meanwhile, similarly in rat/mouse model and in Human, capillarization progressively declines (decreased CD) and capillary to fiber ratio (C/F) increases in all fiber types consistent with post-natal muscle capillary growth and myofiber enlargement, respectively (Sallum et al., 2013; Smith et al., 1989).

Signaling mechanisms involved in embryonic development and more particularly in vasculogenesis and myogenesis have been deeply studied but mechanisms that may orchestrate and interegulate the two processes remain poorly understood (Buckingham and

Vincent, 2009). In particular, the Notch signaling pathway has been involved in satellite cell activation and cell fate determination in postnatal myogenesis (Conboy and Rando, 2002) and also appears to play myriad roles during vascular development (Gridley, 2010). The role of Notch signaling in regulating vascular development is intertwined with another major regulator of vascular development and physiology, the VEGF pathway. Myofibers targeted-VEGF deficient mice ($mVEGF^{-/-}$) present a significant decrease of muscle capillary to fiber ratio (-48%) and in capillary density (-39%) in gastrocnemius, without changes in muscle fiber type composition, leading to a major intolerance to aerobic exercise. These results indicate that since muscle-VEGF-deficient mice survive to adulthood, VEGF is essential to the physiologic regulation of postnatal muscle capillarity and therefore to the maintenance of adult skeletal muscle microvasculature (Olfert et al., 2009). Thus, the development of muscle vasculature before and after birth needs coordinated angiogenesis and myogenesis. Interactions between vessels and muscle are also required upon various physiological conditions (hypoxia, exercise, and aging) in which both muscle fibers and vessels adapt to changing demands by altering myofiber size or type composition and capillary density, respectively. All the pathways studied during development may be also recruited postnatally in response to muscle injury. For example, the Hedgehog (Hh) signaling was demonstrated to be further reactived in adult ischemic tissues and to be impaired in aging mice (Pola et al., 2003; Renault et al., 2013a, 2013b).

3. Physiological adaptation of the skeletal muscle microvascular bed

Skeletal muscle is the organ containing the highest microvascular mass in Human and constitutes a highly adaptable tissue, responding to environmental and physiological demands.

The vasculogenesis/angiogenesis processes described above are initiated during fetal development. By contrast, postnatal physiological (*i.e.* non pathological) angiogenesis is relatively rare, limited to uterine changes during the estrous cycle, and to exercise and altitude-induced angiogenesis in skeletal muscle (Egginton, 2011; Olfert and Birot, 2011; Shimizu-Motohashi and Asakura, 2014). The following paragraph aims at focusing on current knowledge about molecular aspects in some physiological conditions (exercise, hypoxia and aging) to highlight specific interactions between muscle cells and vessels.

3-1. Exercise

Exercise is a potent angiogenic stimulus and is one of the few situations of non-pathological angiogenesis that occurs in mammals after development (Egginton, 2009; Malek et al., 2009). Because the vascular supply to muscles is a major contributor to endurance capacity, physiological angiogenesis has been studied in trained and untrained subjects as well as after training or detraining (Hoier and Hellsten, 2014). The increase of capillarity that occurs in skeletal muscle in response to endurance exercise training is a major example of physiological capillary growth in a mature differentiated tissue (Malek et al., 2009). Indeed, the number of capillaries *per* fiber is higher in endurance athletes than in sedentary subjects and it increases with endurance training in parallel with the changes in oxidative metabolism (Olenich et al., 2013). Under exercise, skeletal muscle presents increased blood flow. Capillaries are exposed to repeated shortening and elongation due to changes in sarcomere length during contractions (Egginton, 2011). However, how exercise regulates the complex process of physiological angiogenesis remains poorly described. One prevailing notion is that the metabolic needs during exercise lead to a local hypoxia with induction of VEGF secretion (Breen et al., 1996; Richardson et al., 1999). Among possible cellular sources, myocyte is a critical source for paracrine VEGF production during exercise. In myocyte-VEGF$^{-/-}$ mouse model, the

physiological angiogenesis (*i.e.* increase in capillarity) does not occur and metabolic enzyme activity levels after training are not increased. This may indicate that other cellular sources of VEGF such as endothelial cells, fibroblasts, pericytes and macrophages are unable to compensate for the loss of myocyte-derived VEGF (Delavar et al., 2014; Olfert et al., 2010). The mechanism by which myocyte-derived VEGF controls skeletal muscle angiogenesis is not well understood. Confocal microscopy has revealed an increase of the density of immunostained VEGF vesicles in the subsarcolemmal region of teased human muscle fibers after exercise suggesting that VEGF is pre-stored in vesicles and secreted to the extracellular space (Hoier et al., 2013). This release seems to be partially mediated by adenosine *via* mitogen activated protein kinase (MAPK) (Høier et al., 2010a).

Factors capable of coordinating the complex process leading to VEGF dependent angiogenesis remain elusive. Several studies have investigated regulatory factors proposed to be related to VEGF expression in skeletal muscle. Matrix remodeling *via* Matrix Metalloproteases (MMP) as well as angiopoietin-2 (Ang-2) are important for the destabilization of the capillary and the division of capillary lumen (Høier et al., 2010b). They have been shown to both induce VEGF secretion and regulate skeletal muscle angiogenesis (Bobadilla et al., 2014; Hoier and Hellsten, 2014). VEGF is a downstream target of hypoxia-inducible factor (HIF). HIF is a heterodimeric complex composed of a constitutively expressed HIF β-subunit and an oxygen sensitive HIF α-subunit (Semenza, 2003). Three α-subunits are known to date (HIF-1α, -2α, and -3α). In skeletal-muscle-specific-HIF-1α-KO mice, the increase of expression of HIF-1α target genes, including *VEGF*, normally observed in response to exercise is lacking, suggesting a HIF dependent adaptation of skeletal muscle to exercise (Mason et al., 2004). The peroxisome proliferator-activated receptor gamma (PPARɤ) coactivator-1 alpha (PGC)-1α, a potent metabolic sensor involved in multiple aspects of skeletal muscle physiology, has been also described as a key regulator of skeletal

muscle angiogenesis. PGC-1α is robustly induced in the skeletal muscle in response to exercise (Baar et al., 2002; Gouspillou et al., 2014) resulting in mitochondrial biogenesis, a switch from glycolytic fibers to mitochondrial-rich oxidative fibers (Handschin and Spiegelman, 2011; Miura et al., 2008; Wende et al., 2007). PGC-1α induces VEGF expression by co-activating the transcription factor estrogen related receptor alpha (ERRα) on an enhancer located in the first intron of the *VEGF* gene (Arany et al., 2008; Leick et al., 2009). Furthermore, deletion of PGC-1α in skeletal muscle prevents exercise-mediated angiogenesis (Chinsomboon et al., 2009; Rowe et al., 2014). Several studies have pointed out the role of non-myocyte cell types in exercise-induced angiogenesis. Expression microarray analysis using RNA from muscles of an inducible mice transgenic model of PGC-1α overexpression has shown that the vast majority of upregulated genes are known to be strongly expressed in macrophages. It was demonstrated that PGC-1α induces the recruitment of macrophages to skeletal muscle and the secretion of phosphoprotein 1 ([SPP1]; also known as osteopontin) by myocytes. It was suggested that SPP1 could lead to secretion of monocyte chemoattractant protein-1 (MCP-1) from macrophages, which in turn would activate adjacent endothelial cells, pericytes and smooth muscle cells (Rowe et al., 2014) (Figure 6). Thus, proper temporal and spatial interactions between myocytes, the main source of VEGF in muscle and their microenvironment are crucial to ensure that the metabolic demands of the muscle during exercise are met.

Figure 6: Proposed model for PGC-1α-mediated orchestration of different cell types, myokines, and cytokines to mediate functional angiogenesis in skeletal muscle (adapted from Rowe et al.,2014).

3-2. Hypoxia

Similarly, modifications of the muscle vascular bed also occur as an adaptation to exposure to hypoxia defined by the decrease of partial pressure of oxygen. Whatever the origin of the hypoxic stimulus may be (environmental or pathological (chronic obstructive pulmonary disease, stroke, cardiac dysfunction...), the ultimate consequence is an inadequate oxygen delivery at the tissue level leading to ischemia. Exposure to systemic chronic hypoxia in rats stimulates significant arteriolar changes including an increase of the number of terminal arterioles and of arcade arteriole loops (Bailey et al., 2008). Additional branches are also formed along each category of arterioles to maintain an adequate tissue perfusion and oxygenation. This reduction of the branching interval might be attributed to an increase in number of newly formed arterioles from pre-existing capillaries (Price and Skalak, 1998; Smith and Marshall, 1999). These arteriolar remodeling begin within the first few days after the onset of hypoxia but gradually develop over the following 3-4 weeks (Olfert et al., 2001; Ou et al., 1985). However, the question of whether chronic hypoxia induces angiogenesis within skeletal muscle is still controversial. Due to the high variations in experimental protocols (duration, oxygen pressure, sedentary *vs*. trained subjects…), animal and human studies show discrepant results regarding the effect of hypoxia on VEGF and on growth of skeletal muscle capillaries. Generally, it is accepted that in response to chronic hypoxia, the resting mRNA levels of VEGF, and of its receptors (VEGFR1/Flt1, VEGFR2/Flk1) increase, CD is unaltered or somewhat increased and the C/F remains unchanged (Desplanches et al., 1996; Lundby et al., 2009; Olfert et al., 2001, 2009; Mounier et al., 2009, 2011; Pisani, 2005; Vogt et al., 2001; Tuomisto et al., 2004). While many cellular functions such as overall protein synthesis are down regulated under hypoxia, selected subsets of gene are upregulated. Prominent among them is the family of genes governed by the transcription factor HIF-1. HIF-1 is a heterodimer composed of an alpha and a beta subunit. HIF-1α protein is usually not present at high levels in tissues or cells in a normoxic environment (Brown et al., 2005; Flann

et al., 2014; Hudlicka and Brown, 2009; Semenza, 2011; Silvestre et al., 2013). HIF-1α is hydroxylated, ubitiquined and degraded in normoxia but is stable in hypoxia and translocates into the nucleus to form an active complex with HIF-1β, which is constitutively expressed (Jaakkola et al., 2001). HIF-1 induces transcription of numerous target genes involved in erythropoiesis, energy metabolism and angiogenesis (Forsythe et al., 1996; Hudlicka and Brown, 2009; Jewell et al., 2001; Semenza, 2011; Silvestre et al., 2013). Human and mice studies show also discrepant results regarding the effect of hypoxia on HIF expression according predominantly oxidative or glycolytic muscles (Mounier et al., 2010; Pisani, 2005).

HIF-1α likely plays a more prominent role in pathological angiogenesis (Semenza, 2011) whereas deletion of HIF-1α in skeletal muscle leads to more blood vessels, rather than fewer (Mason and Johnson, 2007). By contrast, PGC1-α expression appears to play a major role in physiological angiogenesis. In human skeletal muscle, PGC1-α expression is coupled to HIF-1α dependent gene expression by increasing mitochondrial consumption, leading to a decrease in intracellular oxygen availability for HIF hydrolases, resulting in activation and stabilization of HIF-1α (O'Hagan et al., 2009).

Furthermore, the hypoxic responsiveness of satellite cells, the main muscle stem cells, in term of their angiogenic capacity remains to be defined. Hypoxia induces modifications in the normal interactions between vessels and satellite cells for maintaining muscle homeostasis and therefore the mechanical properties, to meet the functional demand. Satellite cells seem to prefer hypoxic niches, which is in apparent contradiction with satellite cell proximity to vessels (Latil et al., 2012). VEGF expression in satellite cells is modulated by hypoxia (Germani et al., 2003; Rhoads et al., 2009; Rissanen et al., 2002a). A second potential candidate that may modulate satellite cell angiogenic capacity is Hepatocyte Growth Factor (HGF). HGF possesses a dual role regulating angiogenesis and myogenesis, raising the possibility that it is a critical factor coordinating both aspects during skeletal muscle

regeneration. Hypoxic conditions increase satellite cell HIF-1α and VEGF protein content but decrease HGF mRNA content compared to normoxic satellite cells. This reduction of satellite cell HGF expression under hypoxia directly impacts the ability of satellite cells to drive angiogenic process (see below, paragraph 4.3) (Flann et al., 2014).

3-3. Aging

Aging is another physiological condition leading to significant modifications in the angiogenic and regenerative capacity of skeletal muscle. Progressive generalized loss of skeletal muscle mass and function (sarcopenia) occurs as a consequence of aging. The reduced regenerative potential associated with age is correlated with a decline in satellite cell number (Day et al., 2010; Renault et al., 2013a; Verney et al., 2008). Multiple mechanisms are thought to be involved in these age-induced alterations of satellite cell niche and microenvironment, which ultimately have an effect on satellite cell activity. Recent studies have highlighted that both intrinsic and extrinsic factors are responsible for the loss of myogenic capacities of satellite cells with age but the exact etiology of sarcopenia remains unknown (Bernet et al., 2014; Biressi et al., 2014; Brack et al., 2007; Cosgrove et al., 2014; Fry et al., 2015; Price et al., 2014; Sousa-Victor et al., 2014; Tierney et al., 2014). In particular Notch ligand Delta is down regulated in old satellite cells resulting in defective satellite cell proliferation and an inability to generate myoblasts during regeneration (Conboy et al., 2003) whereas Wnt signaling is hyperactivated (Brack et al., 2007). Furthermore, with increasing age, activation of JAK-STAT signaling in satellite cells substantially contributes to myogenic commitment and results in their regenerative deficiency by exhausting the pool of satellite cells (Doles and Olwin, 2014; Price et al., 2014; Tierney et al., 2014). Aging is associated with higher expression of known activators of JAK-STAT signaling, including basic fibroblast growth factor (bFGF, also called FGF2), inflammatory cytokines including interleukin-6 (IL-6), PDGF, and Epidermal Growth Factor (EGF) (Shuai and Liu, 2003).

Changes in the microenvironment in aging muscle could impede the physiological angiogenesis and myogenesis and thus alter muscle capacities to regenerate. In parallel, the expression of VEGF has been shown to be down regulated in aged animals (Rivard et al., 1999). Moreover downregulation of VEGFR2/Flk1 observed in old mice has been suggested to be responsible for impaired VEGF-induced angiogenesis in the ischemic limb of old mice (Pola et al., 2001; Qian et al., 2006). From a histological perspective, muscle aging is characterized by a decrease in myofiber size and number, with a preferential loss of fast type II myofibers (type II atrophy) (Piec et al., 2005). Data on the impact of aging in skeletal muscle capillarization are variable, depending on species and muscles studied as well as the methodology used (Degens et al., 1994). They show either unchanged or increased C/F ratio (Mathieu-Costello, 2005). Impaired microvascular functions associated with aging have been poorly investigated in skeletal muscle. They involve several processes likely to interfere with the homeostasis of myofibers and myogenic cells, such as a decreased NO activity, increased production of vasoconstrictor factors, increased oxidative stress associated with increased expression of pro-inflammatory cytokines/compounds (Baraibar et al., 2013; Herrera et al., 2010). In addition, aged satellite cells exhibit decreased ability to promote angiogenesis*)* (Rhoads et al., 2013) *(see below part 4).* Hedgegog (Hh) signaling and Hh dependent regulation of angiogenesis and myogenesis (cf below paragraph 4.3) is impaired in aged mice (Renault et al., 2013a). Evidence indicates that apoptosis is involved in mediating the progression of sarcopenia in old mice. Apoptosis is not only confined to myofibers but is preponderant (over 75%) in capillary endothelial cells (Wang et al., 2014). Altogether, these findings indicate that age related changes affecting both myogenic cells and endothelial cells may unbalance muscle homeostasis and alter the normal muscle angiogenesis abilities.

In summary, the adaptation to physiological conditions (exercise, hypoxia and aging) needs specific and proper interactions between muscle and vessels at the tissue level. These

interactions are substantiated at the cellular level by a close proximity between endothelial and myogenic cells.

4. Vascular niche (cellular and molecular aspects)

A stem cell niche can be defined as a spatial structure in which stem cells are housed and maintained by allowing survival and slow self-renewal in the absence of differentiation. The niche comprises cellular structures, extracellular matrix proteins, and soluble factors (Rezza et al., 2014). Muscle stem cells, *i.e.* satellite cells play a key role in muscle regeneration process (Wang et al., 2014). They lie along the myofiber in a quiescent state until a damage signal stimulates their entry into the cell cycle. These myogenic precursor cells or transit-amplifying myogenic cells proliferate and further commit into terminal myogenic differentiation to replace the damaged myofibers while a subset of these cells self-renew to maintain the satellite cell pool (Wang et al., 2014). To achieve these processes, satellite cells interact with several cell partners in the muscle tissue, among them endothelial cells, of which they are in close proximity. The vascular stem cells niche concept has been characterized in several tissues: hematopoietic stem cells (HSCs) and neural stem cells (NSCs) while it remains poorly characterized in skeletal muscle, particularly at the molecular level.

4-1. Hematopoietic stem cell vascular niche

HSCs give rise to all hematopoietic lineages and provide appropriate numbers of mature blood cells throughout the lifetime. A plethora of studies has investigated HSC niche. Due to the particular organization of bone marrow, HSCs may find several cell types as a niche support including osteoblasts, macrophages, platelets, specific interstitial cells (Mendelson

and Frenette, 2014). We will focus here on the interactions HSCs develop with endothelial cells. It seems established that a hypoxic HSC microenvironment is crucial for HSC maintenance and survival (Rehn et al., 2011). HSCs reside in a hypoxic microenvironment as pharmacologic increase in HIF-1α enhances HSC homing (Speth et al., 2014; Suda et al., 2011). During several years, the concept of two main HSC niches prevailed, with the "endosteal or osteoblastic niche" serving as a quiescent storage niche for dormant HSCs and the "vascular or sinusoidal niche" for HSC differentiation and mobilization (Colmone and Sipkins, 2008; Wilson and Trumpp, 2006) (Figure 7). However, recent studies broke this paradigm and demonstrated that vascular niche is indispensable for maintaining HSC quiescence (Scadden, 2014; Spencer et al., 2014). HSCs in close proximity to sinusoids would allow the constant screening of the status of hematopoietic system in the vascular network (Wilson and Trumpp, 2006). A detailed analysis of the location of HSCs and progenitors along the entire femur at short time points after transplantation revealed that they preferentially and consistently migrate through endothelium and reside in an endosteal niche in close association with blood vessels, which do not form a separate niche (Ellis et al., 2011). Similarly, 3D analysis of bone marrow vascular structures demonstrated that quiescent HSCs specifically associate with small arterioles that are preferentially found in the endosteum, indicating that arteriolar niches are indispensable for maintaining HSC quiescence (Kunisaki et al., 2013; Morrison and Scadden, 2014; Scadden, 2014) A large number of molecular signaling delivered by the various components of the HSC niche have been shown to regulate and control HSC homeostasis (Mendelson and Frenette, 2014). Some are specifically delivered by endothelial cells, such as Stem Cell Factor (SCF) (Ding et al., 2012)**.** HSCs are located adjacent to perivascular cells (reticular cells) highly expressing chemokine (C-X-C motif) ligand 12. CXCL12 is involved in the regulation of HSC trafficking between the bone marrow niche and the peripheral circulation (Guerrouahen et al., 2011). Platelet endothelial

cell adhesion molecule (PECAM-1) also known as cluster of differentiation 31 (CD31) expressed by vascular cells and HSCs regulate their ability to respond to a CXCL12 gradient (Ross et al., 2008**).** VEGF, which expression in HSCs is upregulated by a hypoxic environment, is involved in HSC survival (Rehn et al., 2011), as well as in the regeneration of the bone marrow vascular niche after myelosuppression (Kopp et al., 2009).

Figure 7: The model of HSCs niche. HSCs niche is composed of complex components including HSCs and other functional elements such as vessels, stromal cells, ECM proteins, neural inputs, and endothelial cells**.** HSCs are found mainly adjacent to sinusoids throughout the bone marrow, where endothelial cells and mesenchymal stromal cells promote HSC maintenance by producing SCF, CXCL12 and probably other factors (adapted from Morrison and Scaden, 2014).

4-2. Neural stem cell vascular niche

Neurogenesis in the adult brain has been demonstrated within the subventricular zone (SVZ) and hippocampus (Kuhn et al., 1996). Neurogenesis and angiogenesis are closely linked in the germinal zones of the adult brain where neural stem cells (NSCs) reside associated with the vasculature (Capela and Temple, 2002; Palmer et al., 2000). Bursts of angiogenesis occur at the same time as neurogenesis and endothelial cells secrete soluble factors that regulate neuronal differentiation *in vitro* (Alvarez-Buylla and Lim, 2004; Shen, 2004). Adult neurogenesis supported by proliferative cells that generate neurons are found in dense clusters associated with the vasculature (Palmer et al., 2000). Anatomically, NSCs are closely apposed to the laminin-containing ECM surrounding endothelial cells (Shen et al., 2008). Moreover, transplanted human NSCs were found in the proximity of cerebral microvessels upon induction of angiogenesis by cerebral infusion of VEGF into the murine brain (Schmidt et al., 2009; Shen et al., 2008). Blocking the laminin receptor α6β1 integrin, which is expressed by NSCs, inhibits their adhesion to endothelial cells and alters their proliferation, indicating that direct contact with vessel plays a functional role in regulating NSC properties (Shen et al.,

2008). Indeed, co-transplantation of endothelial cells with NSCs increases their survival and proliferation and accelerates neuronal differentiation (Nakagomi et al., 2009). Unique neurovascular niche was defined in which angiogenesis and neurogenesis are linked through specific vascular growth factors and chemokines. A focal cortical stroke in the cortex induces the long-distance migration of neuroblasts originate from NSCs in the SVZ, which form close associations with peri-infarct blood vessels. These interactions are, at least, in part mediated by the vascular ligands CXCL12 and Angiopoetin 1 (Ang1) acting on neuroblast receptors CXCR4 and Tie-2, respectively, which exert a tropic effect on migrating neuroblasts (Ohab et al., 2006). Ang1 has a unique role in neurogenesis independent of its role in angiogenesis. Ectopic expression of Ang1 promotes neuronal differentiation and neurite outgrowth in neuronal progenitors, while this effect was blocked by the presence of anti-Tie-2 receptor antibody (Bai et al., 2009). Of note, Ang1 stimulates *in vitro* neurogenesis in neural progenitor cells (NPCs) through the Akt pathway (Bai et al., 2009). VEGF also plays a role in the proliferation, homing and recruitment of NSCs to the site of injury. *In vivo*, microvasculature modulates the local guidance of NSCs through endothelial cell-derived chemo-attractants such as PDGF-BB, chemokine (C-C motif) ligand 5 (CCL5) also known as RANTES, chemokine (C-X-C motif) ligand 11 (CXCL11) also known as I-TAC, chemokine (C-X-C motif) ligand 1 (CXCL1) also known as GROα, Neurophil-activating peptide 2 (NAP-2), Angiopoietin 2 (Ang2), and macrophages-colony stimulating factor (M-CSF). Moreover, *in vitro* chemotactic migration of human NSCs is enhanced in the presence of conditioned media from human endothelial cells stimulated with VEGF (Schmidt et al., 2009). Reconstitution of NSC-vascular niche in 3D with vascular cells and extra cellular matrix provides precise control of NSC self-renewal, proliferation and differentiation into astrocytes and oligodendrocytes through Notch effectors. Astrocyte differentiation is more active when NSCs are in close proximity to brain vasculature (Shin et al., 2014). Indeed,

endothelial cells participate in the regulation of NSC homeostasis by secreting soluble factors that activate Notch and Hes 1 to promote self-renewal (Shen, 2004).

4-3. Satellite cell vascular niche

Recent studies identified vessel cells as privileged partners of satellite cells and myogenic precursor cells (MPCs) and showed that vessels contribute to the regulation of satellite cell fate (Mounier et al., 2011). Skeletal muscle is laced with a dense microvasculature, and most quiescent satellite cells are found strikingly close to capillaries. At the tissue level, angiogenesis and myogenesis take place concomitantly during muscle regeneration after ischemia (Scholz et al., 2003). Christov et al. indicated that satellite cells and endothelial cells were tightly juxtaposed at steady state in normal adult muscle. Satellite cell number was significantly correlated with capillarization of myofibers, regardless to their type, in normal muscle. They also varied in paradigmatic physiological and pathological situations associated with variations of capillary density. Satellite cell number was decreased in amyopathic dermatomyositis, a condition in which muscle capillary loss occurs without myofiber damage, while it was increased in athlete muscles presenting a higher number of capillaries (Christov et al., 2007). *In vitro* analysis using human cells in coculture showed that myogenic cells and endothelial cells reciprocally interact to promote both angiogenesis and myogenesis. Endothelial cells support myogenesis through the secretion of a series of growth factors such as Insulin Growth Factor (IGF-1), HGF, bFGF, PDGF-BB and VEGF (Christov et al., 2007). Reciprocally, myogenic cells promote angiogenesis, a process that mainly depends on VEGF, which expression was increased in myogenic cells while they differentiate along the myogenic program (Chazaud, 2003; Christov et al., 2007). This was confirmed in a 3D co-culture model composed of rat satellite cells and microvascular fragments, a multicellular structure consisting of endothelial cells, pericytes, and smooth muscle cells. Active myogenic

cells possess a potent pro-angiogenic program that may participate in revascularization of damaged muscle through the secretion of soluble factors, such as VEGF, HGF, IGF and FGF (Rhoads et al., 2009). VEGF is involved in myogenesis and angiogenesis regulation as satellite cells express Flk1 and Flt1 receptors for VEGF that modulate their migration and survival (Germani et al., 2003). Several studies have demonstrated that VEGF is necessary for muscle repair: intramuscular AAV-VEGF treatment or recombinant proteins VEGF associated with IGF1 enhanced muscle regeneration, innervation and revascularization after ischemia (Arsic et al., 2004; Borselli et al., 2010). It has been shown that *in vitro* VEGF stimulates myogenic differentiation of MPCs and that *in vivo* it mediates skeletal myogenesis (Bryan et al., 2008; Chazaud, 2003). Increase of VEGF expression in myogenic cells is mediated by β-catenin signaling and induces both angiogenesis through endothelial cell proliferation, and muscle regeneration (Kim et al., 2006). Controlled overexpression of VEGF in muscle induces vessel splitting whereas uncontrolled expression causes aberrant vascular structures (Gianni-Barrera et al., 2013; Karvinen et al., 2011).

Analysis of Hh signaling showed the tight coregulation of myogenesis and angiogenesis in the context of post-ischemia muscle regeneration (Renault et al., 2013a). Specific depletion of Gli3, a transcription factor mediating Hh signaling in myofibers induces both impaired myogenesis and angiogenesis. Gli3 regulates myogenic differentiation as well as the delivery of proangiogenic factors by myogenic cells, including thymidine phosphorylase and Ang1. This study demonstrates that impaired myogenesis affects angiogenesis in the context of skeletal muscle regeneration (Renault et al., 2013b). Other factors such as Ang1, Ang2, FGF, Nerve Growth Factor (NGF) and chemokine (C-C motif) ligand (CCL-2/MCP-1) are implicated in angiogenesis and their expression is increased after an injury at early stages during muscle regeneration (Wagatsuma, 2007). Ang2 stimulates angiogenesis during muscle regeneration (Bellamy et al., 2010). NGF plays a functional role in neovascularization after

treatment of ischemic muscle, through stimulation of angiogenesis and protecting myofiber from necrosis (Emanueli et al., 2002). At steady-state, vessels are surrounded by peri-endothelial cells including smooth muscle cells, pericytes and interstitial fibroblastic cells. These cells are known to secrete Ang1 that binds to its Tie-2 receptor on endothelial cells to stabilize vessels. This Ang1/Tie-2 signaling has also been shown to act on muscle stem cell behavior (Abou-Khalil et al., 2009; Bentzinger et al., 2013). In an autocrine manner, myogenic cell-derived Ang1 signals on Tie-2, through ERK1/2 pathway, to decrease both proliferation and differentiation and increase their own self-renewal. Peri-endothelial cells, by secreting Ang1, reinforce and maintain the quiescent state in satellite cells in a paracrine manner (Abou-Khalil et al., 2009). Thus endothelial cells and peri-endothelial cells have opposite effects on satellite/myogenic cells. During muscle regeneration, endothelial cells, free from peri-endothelial cells due to vascular remodeling, may interact with myogenic cells to promote angiogenesis and myogenesis. Then peri-endothelial cells promote quiescence of both satellite cells and vessels once homeostasis of the skeletal muscle is recovered (Abou-Khalil et al., 2010). While few studies, described above, have investigated the concomitant regulation of angiogenesis and myogenesis during skeletal muscle regeneration, a number of molecules have been separately described to be involved in these two processes. The "musculo-vascular niche" should be envisaged in a broader aspect than strictly defines the place where stem cells reside in a quiescent state, since interactions with endothelial cells have been demonstrated for both quiescent, cycling and differentiating myogenic cells (Christov et al., 2007). The characterization of this niche will benefit from further identification of molecular regulators of these dynamic interactions, as well as the potential identification of satellite cell subsets exhibiting different interactions with vessels. Nevertheless, vessels fully participate to the coordination of the acute satellite cells response as well as the sequential steps of muscle regeneration until the returns to homeostasis

(Bentzinger et al., 2013) (Figure 8). It is therefore likely that endothelial cell/myogenic cell interactions are affected in pathological contexts.

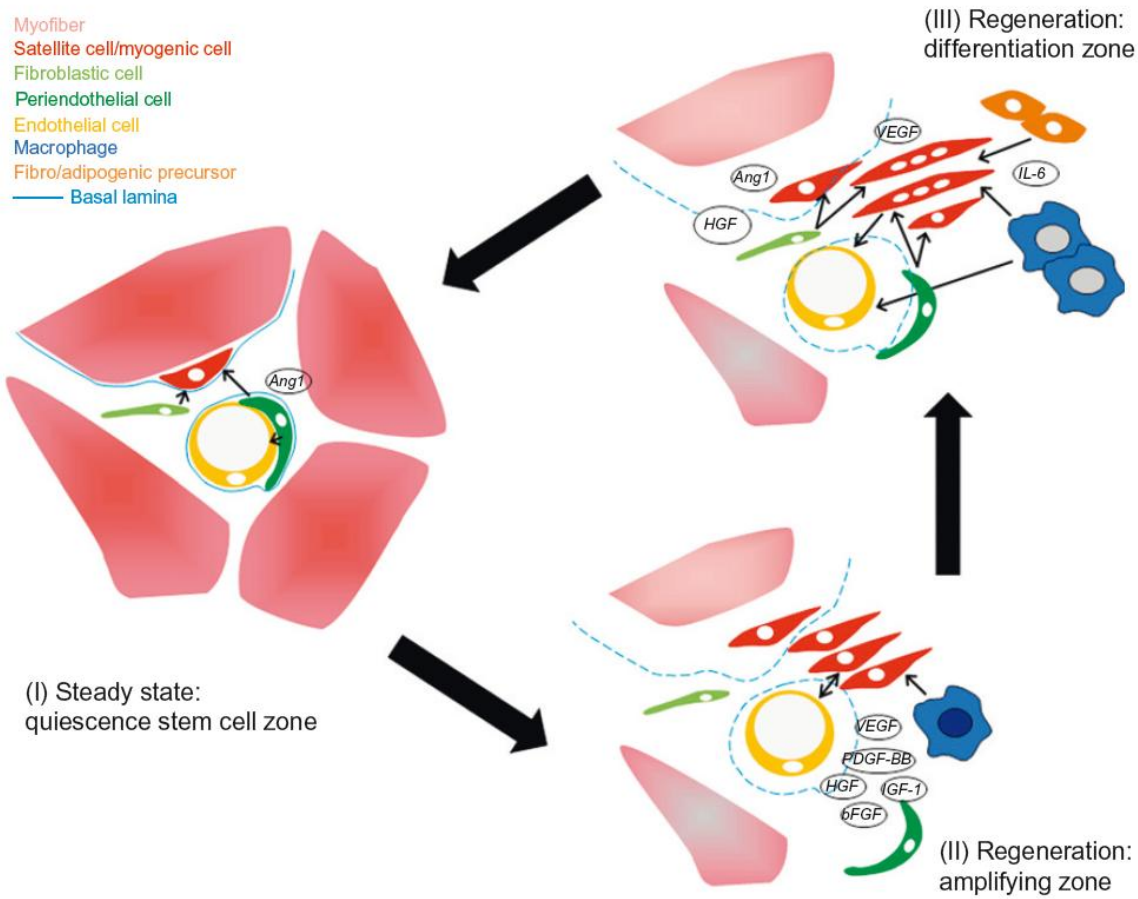

Figure 8: Proposed model of interactions between vessels and satellite cells during muscle regeneration.
(I) At steady state, satellite cells lay at quiescent state under basal lamina, under the influence of perivascular Ang1 that helps the maintenance in the G0 state. (II) At the time of regeneration, degenerating/regenerating fibers are still surrounded by basal lamina or at least remnants but cells seem to easily cross it. Vessels are growing, thus ECs are free of vascular mural cells. Expanding myogenic cells and ECs, facing each other, can bidirectionally interact to promote myogenesis and angiogenesis through the secretion of various growth factors (VEGF, PDGF, HGF, IGF-1, bFGF…). Early infiltrating macrophages, that have an inflammatory phenotype, also stimulate the amplification of myogenic cells. (III) Later during the repair process, macrophages have changed their phenotype into antiinflammatory cells that promote differentiation of myogenic cells. Fibro/adipogenic cells also stimulate myogenic differentiation (through IL-6 secretion). Young differentiating myogenic cells promote angiogenesis (through VEGF secretion). Further, macrophages are renowned to have angiogenic properties. When myogenic progenitor expansion is ending, cells have to choose between differentiation and self-renewal. This can be achieved, at least through high concentrations of HGF and through Ang1/Tie-2 signaling that arises from myogenic progenitors themselves, and may be from perivascular cells (fibroblastic or smooth muscle cells) that start to stabilize the newly formed vessels (adapted from Mounier et al., 2011).

5. Skeletal muscle microvasculature under pathological conditions

After an injury, skeletal muscle regeneration is a multifaceted process requiring the temporal coordination of myogenesis as well as angiogenesis. To explore the regulation of neovascularization and angiogenesis in chronic muscle regeneration, two human muscle diseases may serve as models: the juvenile dermatomyositis (JDM), the most common inflammatory myopathy in childhood, and Duchenne muscular dystrophy (DMD), the most frequent genetic neuromuscular disorder in children. Both muscular disorders share similar mechanisms of necrosis-inflammation associated with alterations in angiogenesis.

5-1. Juvenile Dermatomyositis

5-1-1. Epidemiology and genetic factors

JDM is an extremely rare disease, with an incidence estimated between 2 and 5 cases per million children under 16 (McCann et al., 2006; Symmons et al., 1995). The female/male ratio varies to 2/1 to 5/1. The median age at disease onset is around 7 years (Pachman et al., 2005). There are extensive data suggesting a geographical or seasonal clustering with the onset of disease and linking human leukocyte antigens (HLA) with JDM susceptibility. HLA-DQA1*0501, HLA-DQA*0301, HLA-DRB1*0301, and HLA-B8 have been found more frequently in patients with JDM (Feldman et al., 2008). Cytokine polymorphism including a tumor necrosis factor (TNF alpha promoter polymorphism) and an intronic polymorphism of the interleukin 1 receptor antagonist (IL-1ra) are also risk factors in Caucasian patient

(Batthish and Feldman, 2011). Although some studies allow speculation about the role of environmental agents as triggers of JDM, no specific antigen-antibody conflict have been consistently identified (Reed et al., 2012).

5-1-2. Diagnosis criteria

JDM is characterized by proximal muscle weakness, specific skin rashes and the potential for involvement of other systems, including pulmonary, cardiac and gastrointestinal systems. JDM are highly heterogeneous conditions and no reliable tests or validated predictive tests are now available to facilitate the identification of patients at risk of severe complication or outcome. The diagnosis remains based on criteria published in 1975 which are now outdated and do not include modern imaging techniques such as Magnetic Resonance Imaging (MRI) and screening of myositis specific autoantibodies (MSAs) (Bohan and Peter, 1975; Brown et al., 2006). Some recent evidence suggests that JDM may be classified according to the presence of MSAs which can now be detected in about 50% of children with idiopathic inflammatory myopathies (Consolaro et al., 2014; Tansley et al., 2013). MSAs frequently target components involved in gene transcription, protein translocation and antiviral responses. Although their mechanistic relevance to disease pathogenesis is not fully understood, specific MSAs including anti-transcriptional intermediary factor 1ɣ (TIF1ɣ), anti-melanoma differentiation associated gene 5 (MDA5) and anti-nuclear matrix protein 2 (NXP2) autoantibodies may define homogenous groups of patients with similar clinical features or outcome. TIF1ɣ is a nuclear factor that plays an important role in transforming growth factor beta (TGFβ) signaling and suppression of cell growth *via* the transcription factor Smad4 (Mohassel et al., 2014). NXP2 regulates the activation and subcellular localization of the tumor suppressor gene p53 (Tansley et al., 2013). Increasing number of published series have reported MSAs associated with various clinical phenotypes (Casciola-

Rosen and Mammen, 2012; Kobayashi et al., 2014; Tansley et al., 2014a, 2014b). Furthermore, the different patterns of muscle MRI changes could also provide in the near future new cues regarding the prognosis and could help to determine different subgroups in JDM (Davis et al., 2011; Malattia et al., 2013). Intensity of inflammation on short tau inversion recovery (STIR) sequences whole body muscle MRI is positively correlated to the disease activity. Furthermore, a patchy distribution of muscle inflammation was recently described, which substantially confirms the heterogeneous and multifocal muscle injury in JDM (Malattia et al., 2013).

Table 2. Bohan and Peter diagnosis criteria of JDM (adapted from Bohan and Peter, 1975)

Dermatological features:
Gottron's papules, heliotrope, involvement of knees, elbows, medial maleoli, face, neck and upper torso
Together with at least 2 *(probable JDM) or 3 (JDM) of the following 4 items:*
1. symmetrical, proximal muscles weakness, progressing over weeks to months
2. elevated serum muscle enzymes: creatinine kinase, aldolase
3. electromyographic findings typical of JDM
4. typical muscle biopsy findings (perifascicular inflammation with or without atrophy, necrosis, regeneration)

5-1-3. Clinical features

JDM presenting features and outcome are protean. JDM has often an insidious onset and the diagnosis is established after several weeks in most cases (Feldman et al., 2008). In some patients however, a more severe course may be life-threatening within a couple of weeks and leads these patients to an intensive care unit. The cardinal signs are erythematous skin lesions

over the metacarpo-phalangeal and interphalangeal joints (Gottrons papules), a “heliotrope” eyelid, malar and truncal rashes and muscle weakness with markedly increased creatine phosphokinase (CPK). The first sign of JDM is usually a skin rash. The rash may be red and patchy, with typically red or purplish color on the eyelids (“heliotrope” rash), cheeks or both. A malar rash may involve the naso-labial fold. Truncal rash in “V” is common. Gottron’s papules develop over the metacarpophalangeal and interphalangeal joints, knees and medial malleolus Nailfold telangiectasiae are sometimes visible. The skin rash may be preceded, accompagnied or followed by myalgia, a predominantly proximal muscle weakness, arthralgia, dysphonia, dysphagia or anorexia. Some patients present a multisystemic organ involvement, including oesophagitis, gastritis, bowel disease and colitis with a risk of perforation in a few cases, pancreatitis, anasarca, contractures, interstitial lung disease, cardiac involvement, or renal disease (Quartier and Gherardi, 2013).

The clinical features are detected at the time of diagnosis with various frequency among different series, emphasizing difficulties of a reliable classification of JDM based only on clinical features (Robinson and Reed, 2011). Nonetheless, some characteristic clinical features would deserve further discussion. Indeed, all the manifestations presented in the following paragraph are thought to be related to vasculopathy. Evidence of small vessel inflammation can be seen in the nailfolds, eyelids, and gums as telangiectasias of the capillary loops. The number of end row nailfold loops can be quantified, and normal numbers of end row loops in JDM has been correlated with earlier diagnosis and less severe skin disease. Persistent capillary abnormalities at 6 months may be associated with longer time to remission in children (Schmeling et al., 2010). Severe vascular inflammation can cause cutaneous ulcerations (10%) and might be an indicator of increased severity and poor prognosis (Feldman et al., 2008; Robinson et al., 2013). In addition, early subcutaneous limb edema (widespread edema anasarca) and gastrointestinal involvement are thought to be

related to vasculopathy. The exact mechanism of increased capillary permeability in edematous DM (Milisenda et al., 2014; Mitchell et al., 2001) remains elusive, but muscle microinfarcts are much more frequently found in edematous (80%) compared to non-edematous (34%) adult DM, suggesting a prominent role of ischemia (Milisenda et al., 2014; Ravelli et al., 2010). Gastro-intestinal tract involvement is uncommon in JDM (Robinson et al., 2013) and has been linked to inflammatory vasculopathy with lumen narrowing or complete occlusion of multiple small and medium arteries causing gastrointestinal ulceration and perforation (Mamyrova et al., 2007). Furthermore, the JDM outcome is characterized by JDM bystanders: lipodystrophy and calcinosis. They are thought to be associated with long-standing or undertreated disease in JDM and are uncommon in adults (Marhaug et al., 2008; Tansley et al., 2014b). Calcinosis is reported in up to 30% of patients with JDM, and most often begins 1-3 years after the disease onset. The intensity of the inflammation may contribute to the development of the calcinosis. Increased local production of TNF alpha is associated with calcinosis and is associated with the TNF alpha 308 polymorphism (Pachman et al., 2000). Recently the presence of anti-NXP2 autoantibody was associated with the risk of the development of calcinosis (Tansley et al., 2014b). Lipodystrophy, reported in 10% of children with JDM, clinically results in a progressive loss of subcutaneous and visceral fat, and might be associated with a metabolic syndrome with insulin resistance, acanthosis, hypertriglyceridemia and abnormal glucose tolerance (Mathiesen et al., 2012). Brawny erythematous thickening of the skin with patches of pigmentation and depigmentation over the extensor surfaces of joint (poilikoderma) mark the more chronic stage of the disease.

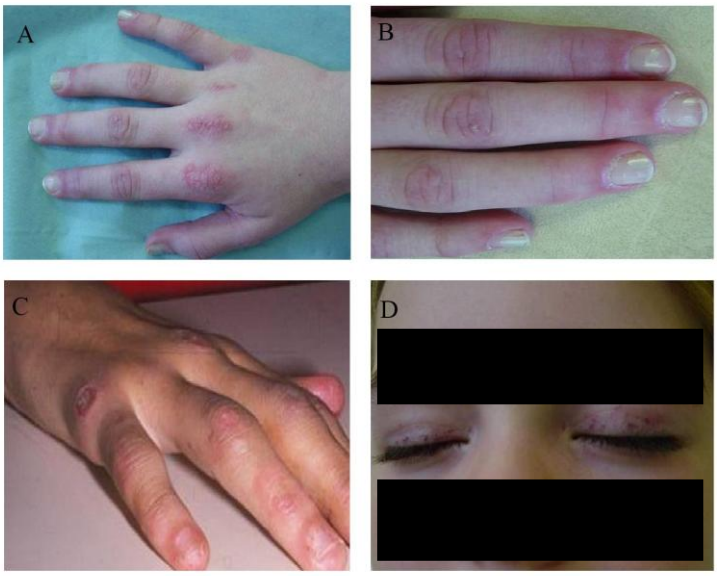

Figure 9: Clinical characteristic feature of juvenile dermatomyositis, (A) and (B) scaly red rash on the knuckles with Gottron's papules. (C) Ulcerations (D) Eyelid telangiectasias,

5-1-4. <u>Prognosis</u>

The duration of the disease activity is highly variable (Huber et al., 2000) . International study group have standardized and validated measures of disease activity. Core sets of measure for clinical study have been proposed. These measures have been combined to develop criteria to show response to treatment. The muscle strength and physical function are mostly assessed by two scales: (i) the Childhood Myositis Assessment Scale (CMAS 0-52), a 14-item observational, performance-based instrument that was developed to assess muscle strength, functional capacity and endurance in JDM (Huber et al., 2004), and (ii) the Manual Muscle

Testing (MMT 0-80) of eight muscle groups (Huber et al., 2004; Jain et al., 2006). Moreover, tools have been proposed to assess not only the muscles but also involvement of the skin, the joints and other organs. The JDM disease activity score (DAS) assesses the extent and distribution of cutaneous involvement, muscle weakness functional status and vasculopathy (Bode et al., 2003). The Physician global assessment of disease activity and patient/parent global assessment on an overall wellbeing and pain on a 10 cm visual analysis scale are simple and useful tools (Rider et al., 1997). They are part of composite assessment tools proposed by the Pediatric international Trial Organization PRINTO (Ruperto et al., 2003). PRINTO remission criteria include at least three out of four of the following criteria: creatine kinase ≤150, CMAS ≥48, MMT ≥78 and physician global assessment of overall disease activity (PhyGloVAS) ≤0.2 (Lazarevic et al., 2012).

Early studies described three different courses of JDM: monophasic (response to a limited treatment with remission within 2 years), chronic polycyclic and chronic relentless disease (Crowe et al., 1982; Spencer et al., 1984). Long-term outcome studies showed that 40-60% of patients develop a chronic course requiring long-lasting, often multiple, immunosuppressive treatments (Mathiesen et al., 2012; Ravelli et al., 2010; Sanner et al., 2010). However, clinical and histopathological predictive factors of poor response to classical treatment have not yet been clearly identified. The role and measurement properties of immunological and endothelial activation markers that might also help in the assessment of disease activity (especially in refractory patients) including interferon and cytokines signature has to be further evaluated (Baechler et al., 2007). For instance, recently, tumor necrosis factor type 2, galectin 9, inducible protein 10 kD (IP-10/CXCL10) and Myeloid related protein (MRP) 8/14 were identified as novel markers of active JDM (Bellutti Enders et al., 2014; Nistala et al., 2013).

5-1-5. Pathologic changes and pathophysiology

JDM combines inflammation, myofiber alterations and microvascular changes (Carpenter et al., 1976; Crowe et al., 1982; Emslie-Smith and Engel, 1990; Greenberg and Amato, 2004, 2004; Kissel et al., 1986). It typically shows a mixture of inflammatory changes in the vicinity of perimysial arteries and myofiber changes including perifascicular atrophy, microinfarcts and ischemic vacuoles. Moreover, JDM is characterized by specific microvascular changes including: a) an early capillary deposition of the complement C5b-9 membranolytic attack complex (MAC); b) endothelial cell hyperplasia; c) destruction of endothelial cells, which results in focal capillary loss. Muscles of patients with dermatomyositis present arterialization of capillaries: capillaries are replaced by microvessels with widely opened lumens and thickened walls, due to the proliferation of vascular smooth muscle cells, in place of pericytes, as observed after arterial occlusion (Dobaczewski et al., 2004). Despite increasing attention paid to microcirculatory changes, the pathophysiological mechanism of capillary depletion remains uncertain in DM (Gitiaux et al., 2013). It is believed to begin when putative antibodies directed against endothelial cells activate the complement cascade, leading to MAC formation. As a result of these deposits, capillary obliteration and arterial lumen occlusion are supposed to cause secondary ischemic changes in muscle associated with immune mediated primary myofiber injury (Crowe et al., 1982). JDM is thus usually thought to be an "autoimmune disease" (Huber and Feldman, 2013). Factors supporting its autoimmune basis include: familial aggregation of autoimmune disease in families of children with JDM (Niewold et al., 2011), the presence of circulating serum autoantibodies (Tansley and McHugh, 2014) and their response to immunosuppressive or immunomodulatory therapy (Robinson and Reed, 2011). Furthermore, the observations that treatment for autoimmune disease in adult can induce DM as a rare complication give additional evidence of the importance of type 1 interferons (IFNs) in the JDM pathology

(Somani et al., 2008). Although evidences suggest that innate immunity plays an important role in JDM pathogenesis, neither putative antigens nor factors activating complement, such as immune complexes, have been reliably identified.

Recent studies have identified type1 IFNs or their inducible gene products as biomarkers of DM (Greenberg et al., 2012), suggesting a mechanism of myofiber and capillary injury driven by type 1 IFNs. Some of the $CD4^+$ cells in the perivascular infiltrates are not T-cells but BDCA 2^+ plasmacytoid dendritic cells (PDCs). PDCs are primarily type 1 IFNs-secreting cells and gene expression profiling analyses of blood or muscle tissue showed a specific JDM "signature" and an over-expression of type 1 IFNs-dependent genes in most of the patients (Baechler et al., 2007). An expanding number of IFN upregulated genes including the IFN stimulated gene 15 (ISG-15) and a type 1 interferon inducible antiviral molecule (MxA) are found in the muscle and skin of patients with JDM (O'Connor et al., 2006; Salajegheh et al., 2010) (Figure 10). Type 1 IFNs impair myotube differentiation of both C2C12 mouse myoblasts and human myoblasts (Franzi et al., 2013). These findings are consistent with other studies demonstrating toxic and antiproliferative effects of type 1 IFNs in other cell lineages (endothelial cells and vascular smooth muscle) (Schirmer et al., 2010; Xiao et al., 2012). Type 1 interferons may upregulate the expression of class 1 HLA on muscle cells. It has been proposed that MHC class I upregulation by α-IFN in myofibers might cause activation of the endoplasmic reticulum stress response in DM, which could lead to muscle tissue injury and resulting myositis (Nagaraju et al., 2000). The stimulation of secretion of pro-inflammatory cytokines and chemokines might also contribute to the pathogenesis. An expanding number of cytokines and chemokines inducible by IFN have been reported, all involved in angiostasis, myogenesis and immune cell recruitment (Baechler et al., 2007; Caproni et al., 2004; Lopez-Vales et al., 2008; Zhao et al., 2007). For example the level of IL-6 is elevated in the peripheral blood of JDM patients and serum levels are correlated with DM disease activity

(Bilgic et al., 2009). Using an *in vivo* experimental model of myosin-induced myositis, it was demonstrated that IL-$6^{-/-}$ mice were disease free, with no clinical sign of muscle weakness nor any histological evidence of inflammatory infiltrates (Scuderi et al., 2006), underlining the role of IL-6 in the local inflammatory reaction. In addition, IL-6 acts as a central factor of a complex network involved in both angiogenesis and myogenesis (Muñoz-Cánoves et al., 2013; Rowe et al., 2014; Tierney et al., 2014). The expression of chemoattractant cytokines (chemokines) termed CXCL and CCL chemokines can either be induced or inhibited by IFNs. Angiostatic ELR- CXC chemokines, named for the absence of a 3-amino-acid sequence, glutamic acid–leucine–arginine, immediately proximal to the CXC sequence, including inducible protein 10 kDa (IP-10/CXCL10), monokine induced by interferon-c (MIG/CXCL9), interferon-c–inducible T-cell a chemoattractant (I-TAC/CXCL11) and CC chemokine monocyte MCP-1/CCL2, are expressed in the peripheral blood during active disease correlating with the degree of capillary loss and mononuclear cell infiltration (Baechler et al., 2007; Bilgic et al., 2009; Crescioli et al., 2012; Fall et al., 2005; López de Padilla et al., 2007; O'Connor et al., 2006; Sugiura et al., 2000; Zhao et al., 2007). Thus, high levels of antiangiostatic chemokines in affected tissues are related to the vasculopathy in JDM (Fall et al., 2005). Particularly, high serum level of MCP-1 was correlated with disease duration and cumulative organ damage at follow up (Sanner et al., 2014). Furthermore, neovascularization of capillaries is suggested to occur later in JDM disease after a transient capillary loss involving additional key interactions including leucocytes and endothelial cells through specific adhesion receptors. Intercellular adhesion molecule VCAM 1 and ICAM 1 are upregulated in endothelial cells (Sallum et al., 2006). It was demonstrated that VCAM 1 expression is increased in muscle biopsy both in the inflammatory muscle tissue and in the vasculature from JDM children who have a short duration of untreated disease, as compared with those who have a long duration of untreated disease (Kim et al., 2012). In addition to its

role in the immune system, VCAM-1 is also expressed in a developmentally specific pattern on differentiating skeletal muscle, where it mediates cell-cell interactions important for myogenesis through interaction with α4β1 integrin (Iademarco et al., 1993). These findings support the participation of these adhesion molecules in the vascular plasticity in JDM.

Figure 10: Type 1 interferon pathway. Mechanistic pathway showing production of type 1 IFNs, signaling pathway induced by IFNα and -β, and downstream effects including stimulation of genes, production of proteins, and resulting inflammation. IFNAR, IFNa receptor; JAK, Janus Kinase; Tyk2, Tyrosine Kinase 2; STAT, Signal Transducer and Activator of Transcription; ISGF3, Interferon Stimulated Gene Factor 3; IRF, Interferon Regulatory Factor; ISRE, Interferon Stimulated Response Element; ISGs, Interferon Stimulated Genes; ss, single-stranded; ds, double-stranded; LPS, Lipopolysaccharides; TLR, Toll-like receptor; NF-Kb, nuclear factor kappa-light-chain-enhancer of activated B cells; TBK1, TANK-binding kinase 1. Activation and positive feedback pathways of the type I IFN receptor are shown with dotted arrows (adapted from Arshanapalli, 2014).

Table 3: Angiogenic and Angiostatic Chemokines and Chemokine Receptors

ANGIOGENIC	
Receptor	*Chemokine Ligands*
CCR1	MIP-1α, CCL5 (RANTES), MCP-3
CCR2	CCL2 (MCP-1α), MCP-2, MCP-3
CCR3	CCL11 (eotaxin), CCL5 (RANTES), MCP-3, MCP-4
CCR8	CCL1 (I309)
CXCR1	CXCL8 (interleukin-8), CXCL6 (GCP2)
CXCR2	CXCL8, CXCL1 (GROα), CXCL2 (GROβ), CXL3 (GROγ), CXCL5 (ENA-78), CXCL6, CXCL7 (NAP-2)
CXCR4	CXCL12 (SDF-1)
CX3CR1	CX3CL1 (fractalkine)
ANGIOSTATIC	
Receptor	*Chemokine Ligands*
CXCR3	CXCL4 (PF4), CXCL9 (MIG), CXCL10 (IP-10), CXCL11 (I-TAC)
CXCR5	CXCL13 (BCA-1)

MCP monocyte chemotactic protein, GCP granulocyte chemotactic protein, GRO growth-regulated oncogene, ENA epithelial-cell-derived neutrophil-activating peptide, NAP neutrophil-activating peptide, SDF stromal-cell-derived factor, PF platelet factor, MIG monokine induced by interferon-γ, IP-10 interferon-inducible protein 10, I-TAC interferon-inducible T-cell alpha chemoattractant and BCA-1 B-cell chemoattractant 1, table derived from Shireman, 2007.

A comprehensive review by Greenberg has summarized uncertainties in the pathogenesis of DM, and has pointed out ischemia as the single pathogenic mechanism in DM which evidence can be scaled as strong (Greenberg and Amato, 2004). We have identified that capillary loss in DM distinctly takes form of 6-by-6 capillary drop-out, corresponding to multiples of the MVU, suggesting that capillary loss in DM primarily reflects upstream pathogenic events (Gitiaux et al., 2013). In addition, some evidence suggests that histopathological feature indicative of vasculopathy correlates with more aggressive disease or that features of vasculopathy and necrosis may predict chronicity. Indeed, zonal loss of capillary bed, muscle infarction and non-inflammatory of perymisial arterioles seem to be associated with chronicity. Conversely, absence of parameters of severe vasculopathy may predict more limited disease (Carpenter et al., 1976; Crowe et al., 1982). A spectrum of capillary changes that progress from swelling to necrosis and obliteration has been observed. The basal lamina was often thickened, duplicated and interrupted. Small infarcts of skeletal muscle in DM are typically associated with arterial occlusion caused by endothelial swelling with or without superimposed thrombosis (Carpenter et al., 1976; Miles et al., 2007). It is likely that microcirculatory disturbances associated with muscle infarction play a major role in the pathophysiology of DM. This central importance of vasculopathy as hallmark of the severe form of DM has to be confirmed (Figure 11).

Thus, JDM pathophysiology exemplifies how homeostasis of microvasculature controls whole skeletal muscle physiology. JDM combines microvascular changes showing a destruction of endothelial cells assessed by focal capillary loss, and a myofiber injury associated with an immune response. The tissue remodeling is efficient in most cases and muscle progressively recovers its function. However, in case of dramatic vascular damage, muscle recovery does not occur, leading to chronic damage.

Figure 11: Components of the pathogenesis of juvenile dermatomyositis (Feldman et al., 2008).

5-2. Duchenne muscular dystrophy

5-2-1. Genetic and clinical features of Duchenne dystrophy

DMD is the most common inherited myopathy of childhood associated with a progressive muscle degeneration leading to death (Brooke et al., 1989). Its incidence is close to 1/3500 live male births (Muntoni et al., 2003). DMD is caused by mutations in the dystrophin gene, the largest human gene, located on the human X chromosome at Xp21 and is usually associated with a marked deficiency or the absence of dystrophin protein. The full length 14 kb mRNA transcribed from the DMD gene and its corresponding 427 kDa protein are predominantly expressed in skeletal and cardiac muscles, with a smaller amount in brain. Dystrophin in the skeletal muscle is a subsarcolemmal cytoskeletal protein interacting with a protein complex, composed of at least 10 different proteins and membrane proteins such as dystroglygans and sarcoglycans (Campbell and Kahl, 1989). Interactions between dystrophin and its associated glycoprotein complex act as a bridge across the sarcolemma to connect the basal lamina of the extracellular matrix to the inner actin-based cytoskeleton. As the Duchenne muscular Dystrophy is transmitted by X linked recessive inheritance, nearly all patients are male. In a few female heterozygotes severe disease becomes manifest because of a failure of inactivation of the maternal X chromosome. Symptoms usually appear in male children before age of 5 and may be visible in early infancy. Typically, DMD patients are

clinically normal at birth, although serum levels of the muscle isoform of creatine kinase are elevated. Weakness starts to appear when a significant part of skeletal muscle has degenerated and been replaced by fibrosis, or fibro-adipose tissue. Early symptoms are developmental delays, difficulty in running, climbing stairs, frequent falls and enlargement of the calf muscles. Muscle weakness is progressive and by the age of 12, 95% of patients are no longer ambulatory and become wheelchair-bound. Significant weakness of respiratory muscle begins at the age of 8 or 9 and decreases consistently, the forced vital capacity declining annually by about 4% of the predictive value (Tangsrud et al., 2001). Most patients die in their early thirties as a result of cardiac dysfunction with cardiomyopathy and of respiratory complications due to intercostal muscle weakness and respiratory infection (Schade van Westrum et al., 2011).

5-2-2. The muscle microvasculature in DMD

The myopathological changes in DMD are characterized by a "dystrophic process" including necrotic and regenerating myofibers with progressive replacement of muscle tissue by fibrosis, or fibro-adipose tissue (Bell and Conen, 1968). In the 70s, before the discovery of the dystrophin, because the small cluster of necrotic fibers was similar to experimentally induced microinfarcts in muscle (Hathaway et al., 1970), the fiber necrosis was initially attributed to ischemia. This notion gave rise to the vascular hypothesis of DMD. This vascular theory was strongly debated as some researchers brought out minimal vascular abnormalities as they experimented an aortic ligation in rats followed by treatment with vasoactive amines in order to experimentally reproduce DMD lesions (Mendell et al., 1971). Several studies did not observe marked modifications of the vascular bed using electronic microscopy (Koehler, 1977; Musch et al., 1975). On the contrary, Jerusalem et al showed that two thirds of the capillaries display a replication of their basal lamina and that the capillary lumen was larger

than normal although they admitted that there was no evidence that DMD is caused by a primary abnormality of muscle microcirculation (Jerusalem et al., 1974). This controversy finally died out with the discovery of the dystrophin gene in 1987 (Koenig et al., 1987). However, the reason for the grouping of necrotic and regenerating fibers remains not fully understood. Since dystrophin is expressed in vascular smooth muscle cells, the dystrophin deficiency could hypothetically result in an angiopathy. Blood vessel disorganization and its impact on dystrophic myopathies were investigated, as it was suggested that a state of ischemia further aggravates the pathogenesis. In Golden Retriever muscular dystrophy (GRMD) dogs, the canine model for DMD, mimicking more closely the human disease than other existing mammalian model of dystrophin deficiency (Valentine et al., 1988), it was observed that the microcirculation in skeletal muscle is not altered in the first 3 first months of life. But by 4 month-old, dogs present a decrease in capillary density with normal C/F ratio suggesting that fiber atrophy and fibrosis are the major factor influencing microvascular architecture in skeletal muscle (Nguyen et al., 2005). The accumulation of endomysial and perimysial connective tissues may contribute to the impairment of intra-muscular blood circulation, and the decrease in capillary density associated with an increase in the distance capillary-fiber may, in turn, lead to an increase of the amount of connective tissue, beginning a vicious circle. In human DMD, microvascular networks in DMD muscle showed arteriolization and capillary tortuosity, and high variability of capillary domain sizes. Furthermore, endomysial fibrosis correlates with the severity of motor outcome of patients and accumulation of ECM components in the endomysium progressively increases the capillary-to-fiber distance suggesting that fibrosis favors an ischemic state of the muscle (Desguerre et al., 2009) (Figure 12). Fibrosis is one of the limiting factors of new therapeutics and is still a therapeutic target. Increasing distance between vessels and myofibers impairs muscle fiber mechanical function as the muscle-to-capillary interface is an important factor

involved in oxygen supply to the muscle (Chilibeck et al., 1997; Eliason et al., 2010) and could potentially impede their reciprocal stimulation by soluble factors during muscle repair.

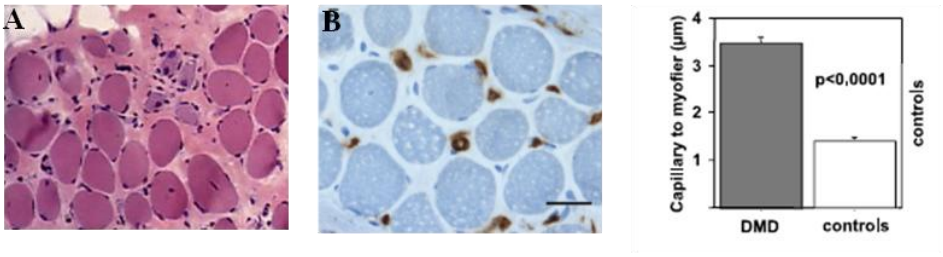

Figure 12: Vascular changes in DMD. (A) Grouped necrotic myofibers (B) There was a highly significant increase of the capillary-to-muscle fiber distance in Duchenne muscular dystrophy (DMD) patient biopsies compared with normal controls (mean+/-SEM) (adapted from Desguerre et al., 2009).

Different results from those observed in large animal models were described in smaller organisms, suggesting the importance of animal model as well as the choice of the vessel morphometric indexes. The best known murine model of DMD is the *mdx* mouse which also lacks dystrophin, identified from a colony of C57BL/10ScSn mice (Bulfield et al., 1984). *Mdx* does not reflect human DMD disease, as only old mdx presenting similar myopathologic features than in human (Lynch et al., 2001; Pastoret and Sebille, 1995; Tidball et al., 1995). In this model, a significant increase in arteriole density is found after hindlimb ischemia. Arteriogenesis is also enhanced in *mdx* mice in response to growth factors such as bFGF, MCP-1, NGF or SDF-1, suggesting that DMD is characterized by an imbalance of growth factors involved in neovascularization (Germani et al., 2003; Straino, 2004). Transplantation of satellite/myogenic cells expressing VEGF in *mdx* mice is associated with an improvement

of the vascularization, muscle regeneration and a decrease of fibrosis (Deasy et al., 2009). Treatment with and adeno-associated virus encoding for VEGF also improves the pathology and functional parameters in *mdx* mice with pro-regenerative and pro-angiogenic effects (Messina et al., 2007). Similarly, in *mdx* mice bearing one allele of the VEGF decoy receptor Flt-1, endothelial cell proliferation and vascular density are increased and this is associated with an improved muscle histology (decreased fibrosis and calcifications) and an increased muscle blood flow and force production (Verma et al., 2010). Additional evidence of an interdependent relationship between angiogenesis and muscular dystrophy is provided by the finding that, in *mdx* mice, reducing angiogenesis by ablating MMP-2 gene results in impaired growth of regenerating muscle fibers (Miyazaki et al., 2011). Therefore, it is possible that an increase in the vascular niche might promote muscle regeneration via stimulation of satellite cell proliferation or survival. A study in human DMD and BMD (Becker Muscular Dystrophy) patients revealed that levels of VEGF have a tendency to be higher as compared with control groups, suggesting that VEGF may reflect hypoxic and/or ischemic conditions in muscle tissues and be partly related to the process of disease progression (Saito et al., 2009). These results are compatible with a probably hypoxia induced, proangiogenic response in DMD and suggest that promoting angiogenesis is beneficial for dystrophic muscle pathology. At the molecular level, the role of nitric oxide (NO) has been investigated. In both mouse and human skeletal muscle, dystrophin deficiency results in loss of neuronal nitric oxide synthase (nNOS), the enzyme that produces the freely diffusible NO, which normally is localized to the sarcolemma as part of the dystrophin–glycoprotein complex (Brenman et al., 1995). *In vivo* mouse experiments suggest that skeletal muscle derived NO also may play an important role in the regulation of blood flow in exercising skeletal muscle by modulating the vasoconstrictor response to activation of α-adrenergic receptors. Such modulation was shown to be defective during contraction of nNOS-deficient skeletal muscles both of *mdx* mice, and

nNOS null mice (Froehner et al., 2015). This protective mechanism in children with DMD is also affected, because the vasoconstrictor response to reflex sympathetic activation, thereby optimizing muscle perfusion, was not upregulated during exercise of the dystrophic muscles, resulting in functional muscle ischemia (Sander et al., 2000). Transgenic *mdx* mice expressing dystrophin only in vascular smooth muscle cells exhibit an intermediate phenotype, with partial restoration of the NO-dependent modulation of α-adrenergic vasoconstriction in active muscle and muscle improvement (Ito, 2006). Flow is a major stimulus for vascular cell growth and angiogenesis. An impaired flow-mechanotransduction due to the absence of dystrophin could be deleterious for the angiogenic process. The same team realized several studies showing that: i) dystrophin plays a key role in the mechanotransduction of shear stress as impaired microvascular system adaptation to chronic changes in blood flow is detected in mesenteric arteries isolated from *mdx* mice and ii) DMD is associated with impaired NO-dependent dilation and a decrease in NOS expression (Loufrani, 2004; Loufrani et al., 2001, 2002). At the cell level, few studies have showed altered relationship between endothelial cells and myogenic cells that may contribute to the development and progression of muscle damage and degeneration. *Mdx*-derived endothelial cells have impaired angiogenic properties, in terms of migration, proliferation, and tube formation than wild-type controls. They undergo increased apoptosis *in vitro* and exhibit increased senescence. Moreover, m*dx*-derived endothelial cells display reduced ability to support myoblast proliferation when cocultured with myogenic cells (Palladino et al., 2013). Inversely, myogenic cells from old *mdx* (14-15 months) exhibit a reduced capacity to promote angiogenesis *in vitro*, as compared with wild-type cells, through the delivery of soluble factors. This altered capacity is correlated with a reduced expression of HIF-1α and VEGF genes in dystrophic satellite cells (Rhoads et al., 2013). As discussed above (see chapter 4), the signaling pathway of hedgehog is reactivated and has a physiologic role in ischemia induced skeletal muscle angiogenesis and regulates the

production of multiple growth factors during muscle regeneration (Pola et al., 2003). This upregulation of the Hh pathways in response to injury and during regeneration is significantly impaired in *mdx* muscle and Shh treatment increases in *vivo and in vitro* the proliferative potential of satellite cells isolated from the muscles of *mdx* muscle (Piccioni et al., 2014). Altogether, these studies demonstrate that DMD is clearly associated with alterations of vessels, which may directly affect the muscle regeneration process. Impaired angiogenesis is a novel player and potential therapeutic target in DMD although alteration of vessels and their impact on myogenesis should be deciphered at the molecular level. Moreover, vessel function is an essential issue in this disease since efficient gene or cell therapy relies on intravascular administration (Ennen et al., 2013) **.**

SPECIFIC AIMS OF THE STUDY

Specific aims of the study

Muscle is highly vascularized, with blood vessels being essential for adequate oxygenation of the tissue and for supporting increased metabolic demands. Beyond oxygen and nutrient supply, new functions have been demonstrated for vessels, through the interactions that vessel cells (endothelial cells) develop with myogenic cells (satellite cells). At steady-state, endothelial cells are surrounded by peri-endothelial cells now known to induce quiescence of satellite cells (Abou-Khalil et al., 2009). During skeletal muscle regeneration endothelial cells reciprocally interact with myogenic cells by direct contact or by releasing soluble factors to promote both myogenesis and angiogenesis processes (Christov et al., 2007). Therefore vessels play an important role in the regulation of muscle homeostasis, and in the tissue remodeling that occurs after an injury. However, little information is available on the role of vessel plasticity during human muscle regeneration. Skeletal muscle regeneration typically occurs as a result of a trauma or disease, such as congenital or acquired myopathies. To better understand the role of vessel plasticity in tissue remodeling, we took advantage of two paradigmatic situations of regenerating skeletal muscle in the child: Juvenile Dermatomyositis (JDM) and Duchenne Muscular Dystrophy (DMD). Although, these two muscular disorders share similar mechanisms of necrosis-inflammation from the histological point of view, they differ regarding the vessel domain. In JDM patients, microvascular changes display a destruction of endothelial cells assessed by focal capillary loss. Even though this transient capillary bed destruction, the tissue remodeling is efficient and muscle may progressively recover its function. By contrast, in DMD an increase of vessels density is observed in an attempt to improve the muscle perfusion but muscle function progressively alters with age (Desguerre et al., 2009).

The process of vessel plasticity is likely different in these two pathologies and my program aimed to define new interactions with muscle cells which characterize vascular remodeling in these skeletal muscle pathologies. The specific objectives were:

- *Clinical/histological aim*. JDM is highly heterogeneous regarding the constellation of pathological muscle changes and the outcome. The clinical part of the program was to identify the clinical and pathological predictive factors of poor clinical outcome in JDM by computing a comprehensive initial and follow-up clinical data set with deltoid muscle biopsy alterations assessed using the consensus JDM score tool controlled by age-based analysis of the deltoid muscle capillarization. This would finally allow stratifying treatment regimens based on the risk factors of poor response to classical first line treatment.

- *Cell aim.* This part includes the identification of specific cell interactions between myogenic cells issued from JDM and DMD patients and normal endothelial cells in coculture systems to explore whether myogenic cells participate to the vessel remodeling observed in the two pathologies. This functional analysis has been completed by a molecular investigation of the angiogenic signature of JDM and DMD myogenic cells, and compared with that of normal myogenic cells, to gain further insights in the pathogenesis of these diseases.

- *Molecular aim*. In this part, a transcriptomic analysis of endothelial and satellite cells purified from JDM and DMD muscle biopsies was realized. Analysis of Gene Ontology enrichment, as well as the main differentially expressed genes allowed to distinguish these two pathologies at the molecular level.

RESULTS

Results

Article 1: Vasculopathy as a major marker of severity in Juvenile Dermatomyositis-

article in review (Rheumatology), oral and poster communications: Société française de Myologie 2013, Société européenne de neuropédiatrie 2014.

The Juvenile Dermatomyositis (JDM) is the main inflammatory myopathy in childhood. The clinical presentation and outcome of JDM are highly heterogeneous. Early recognition of severe or unusual forms of JDM could lead to more favorable outcome if using appropriate treatment strategies. However, there is currently no reliable classification of the patients that can predict disease course, outcome or response to treatment during the acute phase. The main objective of the multiparametric analysis of clinical and histological data of a well defined monocentric cohort was to determine clinical and muscle biopsy features associated with poor outcome and response to treatment. The main results are: (i) JDM can be divided into two distinctive clinical subgroups, (ii) severe clinical presentation and outcome are linked to vasculopathy (iii) A set of simple predictors (CMAS<34, gastrointestinal involvement, muscle endomysial fibrosis at disease onset) allow early recognition of patients needing rapid therapeutic escalation with more potent drugs.

Vasculopathy as a major marker of severity in Juvenile Dermatomyositis

Cyril Gitiaux[1,2,3] MD, Marie De Antonio[4,5] PhD, Jessie Aouizerate[4] MD, Romain K Gherardi[4,5] MD, Thomas Guilbert[3] PhD, Christine Barnerias[1,2] MD, Christine Bodemer[7] MD PhD, Karine Brochard-Payet[8] MD, Pierre Quartier[9] MD, Lucile Musset[10] PhD, Bénédicte Chazaud[3] PhD, *Isabelle Desguerre [1,2,3] MD PhD, *Brigitte Bader-Meunier[9] MD

Authors affiliation:

[1]Department of Pediatric Neurology, Hôpital Necker Enfants Malades, Assistance Publique-Hôpitaux de Paris, Université Paris Descartes, Paris, France.

[2]AP-HP, Referral center for neuromuscular diseases "Garches-Necker-Mondor-Hendaye", France.

[3]INSERM U1016, Paris, France.

[3]CNRS UMR 8104, Paris, France.

[3]Paris Descartes University, Paris, France.

[4]AP-HP, Albert Chennevier-Henri Mondor Hospital, Department of Histology, Department of Pathology, Créteil, France.

[5]INSERM UMRS1138-Team 22, Centre de Recherche des Cordeliers, Paris-Descartes University, UPMC University, Paris, France.

[6]INSERM U955-Team 10, Department of Neurosciences, "Mondor Biomedical Research Institute", Paris-Est University, Faculty of Medicine, Créteil, France.

[7]Department of Dermatology, Hôpital Necker Enfants Malades, Assistance Publique-Hôpitaux de Paris, Université Paris Descartes, Paris, France.

[8]Department of Pediatric Internal Medicine and Nephrology, Hôpital des enfants, CHU de Toulouse, Toulouse, France.

[9]Department of Pediatric Immunology-Hematology and Rheumatology, Paris Descartes University, IMAGINE, AP-HP, Necker Hospital, Paris, France.

[10]Department of Immunology, CHU Pitié-Salpêtrière, Assistance Publique-Hôpitaux de Paris, Paris, France

*These authors equally contributed to this study.

Corresponding Author: Dr Cyril Gitiaux. Hôpital Necker-Enfants Malades, 149 rue de Sèvres, 75015 Paris, France. Tel: +33 1 42 19 26 95, Fax : +33 1 42 19 26 92. Email: cyril.gitiaux@nck.aphp.fr

Conflict of Interest Statement: None of the authors has any conflict of interest to disclose.

Key words: Juvenile dermatomyositis, vasculopathy, muscle biopsy, prognostic factors, outcome.

ABSTRACT

Objectives: Outcome of Juvenile dermatomyositis (JDM) is highly heterogeneous. Our objective was to determine clinical and muscle biopsy features associated with poor outcome and response to treatment.

Methods: Clinical data and muscle biopsy were obtained from a monocentric cohort of 29 patients. Clinical subgroups were defined by latent class model analysis of initial and follow-up parameters. Myopathological features were analyzed using validated scores. Capillary loss was determined on reconstructions of transversal sections and assessed in the different age groups to take into account variations of muscle capillarization during post-natal development. Regression models were used to identify initial predictors of therapeutic response.

Results: Two distinct homogeneous subgroups of patients were identified according to clinical severity and pathological findings. The smallest group of patients (7/29) presented with severe JDM. Compared to the other group (22/29), patients had more severe muscle weakness at disease onset, low remission rate at 12 months, frequent subcutaneous limb edema or gastrointestinal involvement and higher myopathological scores ("capillary dropout", "perifascicular necrosis/regeneration", "fibers with internal myonuclei" and "fibrosis" subscores). Relevance of capillary dropout to JDM severity was substantiated by age-based analysis confirming its major role in JDM pathophysiology. Most of these manifestations could be related to vasculopathy (limb edema, gastrointestinal involvement, capillary dropout). Furthermore, CMAS<34 with either gastrointestinal involvement or muscle endomysial fibrosis at disease onset were the best predictors of poor response to treatment.

Conclusions: Vasculopathy is prominent in severe JDM. Simple criteria can be used at initial evaluation to identify patients who might necessitate specific therapeutic approaches.

INTRODUCTION

Juvenile dermatomyositis (JDM) is a rare pediatric-onset idiopathic inflammatory myopathy. It is a heterogeneous disease regarding: (i) the association, or not, with myositis specific autoantibodies (MSA), anti-MDA5 and anti-NXP2 autoantibodies being associated with different clinical phenotypes [1-3]; (ii) the various possible patterns of muscle magnetic resonance imaging (MRI) changes [4,5]; (iii) the constellation of pathological muscle changes [6] and (iv) the onset and outcome of disease [7,8]. Early studies described three different courses of JDM: monophasic (response to first-line treatment with remission within 2 years), chronic polycyclic and chronic relentless disease [9,10]. Long-term outcome studies showed that 40-60% of patients develop a chronic course requiring long-lasting, often multiple, immunosuppressive treatments [11-13]. A recent collaborative randomized controlled trial in JDM concluded that combination of corticosteroids with methotrexate is the best choice first-line treatment in terms of efficacy and toxicity [14]. However, clinical and histopathological predictive factors of poor response to this treatment have not yet been clearly identified. Classical studies attempting to correlate myopathological features with severity were based on the different courses of JDM described above [9,10,15]. Muscle biopsies showing features indicative of vasculopathy were found to predict severity and chronicity [9], but no definite conclusions were reached regarding possible predictors of response to treatment [15]. These authors pointed out the lack of a reliable consensus histopathological scoring system for muscle biopsy changes, leading to the establishment of a consensus JDM myopathological severity score [16] which was recently validated [17]. The same team yielded significant variations of muscle fiber capillarization during the post natal development of quadriceps femoris and biceps brachialis muscles which should also be taken into account in the assessment of JDM vasculopathy [18].

The objective of the present retrospective monocentric study was to identify the clinical and pathological predictive factors of poor clinical outcome in JDM by computing a comprehensive initial and follow-up clinical data set with deltoid muscle biopsy alterations assessed using the consensus JDM score tool [16,17], controlled by age-based analysis of the deltoid muscle capillarization. This would finally allow stratifying treatment regimens based on the risk factors of poor response to classical first-line treatment.

PATIENTS AND METHODS

Patients

We conducted a retrospective cohort study of patients with JDM followed in the French referral center for rare pediatric inflammatory diseases (CERHUMIP). Patients diagnosed from November 2007 to April 2013 were recruited. Indeed, since November 2007, muscle biopsy at onset of JDM was systematically performed. Patients were referred to the referral center either because they lived in the geographical area "Ile-de-France" or because they presented severe disease. Patients were registered in the CEMARA database, a nation-wide information system for rare diseases after parental information [19]. This system benefits from an agreement of the French National Committee on Informatics and Liberty (CNIL). Inclusion criteria were: (i) diagnosis of JDM according to conventional clinico-pathological criteria [20], (ii) muscle biopsy performed, (iii) disease duration <12 months before deltoid muscle biopsy, (iv) follow up > 12 months. Myositis specific autoantibodies were not systematically screened in this retrospective study. Patients were assessed and treated according to a defined protocol including prednisone alone (16/29) or prednisone and methotrexate (13/29) as a first-line of treatment. At each visit, patients had a standardized assessment of skin, muscle and other organs involvements. Clinical, biological and pathological data collected at disease onset and during follow-up (at 6 months and every year until last evaluation) were retrospectively reviewed. They included: (i) demographics; (ii) the

description of skin manifestations such as characteristic skin rash (e.g. facial and malar erythema, "V" or shawl sign), Gottron's papules, subcutaneous edema, telangiectasia, poïkiloderma, ulcerations, and muscle involvement at onset and during follow-up. with a score adapted from the DAS skin score (0 to 2; 0: erythema absent or completely resolved, 1: mild or moderate erythema, 2: severe and active erythema) [21], the Childhood Myositis Assessment Scale (CMAS 0-52), [22], and the Manual Muscle Testing (MMT 0-80) of eight muscle groups [23]; (iii) biological tests including creatine kinase (CK) levels (score 0: <145; 1: <5000; 2: 5000-10000; 3>10000 IU), antinuclear antibodies (ANA) (score 0:<1/100; 1:]1/100-1/600]; 2>]1/600-1/1000] ; 3:>1/1000), Myositis Specific Autoantibodies (MSA) and Myositis Associated Autoantibodies (MAA) (score 0: absent, 1: present); (iv) treatments scored as 1: prednisone or prednisone and methotrexate (MTX); 2: prednisone/MTX+ 1 other line; 3: prednisone/MTX+ 2 other lines; 4: prednisone/MTX+ > 2 other lines; (v) visceral involvement: pulmonary (assessed by chest X ray, tomodensitometry, pulmonary function testing), cardiovascular, gastrointestinal tract involvement (abdominal pain, diarrhea, perforation); (score 0 if absent or 1 if present); (vi) presence of calcinosis or lipodystrophy (score 0 if absent or 1 if present).

Remission was defined as the presence of CMAS ≥48, the absence of active skin disease and a Physician's Global Assessment Score (PGAS) <1 [2]. When possible, the PRINTO definition of JDM disease inactivity was used [24].

Muscle biopsy

Scoring of muscle biopsy

For each patient, deltoid muscle biopsy sampling, histological staining and immunohistochemistry were carried out on 7 μm cryostat sections, including hematoxylin-eosin staining, Gomori's trichrome, immunohistochemistry for endothelial cells (CD31, 1/20, Dako, Glostrup, Denmark, M0823), regenerating myofibers (CD56, 1/100, Novocastra,

Antony, France, NCL-CD56-1B6), macrophages (CD68, 1/300, Dako, Glostrup, Denmark, M0814), T cells (CD3, 1/100, Dako, Glostrup, Denmark, A0452), CD4+ cells (CD4, 1/200, Novocastra, Antony, France, NCL-CD4-1F6), CD8+ cells (CD8, 1/400, Dako, Glostrup, Denmark, M7103), B cells (CD20, 1/500, Dako, Glostrup, Denmark, M0755), anti-human major histocompatibility complex (MHC) class I (HLA-ABC, 1/4000, Dako, Glostrup, Denmark, R7000), and C5b-9/MAC (1/50, Dako, Glostrup, Denmark, M0777) [25]. All biopsies were reviewed blindly for clinical data by two of us (CG, RKG), using the recently validated score tool for muscle biopsy evaluation in patients with JDM [16,17]. Particularly, endomysial fibrosis was considered to be present when fibrous tissue was distinctly seen in-between at least 3 myofibers on trichrome stain.

Capillary loss assessment

Control muscle biopsies were used to establish normal age-dependent capillary density in the deltoid muscle. They included 21 normal biopsy specimens of 11 boys and 10 girls, aged from 1 to 21y, stored in the muscle bank of the GNMH Neuromuscular Reference Center (Créteil, France). All deltoid muscle biopsies from JDM patients (n=29) and controls (n=21) were subjected to full 2D reconstructions, including 40-100 adjacent images (X10) of CD31 immunostained sections, using a Zeiss Axio Observer Z1 microscope and MetaMorph 7 software (Scan-Slide option). Thus, each biopsy appeared as a single image of the whole sample. Image analyses were performed using homemade ImageJ routines (http://imagej.nih.gov/ij/). Calculation of capillary-fiber (C/F) ratio and capillary density (CD) was done after automatic color segmentation (RGB threshold), on 3-10 selected fascicles of interest per sample, allowing reproducible and unbiased object counts. Furthermore, JDM patients' C/F ratio displaying the most obvious capillary loss was added in order to refine the depiction of capillary changes.

Statistical analyses

Muscle involvement trajectory subgroups.

Latent class model analysis (LCA) was used to identify, within the cohort of JDM patients, subgroups with homogenous muscle involvement trajectory, assessed by CMAS during follow-up [26]. LCA is a statistical method that simultaneously considers a number of variables over time to assign each patient to homogeneous mutually exclusive groups existing within a heterogeneous population. The covariates used to determine these subgroups were: "treatment lines", "CK levels" and "severity of the skin involvement during follow-up". This model was adjusted on age at diagnosis. A two and a three subgroups solutions determined by LCA were performed, and finally the most clinically relevant solution was chosen. Then, comparisons between identified subgroups for initial clinicopathological variables were performed using the Fisher's exact test for qualitative variables and the Mann-Whitney U test for quantitative variables. Spearman's rank correlation coefficient was used to assess correlation between different items of the JDM score tool.

Initial indicators of poor response to a first-line treatment.

In another part of the study, clinicopathological features at the onset of disease were used to assess their ability to help determine patients who will require a rapid therapeutic escalation. JDM patients were classified into *non responders* to treatment if they required ≥ 2 lines of treatment within 6 months after diagnosis, and *good responders* in the other cases. Eleven variables were used as potential predictors in this response to treatment classification model: "subcutaneous edema", "gastrointestinal involvement", "CMAS", "CK", "histo-pathologists' overall severity score (VAS)", "obvious capillary dropout", "fibers with internal myonuclei", "perifascicular necrosis/regeneration", "endomysial fibrosis", "perimysial fibrosis" and "C/F in the most affected fascicle". Logistic regression was used to explain the binary variable (*good vs non responders*) by a subset of the 11 selected potential predictors. For continuous variables, the median was used to split the sample into two categories. First, univariate

analyses were performed, and then forward selection approach was used to obtain the best subset selections. The final models are the models having the smallest Akaike Information Criterion (AIC).

Age-dependent muscle capillarization.

Mixed linear models, using *"age at biopsy"* as a fixed effect and *"subjects"* as a random effect, were performed to assess age-dependent variations of capillary parameters (C/F, CD) in control deltoid muscle biopsies. Spearman's test was applied for correlation on deltoid muscle *vs* age. Analysis of vascular parameters for each JDM patients was performed taking into account the expected value for age of C/F and CD compared to the observed value.

All statistical analyses were conducted using R software [27]. The significance level was set at 0.05 and all tests were two-tailed.

RESULTS

1-Identification of two distinct JDM subgroups .

a) Clinical characterization.

Twenty-nine patients with JDM (20 females, 9 males) were included in the study. Diagnostic criteria consisted in proximal muscle weakness, characteristic skin involvement and muscle biopsy features suggestive of JDM. Median age at onset was 7.7 years (range 2-14) and median disease duration was 1 month (range 0-7) at time of biopsy. The median follow-up was 28 months (range 12-82). Clinical and biological characteristics at disease onset are shown in table 1.

LCA finally identified two subgroups with distinct muscle involvement trajectory: a "severe group" (group 1) and a main "classical group" (group 2), including 7 and 22 patients, respectively (Table 1).

This two subgroups were characterized by highly distinct initial phenotype and outcome (Figure 1): at disease onset, patients of group 1 displayed a severe muscular involvement

[lower CMAS (p=0,007), higher CK rate (p=0,014)] and a constant and significant subcutaneous edema (100 *vs* 45,5%) with distribution in limbs of 57 *vs* 14% in group 2 (p=0.038). Other skin manifestations were similar in the two groups. Evidence of involvement of other organs was also more frequent in group 1. In particular, gastrointestinal involvement at disease onset was a major feature in group 1 (71 *vs* 0% p<0.001). The first treatment line at the onset was similar in the two groups (prednisone alone 43% in group 1 *vs* 59% in group 2 or MTX+prednisone 57% in group 1 *vs* 41% in group 2, p=0,67). Regarding the course of the disease, more treatment lines were clinically required within the first 6 months (≥ 2 lines, 100 *vs* 23%, p<0.001) in group 1. Calcinosis was not significantly associated with group 1 (42% *vs* 14%, p=0,13). Using a recently proposed definition of disease inactivity in JDM [2], less patients of group 1 were in remission at one year post diagnosis (information available for all patients): 14% *vs* 76% p=0,007 and at 3 years post diagnosis (information available for 50% patients): 25% *vs* 80% p=0,07. Of note, there was no significant difference in age (a trend for older age in group 1) and in sex distribution of patients across the different clinical courses.

b) Myopathological features.

Scoring of muscle biopsy in JDM subgroups showed that a prominent vascular injury is associated with severity.

Scoring of all biopsies using the JDM severity score tool were compared in the two groups identified above. The histo-pathologists' overall severity score (VAS) was significantly higher for group 1 (p=0.03). The total score of the vascular domain (p=0.01), the muscle fiber domain (p=0,006) and the connective tissue domain (p=0,02) differed significantly between the two groups (Figure 2A). Regarding subscores, the following items were significantly different (Figure 2B): "capillary dropout" (p=0.003) (Figure 2C), "perifascicular necrosis/regeneration" (p=0.03); "fibers with internal myonuclei" (p=0.002) and "fibrosis"

(p=0.03) (Figure 2D). In contrast, scoring of the inflammatory domain, including both amount and distribution of inflammation, was similar in the two groups (p=0,62) (Figure 2A).

Comparison of capillary loss in relation to age in distinct JDM subgroups.

To avoid bias in the assessment of "capillary dropout" due to immaturity of the microvasculature in young children, capillary density (CD) per fascicular area and capillary-to-fiber (C/F) ratio were established in normal deltoid muscle at various pediatric ages. The C/F ratio showed a mean value lower than 1.0 under the age of 15 years. C/F ratio increased and CD decreased gradually with age, consistently with post-natal muscle capillary growth and myofiber enlargement, respectively. Both CD (Figure 3A) and C/F (Figure 3B) correlated significantly with age. CD and C/F ratio were established in JDM biopsies and their differences from mean normal values at the same age were determined. Patients with poor future clinical outcome (group 1) displayed lower global CD (p=0.04) (Figure 4A and 4C) and lower C/F ratio in the most affected fascicle (p<0.001) (Figure 4B and D) resulting from significantly higher differences in group 1 compared to group 2. Global C/F ratio was not significantly different between the two groups (p=0.13). This confirmed the validity of the JDM severity score tool item "capillary dropout", which needs to be "obvious and marked" regardless of the patient age. Furthermore, these results demonstrated that capillary dropout in JDM occurs as a heterogeneous and focal pattern.

2-Initial indicators of poor response to a first-line treatment.

Finally to help decision-making in defining adequate therapeutic strategies in routine clinical practice we examined whether a reduced set of initial clinical and pathological signs could be used as criteria to predict poor therapeutic response in the JDM cohort. Patients were classified into *non responders* to treatment if they required ≥ 2 lines (corticosteroids or corticosteroids with methotrexate + IV immunoglobulin and/or endoxan and/or plasma exchanges) of treatment within 6 months after diagnosis, and *good responders* in the other

cases. Computation of the associations between the 11 selected clinical and histopathological variables available at the onset of the disease yielded 3 best models predicting therapeutic response (see additional data). The model, including "CMAS", "gastrointestinal involvement", "endomysial fibrosis" (AIC values at each step:15.2; 11.6; 8) was chosen since it allowed 100% of correct classification in the present JDM cohort and included a simple histopathological criterion (i.e. detectable endomysial fibrosis on trichrome stain) appropriate in routine practice. In this model, all patients with initial CMAS≥34 were *good responders*. Among patients with CMAS<34, all patients with GI involvement and/or endomysial fibrosis were *non responders*, while the others (CMAS<34 without GI involvement and without endomysial fibrosis) were *good responders* (Table 2).

DISCUSSION

The present study identifies clinical and pathological manifestations associated with severity and poor response to first-line treatment in JDM. Severe clinical presentation and outcome could be related to vasculopathy, suggesting it is a major factor of severity in JDM.

JDM can be divided into two distinctive clinical subgroups. A majority of patients had "classical" disease and the others had "severe" disease with more pronounced initial muscle weakness, rapid therapeutic escalation requiring adjunctive immunosuppressive treatments, and low remission rate at 12 months. Severe JDM cases more frequently presented with early subcutaneous limb edema (14 *vs* 57%) and gastrointestinal (GI) involvement (0% *vs* 71%). Both manifestations are thought to be related to vasculopathy. The exact mechanism of increased capillary permeability in edematous DM [28-32] remains elusive, but muscle microinfarcts are much more frequently found in edematous (80%) compared to non-edematous (34%) adult DM, suggesting a prominent role of ischemia [31]. GI tract involvement is uncommon in JDM [11,33], and has been linked to inflammatory vasculopathy with lumen narrowing or complete occlusion of multiple small and medium arteries causing

gastrointestinal ulceration and perforation [34]. Consistently, deltoid muscle biopsy showed more pronounced signs of vasculopathy in severe *vs* classical JDM, as assessed by both consensus scoring and age-related morphometry of muscle capillarization. Muscle capillary dropout is a central feature in the pathogenesis of both JDM [9,10,15] and adult DM [25]. The consensus JDM score tool includes 16 items corresponding to 4 domains [16]. Compared to classical JDM, severe JDM cases had significantly higher scores in the "vascular", "muscle fiber" and "connective tissue" domains, but strikingly not in the "inflammatory" domain. Single items found as markers of severity included "obvious and marked capillary dropout", "perifascicular necrosis/regeneration", "fibers with internal myonuclei", and "fibrosis". In keeping with a previous study conducted on human quadriceps and biceps brachialis muscles, we observed that the capillary-to-fiber ratio (C/F) increases whereas the capillary density (CD) progressively declines during post-natal development, reflecting the combination of the capillary bed growth with myofiber cross section increase [18]. On this basis we confirmed in each age group a significant decrease of deltoid muscle capillarization (assessed by C/F in the most affected fascicle) in severe JDM patients, which was not the case in classical JDM cases. This provides the first conclusive documentation of muscle capillary loss in severe JDM. Nevertheless, previous studies have suggested that nailfold capillary changes which likely reflect the degree of systemic blood vessel abnormalities are detected in the more severe forms of JDM [35]. Interestingly, interstitial lung disease (ILD) was rare (3/29) and not associated with severity in our series. Rapidly progressive ILD was recognized as a mortality risk factor [36], whereas MDA5 associated ILD appears to be related with a good prognosis [2].

The study was designed to avoid pitfalls identified in previous studies, including (i) non-validated criteria to segregate JDM severity groups, and (ii) possible bias in the assessment of capillary loss related to physiological variations of capillarization during post-natal muscle

development [15]. The cohort of patients was followed by the same medical team, collecting initial and follow-up data on a systematic basis, and maintaining homogeneous practices along the entire follow-up. The two homogeneous JDM subgroups were distinctly identified by latent class model analysis, a robust statistical tool taking into account both initial and follow-up data. Despite our monocentric study includes relatively small number of patients, this method allowed performing a multivariate analysis taking into account the evolution of data available over time [26].

Although modern treatment has improved JDM outcome, recent long term studies still show significant numbers of patients with ongoing disease or damage [11-13]. Several studies indicate that aggressive early treatment might result in lower morbidity and improve outcome [37-39]. However, guidelines on how to efficiently orient therapeutic interventions in JDM are warranted. Recently, tumor necrosis factor type 2, galectin 9, CXCL10/IP-10 and MRP8/14 were identified as novel markers of active JDM [40,41], but this remains to be validated in practice. Therefore we attempted to define clinicopathological criteria at disease onset, to identify patients deserving rapid therapeutic escalation. Initial muscle weakness severity and GI manifestations of vasculopathy appeared as potentially contributory clinical predictors. “Endomysial fibrosis” emerged as a possible histopathological predictor. As this item was not precisely defined in the JDM score tool, we propose to consider endomysial fibrosis to be present when fibrous tissue is distinctly seen in between at least 3 myofibers on trichrome stain. Of particular interest, endomysial fibrosis associated with capillary loss was correlated with strong expression of angiostatic CXC-Chemokines including CXCL10 and CXCL11 [42]. Furthermore, Miles et al showed that the likelihood of chronic juvenile DM is substantially increased when obliteration of the capillary bed is obvious in foci of prominent endomysial fibrosis [15]. Of note, in the other statistically relevant models (see additional data) “capillary dropout” also emerged as an histopathological predictor. Endomysial fibrosis

was preferred to avoid laborious calculation of the C/F ratio and subsequent comparison to the normal value for age which is uneasy to perform in routine practice. Finally, the set of the combination of initial "CMAS" (< or ≥34), initial "GI involvement" (present/absent), and "endomysial fibrosis' at diagnostic biopsy (present/absent) appeared as predictive of the response to first-line therapeutic response. Although we ensured the homogeneity of the dataset, the monocentric design of our study restricts the number of patients for some aspects of the disease (eg, autoantibodies screening, muscle MRI assessment), calling for further research. Particularly, large series of JDM patients will be of particular interest to decipher the relative contributions of the autoantibodies screening correlated with biopsy features.

REFERENCES

1: Kobayashi N, Takezaki S, Kobayashi I, Iwata N, Mori M, Nagai K, et al. Clinical and laboratory features of fatal rapidly progressive interstitial lung disease associated with juvenile dermatomyositis. Rheumatology (Oxford) 2014;6.

2: Tansley SL, Betteridge ZE, Gunawardena H, Jacques TS, Owens CM, Pilkington C, et al. Anti-MDA5 autoantibodies in juvenile dermatomyositis identify a distinct clinical phenotype: a prospective cohort study. Arthritis Res Ther 2014;16:R138.

3: Tansley SL, Betteridge ZE, Shaddick G, Gunawardena H, Arnold K, Wedderburn LR, et al. Calcinosis in juvenile dermatomyositis is influenced by both anti-NXP2 autoantibody status and age at disease onset. Rheumatology (Oxford) 2014;53:2204-8.

4: Davis WR, Halls JE, Offiah AC, Pilkington C, Owens CM, Rosendahl K. Assessment of active inflammation in juvenile dermatomyositis: a novel magnetic resonance imaging-based scoring system. Rheumatology (Oxford) 2011;50:2237-44.

5: Malattia C, Damasio MB, Madeo A, Pistorio A, Providenti A, Pederzoli S, et al. Whole-body MRI in the assessment of disease activity in juvenile dermatomyositis. Ann Rheum Dis. 2014;73:1083-90.

6: Carpenter S, Karpati G, Rothman S, Watters G. The childhood type of dermatomyositis. Neurology 1976;26:952-62.

7: Feldman BM, Rider LG, Reed AM, Pachman LM. Juvenile dermatomyositis and other idiopathic inflammatory myopathies of childhood. Lancet 2008;371:2201-12.

8: Robinson AB, Reed AM. Clinical features, pathogenesis and treatment of juvenile and adult dermatomyositis. Nat Rev Rheumatol 2011,7:664-75.

9: Crowe WE, Bove KE, Levinson JE, Hilton PK. Clinical and pathogenetic implications of histopathology in childhood polydermatomyositis. Arthritis Rheum 1982;25:126-39.

10: Spencer CH, Hanson V, Singsen BH, Bernstein BH, Kornreich HK, King KK. Course of treated juvenile dermatomyositis. J Pediatr 1984;105:399-408.

11: Ravelli A, Trail L, Ferrari C, Ruperto N, Pistorio A, Pilkington C, et al. Long-term outcome and prognostic factors of juvenile dermatomyositis: a multinational, multicenter study of 490 patients. Arthritis Care Res 2010;62:63-72.

12: Mathiesen P, Hegaard H, Herlin T, Zak M, Pedersen FK, Nielsen S. Long-term outcome in patients with juvenile dermatomyositis: a cross-sectional follow-up study. Scand J Rheumatol 2012;41:50-8.

13: Sanner H, Sjaastad I, Flatø B. Disease activity and prognostic factors in juvenile dermatomyositis: a long-term follow-up study applying the Pediatric Rheumatology International Trials Organization criteria for inactive disease and the myositis disease activity assessment tool. Rheumatology (Oxford) 2014;53:1578-85.

14: Ruperto N, Pistorio A, Oliveira S, Cuttica RJ, Ravelli A, Fischbach M, et al. A randomised trial in new onset juvenile dermatomyositis: prednisolone versus prednisolone plus cyclosporine verus prednisolone plus methotrexate. [abstract]. Arthritis Rheum 2012,64:2473.

15: Miles L, Bove KE, Lovell D, Wargula JC, Bukulmez H, Shao M, et al. Predictability of the clinical course of juvenile dermatomyositis based on initial muscle biopsy: a retrospective study of 72 patients. Arthritis Rheum 2007;57:1183-91.

16: Wedderburn LR, Varsani H, Li CK, Newton KR, Amato AA, Banwell B, et al. International consensus on a proposed score system for muscle biopsy evaluation in patients with juvenile dermatomyositis: a tool for potential use in clinical trials. Arthritis Rheum 2007;57:1192-201.

17: Varsani H, Charman SC, Li CK, Marie SK, Amato AA, Bandwell B, et al. Validation of a score tool for measurement of histological severity in juvenile dermatomyositis and association with clinical severity of disease. Ann Rheum Dis 2015;74:204-10

18: Sallum AM, Varsani H, Holton JL, Marie SK, Wedderburn LR. Morphometric analyses of normal pediatric brachial biceps and quadriceps muscle tissue. Histol Histopathol 2013;28:525-30.

19: Landais P, Messiaen C, Rath A, Le Mignot L, Dufour E, Ben Said M, et al. CEMARA an information system for rare diseases. Stud Health Technol Inform 2010;160:481-5.

20: Brown VE, Pilkington CA, Feldman BM, Davidson JE; Network for Juvenile Dermatomyositis, Paediatric Rheumatology European Society (PReS). An international consensus survey of the diagnostic criteria for juvenile dermatomyositis (JDM). Rheumatology (Oxford) 2006;45:990-3.

21: Bode RK, Klein-Gitelman MS, Miller ML, Lechman TS, Pachman LM. Disease activity score for children with juvenile dermatomyositis: reliability and validity evidence. Arthritis Rheum 2003;49:7-15.

22: Huber AM, Feldman BM, Rennebohm RM, Hicks JE, Lindsley CB, Perez MD et al. Validation and clinical significance of the Childhood Myositis Assessment Scale for assessment of muscle function in the juvenile idiopathic inflammatory myopathies. Arthritis Rheum 2004;50:1595-603.

23: Jain M, Smith M, Cintas H, Koziol D, Wesley R, Harris-Love M, Lovell D, Rider LG, Hicks J. Intra-rater and inter-rater reliability of the 10-point Manual Muscle Test (MMT) of strength in children with juvenile idiopathic inflammatory myopathies (JIIM). Phys Occup Ther Pediatr 2006;26:5-17.

24: Lazarevic D, Pistorio A, Palmisani E, Miettunen P, Ravelli A, Pilkington C, et al. The PRINTO criteria for clinically inactive disease in juvenile dermatomyositis. Ann Rheum Dis 2013;72:686-93.

25 : Gitiaux C, Kostallari E, Lafuste P, Authier FJ, Christov C, Gherardi RK. Whole microvascular unit deletions in dermatomyositis. Ann Rheum Dis 2013;72:445-52.

26: Proust C, Jacqmin-Gadda H, Taylor JM, Ganiayre J, Commenges D. A non linear model with latent process for cognitive evolution using multivariate longitudinal data. Biometrics 2006;62:1014-24.

27: R Core Team (2013). R: A language and environment for statistical computing. R Foundation for Statistical Computing, Vienna, Austria. URL http://www.R-project.org/.

28: Mitchell JP, Dennis GJ, Rider LG. Juvenile dermatomyositis presenting with anasarca: A possible indicator of severe disease activity. J Pediatr 2001;138:942-5.

29: Saygi S, Alehan F, Baskin E, Bayrakci US, Ulu EM, Ozbek N. Juvenile dermatomyositis presenting with anasarca. J Child Neurol 2008;23:1353-6.

30: Chai Y, Bertorini TE, Li YD, Mitchell C, Guan H. Limb edema and anasarca associated with severe dermatomyositis: report of four cases. Neuromuscul Disord 2011;21:439-42.

31: Milisenda JC, Doti PI, Prieto-González S, Grau JM. Dermatomyositis presenting with severe subcutaneous edema: Five additional cases and review of the literature. Semin Arthritis Rheum 2014;44:228-33.

32: Tu J, McLean-Tooke A, Junckerstorff R. Increasing recognition of dermatomyositis with subcutaneous edema - is this a poorer prognostic marker? Dermatol Online J 2014;20:21244.

33: Robinson AB, Hoeltzel MF, Wahezi DM, Becker ML, Kessler EA, Schmeling H, et al. Clinical characteristics of children with juvenile dermatomyositis: the Childhood Arthritis and Rheumatology Research Alliance Registry. Arthritis Care Res (Hoboken) 2014;66:404-10.

34: Mamyrova G, Kleiner DE, James-Newton L, Shaham B, Miller FW, Rider LG. Late-onset gastrointestinal pain in juvenile dermatomyositis as a manifestation of ischemic ulceration from chronic endarteropathy. Arthritis Rheum 2007;57:881-4.

35: Schmeling H, Stephens S, Goia C, Manlhiot C, Schneider R, Luthra S, et al. Nailfold capillary density is importantly associated over time with muscle and skin disease activity in juvenile dermatomyositis. Rheumatology (Oxford) 2011;50:885-93.

36: Huber AM, Mamyrova G, Lachenbruch PA, Lee JA, Katz JD, Targoff IN, et al. Early illness features associated with mortality in the juvenile idiopathic inflammatory myopathies. Arthritis Care Res (Hoboken) 2014;66:732-40.

37: Ramanan AV, Campbell-Webster N, Ota S, Parker S, Tran D, Tyrrell PN, et al. The effectiveness of treating juvenile dermatomyositis with methotrexate and aggressively tapered

corticosteroids. Arthritis Rheum 2005;52:3570-8.

38 : Hasija R, Pistorio A, Ravelli A, Demirkaya E, Khubchandani R, Guseinova D, et al. Therapeutic approaches in the treatment of juvenile dermatomyositis in patients with recent-onset disease and in those experiencing disease flare: an international multicenter PRINTO study. Arthritis Rheum 2011;63:3142-52.

39: Oddis CV, Reed AM, Aggarwal R, Rider LG, Ascherman DP, Levesque MC, et al. Rituximab in the treatment of refractory adult and juvenile dermatomyositis and adult polymyositis: a randomized, placebo-phase trial. Arthritis Rheum 2013;65:314-24.

40: Bellutti Enders F, van Wijk F, Scholman R, Hofer M, Prakken BJ, van Royen-Kerkhof A, et al. Correlation of CXCL10, tumor necrosis factor receptor type II, and galectin 9 with disease activity in juvenile dermatomyositis. Arthritis Rheum 2014;66:2281-9.

41: Nistala K, Varsani H, Wittkowski H, Vogl T, Krol P, Shah V, et al. Myeloid related protein induces muscle derived inflammatory mediators in juvenile dermatomyositis. Arthritis Res Ther 2013;15:R131.

42: Fall N, Bove KE, Stringer K, Lovell DJ, Brunner HI, Weiss J, et al. Association between lack of angiogenic response in muscle tissue and high expression of angiostatic ELR-negative CXC chemokines in patients with juvenile dermatomyositis: possible link to vasculopathy. Arthritis Rheum 2005;52:3175-80.

FIGURE LEGENDS

Figure 1: **Outcome in the two groups identified in JDM** as assessed by (A) the percentage (%) of patients with ≥ 2 treatment lines, (B) the percentage of patients presenting persistent mild or severe cutaneous erythema (C) MMT and (D) CMAS scales over a 3-years follow-up. Group 1 (7/29) is highlighted in dark blue, group 2 (22/29) is highlighted in light blue. All

data are available for 100% of patients at onset, 6 months, and 1 year, for 50% of patients at 3-years follow-up.

Figure 2: **Comparison of biopsy tool score in the two groups identified in JDM**. Group 1 (severe disease, highlighted in dark blue) patients manifested a higher total score of the vascular, muscle fiber and the connective tissue domain (A). Items of the score tool significantly different between the two groups are summarized in (B) and illustrated in JDM deltoid muscle: (C) obvious capillary dropout, (CD31, immunoperoxydase), (D) perimysial and endomysial fibrosis (Masson's trichrome). Bars= 50µm. Indicated p values (* p< 0,05; **p<0,01 *** p< 0,001) are obtained using the Fisher's exact test for qualitative variables and the Mann-Whitney U test for quantitative variables. Variables were summarized using the median and interquartile range.

Figure 3: **Normal deltoid muscle capillarization**: correlation between capillary density (mm^2) (A) and capillary/fiber ratio (B) with age. Spearman's test was applied for correlation on deltoid muscle *vs* age.

Figure 4: **Morphometric analysis of capillary loss in the two groups identified in JDM:** capillary density (mm^2) and capillary/fiber ratio compared in the two groups of clinical severity taking into account the patient age (A, B) or only the observed values (C, D). Group 1 (severe disease) is highlighted in dark blue; group 2 is highlighted in light blue. Indicated p values (*p≤0,05, ***p≤0,001) were obtained using the Mann-Whitney U test for quantitative variables. Variables were summarized using the median and interquartile range.

TABLES

Table 1: Clinical and biological characteristics and comparison between JDM subgroups at the disease onset.

	Total (n=29)	Group 1 (n=7)	Group 2 (n=22)	P values
Gender, female, number (%)	20 (69)	4 (57)	16 (73)	0.642
Age at onset (months), median [IQR]	93 [72;129]	129 [82;134.5]	91 [72;113.5]	0.346
Time between symptoms onset and biopsy (months), median [IQR]	1 [0;3]	4 [0.5;6]	1 [0;2]	0.333
MMT* median [IQR]	61 [44;76.5]	50 [43.75;55.75]	66 [49.5;77.5]	0.144
CMAS† median [IQR]	34 [8;47.5]	8 [6;13.5]	40 [28;49]	**0.007**
CPK rate median [IQR]	1525 [50;4953.25]	5851 [2723;10500]	120.5 [50;2934.5]	**0.014**
skin involvement: n (%)				
Characteristic skin rash#	23 (79)	7 (100)	16 (73)	0.289
Gottron's papules	19 (66)	5 (71)	14 (64)	1
Telangiectasiae	16 (55)	4 (57)	12 (55)	1
Subcutaneous limb edema	7 (24)	4 (57)	3 (14)	**0.038**
Ulcerations	4 (14)	1 (14)	3 (14)	1
Visceral involvement: n (%)				
Interstitial lung disease	3 (10)	1 (14)	2 (9)	1
Cardiovascular involvement	0	0	0	
Gastrointestinal involvement	5 (17)	5 (71)	0	**<0.001**
Treatment used				
as first-line n (%) prednisone+MTX&	13 (45)	4 (57)	9 (41)	0,67
within 6 first months n (%) prednisose/MTX+ other line (≥2 lines)	12 (41)	7 (100)	5 (23)	**<0.001**

malar or facial erythema, V or shawl sign

*MMT, manual muscle testing , possible score 0-80

†CMAS, Childhood Myositis Assessment Score, possible score 0–52.

&MTX: Methotrexate

Indicated p values were obtained using the Fisher's exact test for qualitative variables and the Mann-Whitney U test for quantitative variables

Table 2: Baseline predictors of treatment response (as opposed to non response) in JDM. Results of the multivariate analysis obtained from the model considered as the best choice for predicting the therapeutic response. CMAS: Childhood Myositis Assessment Score, VAS: Histo-pathologists'overall score for severity, C/F: Capillary/fiber

	Non responders n=11	**Good responders** n=17
Initial CMAS <34	11/11 (100%)	2/17 (12%)
Gastrointestinal (GI) involvement	5/11 (41%)	0/17 (0%)
Endomysial Fibrosis (EF)	9/11 (82%)	6/17 (35%)
Initial CMAS ≥34	0/11 (0%)	**15/17 (88%)**
Initial CMAS <34 without GI involvement and without EF	0/11 (0%)	**2/17 (12%)**
Intitial CMAS <34 with GI involvement or EF	**11/11 (100%)**	0/17 (0%)

FIGURES

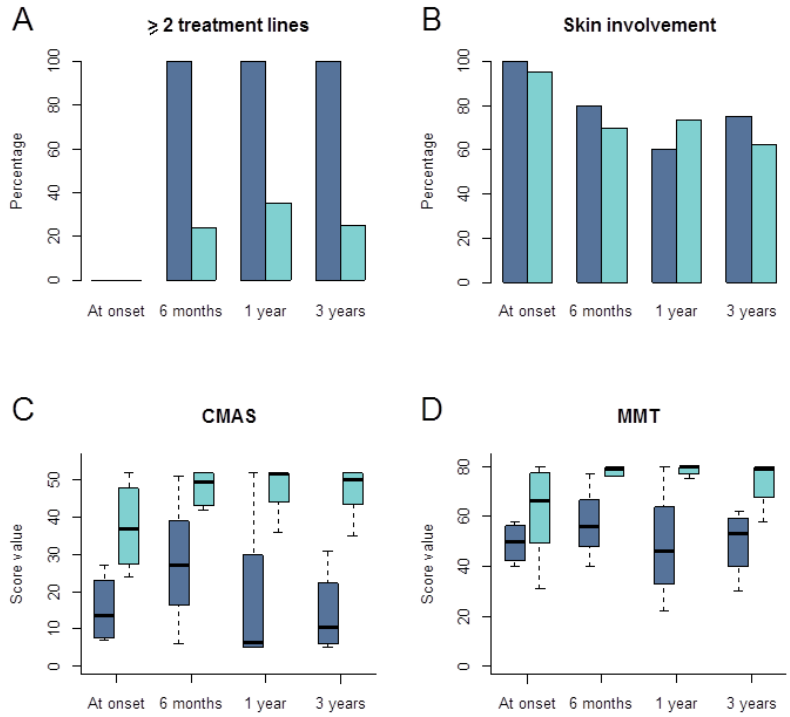

Figure 1: **Outcome in the two groups identified in JDM** as assessed by (A) the percentage (%) of patients with ≥ 2 treatment lines, (B) the percentage of patients presenting persistent mild or severe cutaneous erythema (C) MMT and (D) CMAS scales over a 3-years follow-up. Group 1 (7/29) is highlighted in dark blue, group 2 (22/29) is highlighted in light blue. All data are available for 100% of patients at onset, 6 months, and 1 year, for 50% of patients at 3-years follow-up.

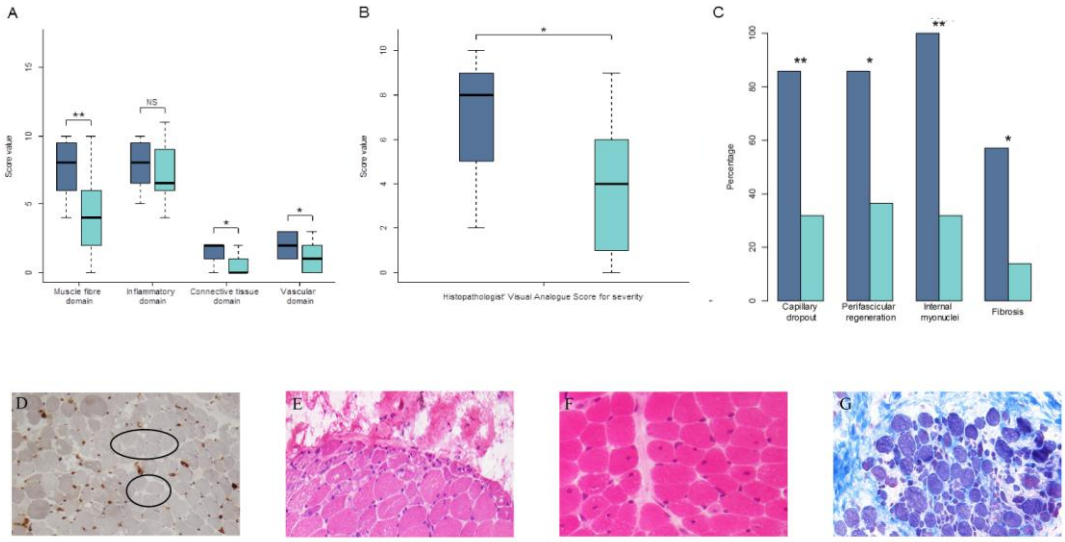

Figure 2: **Comparison of biopsy tool score in the two groups identified in JDM**. Group 1 (severe disease) patients manifested a higher total score of the vascular, muscle fiber and the connective tissue domain. In contrast, scoring of inflammatory domain was similar in the two groups (A). The histo-pathologists' overall severity score (VAS) was significantly higher for group 1 (B). Items of the score tool significantly different between the two groups are summarized in (C) and illustrated in JDM deltoid muscle: (D) "obvious capillary dropout, with circles indicating vessel loss (CD31 immunoperoxidase, x20), (E) "perifascicular necrosis/regeneration" (HE x20), (F) "fibers with internal myonuclei" (HE x20) and (G) "fibrosis" (Masson's trichrome x20). Group 1 is highlighted in dark blue, group 2 is highlighted in light blue. Indicated p values (* p< 0,05; **p<0,01 *** p< 0,001) are obtained using the Fisher's exact test for qualitative variables and the Mann-Whitney U test for quantitative variables. Variables were summarized using the median and interquartile range.

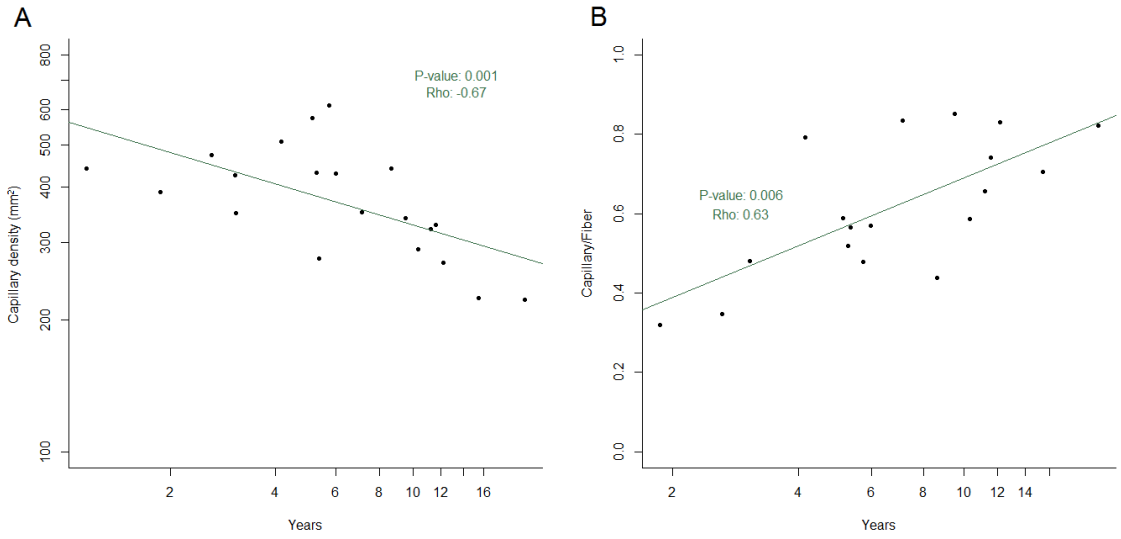

Figure 3: **Normal deltoid muscle capillarization**: correlation between capillary density (mm²) (A) and capillary/fiber ratio (B) with age. Spearman's test was applied for correlation on deltoid muscle *vs* age.

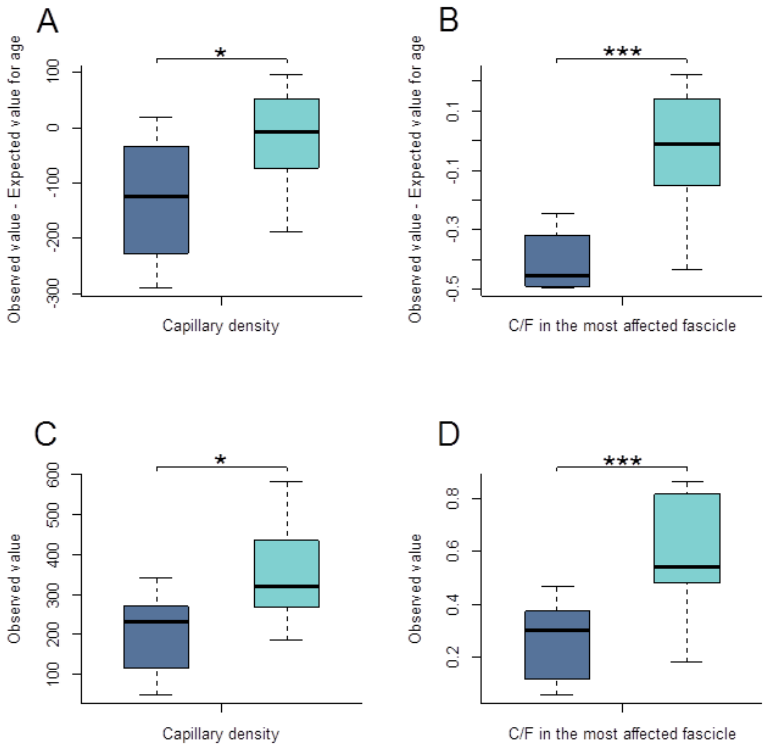

Figure 4: **Morphometric analysis of capillary loss in the two groups identified in JDM:** capillary density (mm^2) and capillary/fiber ratio compared in the two groups of clinical severity taking into account the patient age (A, B) or only the observed values (C, D). Group 1 (severe disease) is highlighted in dark blue; group 2 is highlighted in light blue. Indicated p values (*p≤0,05, ***p≤0,001) were obtained using the Mann-Whitney U test for quantitative variables. Variables were summarized using the median and interquartile range.

Article 2: Myogenic precursor cells differentially participate to vascular remodeling in Juvenile Dermatomyositis and Duchenne Muscular Dystrophy.

Proper activation of myogenesis and angiogenesis is critical for the recovery of skeletal mucle from injury. Recents studies have demonstrated that the close anatomic proximity of muscle progenitor cell (MPCs) and endothelial cell (ECs) and their molecular interactions via various growth factors play an important role in the skeletal muscle's capacities for tissue repair. Our objective was to delineate at the cellular and molecular level the endothelial and satellite cells crosstalk during muscle regeneration in human myopathies using two paradigmatic contexts of regenerating muscle: Juvenile Dermatomyositis (JDM) and Duchenne Muscular Dystrophy (DMD). The main results were: *In vitro* myogenesis/angiogenesis studies demonstrated that MPCs possessed angiogenic properties depending on the pathological environment. In DMD, MPCs promoted the development of establishment of an anarchic, although strong, EC stimulation, leading to the formation of weakly functional vessels. In JDM, MPCs enhanced the vessel reconstruction *via* the secretion of proangiogenic factors. These results were supported by the transcriptomic analysis consistent with a central vasculopathy in JDM with a strong and specific response to an inflammatory environment. On the contrary, DMD cells presented an unbalanced homeostasis with deregulation of several processes including muscle and vessel development with attempts to recover neuromuscular system by MPCs.

Myogenic precursor cells differentially participate to vascular remodeling in Juvenile Dermatomyositis and Duchenne Muscular Dystrophy.

Cyril Gitiaux[a,b,c,d], Claire Latroche[c,d], Stéphane Germain[e], Jamel Chelly[c], Isabelle Desguerre[b,c,d,f], Bénédicte Chazaud[c,d]

Authors' affiliations

[a]Department of Clinical Neurophysiology, Hôpital Necker Enfants Malades, Assistance Publique-Hôpitaux de Paris, Paris, France.

[b]AP-HP, Reference Center for neuromuscular diseases "Garches-Necker-Mondor-Hendaye", France.

[c]Institut Cochin, INSERM U1016, Paris, France.

[c]CNRS UMR 8104, Paris, France.

[d]Paris Descartes University, Paris, France.
[e]UMRS Inserm U1050 CNRS 7241, Collège de France, Center for Interdisciplinary Research in Biology (CIRB), Paris, France.
[f]Department of Pediatric Neurology, Hôpital Necker Enfants Malades, Assistance Publique-Hôpitaux de Paris, Paris, France.

Corresponding Author: Dr Cyril Gitiaux. Hôpital Necker-Enfants Malades, 149 rue de Sèvres, 75015 Paris, France. Tel : +33 1 42 19 26 95, Fax : +33 1 42 19 26 92. Email: cyril.gitiaux@nck.aphp.fr
Conflict of Interest Statement: None of the authors has any conflict of interest to disclose.

ABSTRACT:

Skeletal muscle is highly vascularized. Beyond oxygen and nutriment supply, new functions for vessels have been recently identified, via the interactions that vessel cells establish with muscle progenitor cells. These latter closely interact with endothelial cells for their expansion and their differentiation, while periendothelial cells are involved in muscle cell self-renewal and return to quiescence. Thus, vessels play a central role in the tissue remodeling after an injury while the mechanisms are poorly understood. We investigated myogenic/endothelial cell (MPCs/ECs) interactions in two paradigmatic contexts of regenerating muscle in the child: Juvenile Dermatomyositis (JDM), which is characterized by a transient loss of capillaries, and Duchenne Muscular Dystrophy (DMD) which is associated with an increase in vessel density. We showed *in vitro* specific interactions between myoblasts isolated from muscle of JDM and DMD patients and endothelial cells. In *vitro* myogenesis/angiogenesis studies demonstrated that MPCs exhibited various angiogenic properties depending on the pathological environment. In DMD, MPCs promoted the development of an anarchic, although strong, ECs stimulation, leading to the formation of weakly functional vessels. DMD cells presented an unbalanced homeostasis with nonspecific deregulation of several processes involved in muscle and vessel development. On the contrary, in JDM, MPCs enhanced the vessel reconstruction to efficiently restore the vessel function via the expression of a set of specific angiogenic effectors. MPCs exhibit a strong specific type I IFNs signature and ECs a dysregulation of their angiogenic capacities suggesting a drastic reprogrammation of these cells in response to an inflammatory environment during JDM.

INTRODUCTION

Human skeletal muscle is highly vascularized. The importance of vessels in providing oxygen and nutriments has been known for a long time, illustrated by their crucial role during development (1) and by the highly adaptative behavior of microvessels depending on the muscle demand in physiological settings (2). More recent studies have shown that vessels, and particularly microvessels, fully participate to skeletal muscle homeostasis through the development of specific interactions with neighboring cells including myofibers and myogenic precursor cells (MPCs) derived from satellite cells (3,4). Moreover, angiogenesis and myogenesis take place concomitantly after an ischemia (5) and angiogenesis is a prerequisite for good muscle tissue repair (6,7).

Myogenesis is supported by the activation of satellite cells, the main muscle stem cells, which proliferate as MPCs, migrate, then differentiate into myocytes that fuse to form new myofibers and finally restore the muscle *ad integrum* (8). In normal adult muscle, satellite cells and MPCs are very close to capillaries, whatever their cycling status. The number of satellite cells is correlated with the capillarization of the myofibers (4). This close proximity suggests privileged interactions between vessel cells and myogenic cells. Indeed, MPCs closely interact with endothelial cells (ECs) for their growth and differentiation while their interactions with periECs are associated with their return into quiescence (3,9).

However, although ECs play a main role during muscle repair by close cooperation with MPCs to promote both angiogenesis and myogenesis in muscle, this role remains poorly understood, particularly in a human pathological context where muscle tissue remodeling is observed (10,11). To investigate this issue, we took advantage of two paradigmatic situations of muscle injury in the child: Juvenile Dermatomyositis (JDM), the most common acute inflammatory myopathy in childhood and Duchenne Muscular Dystrophy (DMD) the most frequent genetic neuromuscular disorder in school age children. Although these two muscular

disorders share similar events of necrosis-inflammation, they differ regarding vessels. JDM combines acute inflammation with type1 IFNs inducible genes upregulation, myofiber alterations and specific microvascular changes. These changes include capillary obliteration and arterial lumen occlusion supposed to cause the capillary necrosis which results in focal capillary loss, perivascular inflammation, and muscle ischemia (12-15). Approximately 70% of the patients are responders to immunomodulating treatments and exhibit a progressive recovery of a normal muscle function (16). This recovery could occur as a result of a strong angiogenic response to restore a normal muscle capillary bed following a transient capillary loss (17). In DMD, the lack of the protein dystrophin which serves as a link between cytoskeletal actin and extracellular matrix leads to a progressive exhaustion of the regenerating capacities (18). Dystrophin expression is not restricted to muscle cells and is also present in endothelial and smooth muscle cells. The physiological major role of dystrophin in the vascular endothelium is demonstrated by the fact that skeletal muscle of *mdx* mice (the murine model of DMD) and of children with DMD displays vascular abnormalities through alterations of NO synthase expression causing excessive sympathetic vasoconstriction, focal ischemic muscle damage during contraction and poor endurance exercise performance (19-23). Modification of the microvascular bed including an increase of the capillarity density and of the capillary-to-fiber distance has been observed in Human (24,25), confirmed in the old golden retriever muscular dystrophy *(GRMD)* dog model (26), and has been proposed as a compensatory event for a probable ischemic state. This vessel plasticity to compensate the muscle degeneration is not efficient as the muscle progressively alters with age in correlation with endomysial fibrosis.

To address the role of vessel plasticity in these two pathologies, we explored the interactions between MPCs issued from pathological muscle and ECs. Functionally, various parameters of angiogenesis were analyzed. Molecular investigation included the analysis of the angiogenic

signature of JDM-derived and DMD-derived MPCs, as well as the transcriptome analysis of ECs and MPCs isolated from patient muscle.

MATERIAL AND METHODS

Patients. Duchenne Muscular Dystrophy patients (n=22, median age: 5.3y, range 3-8) showed primary dystrophin deficiency by both western blotting and immunohistochemistry confirmed by mutations in the dystrophin gene. All patients presented onset and progression of clinical symptoms and high levels of Creatine Kinase typical for DMD. Juvenile Dermatomyositis patients (n=12, median age: 7.7y, range 3-14) meet the diagnosis of JDM according to conventional clinico-pathological criteria (27). DMD and JDM biopsies were obtained at time of diagnosis, from deltoid muscle. Control muscle biopsies were obtained from paravertebral muscle of patients which underwent spinal arthrodesis (n=21, median age: 14, 4-16). All biopsies were obtained under institutionally approved protocol and parents or legal representatives gave their written informed consent for participation of the children to the study (protocol registered at the Ministère de la Recherche and Cochin Hospital Cell Bank, Paris, agreement n° DC-2009-944).

Human MPC culture. Pediatric human MPCs were isolated from normal, JDM and DMD pediatric skeletal muscle sample. Cells were obtained and cultured as previously described in HAMF12 medium (Gibco, Life Technologies, Grand Island, NY) containing 15% fetal bovine serum (FBS) and were sorted with anti-CD56 magnetic beads (Miltenyi Biotec, Bergisch Gladbach, Germany) according to the manufacturer instructions (3,4,28). The purity of the cells was assessed for CD56 expression (555518 BD Pharmingen, Franklin Lakes, NJ) by flow cytometry (FC500 Beckman Coulter cytometer, Villepinte, France). All cell cultures were performed at 37°C and 5% CO2 unless otherwise indicated.

HDMEC culture. Human dermal microvascular endothelial cells (HDMECs) isolated from juvenile foreskin were purchased from Promocell (Heidelberg, Germany). For all experiments (except for migration assay), cells were seeded onto collagen-I-coated (Rat tail collagen, Invitrogen, dilution 1:100) flasks and cultured in Endothelial Cell Basal Medium (basal ECGMV2) supplemented with endothelial cell growth supplement (Supplemental mix), and antibiotics (MycoZap Plus-PR, Lonza, Walkersville, USA, dilution 1:500) (growth ECGMV2). Medium and all supplements except antibiotics were purchased from Promocell (Heidelberg, Germany). The cells were used until the 6^{th} passage (P1-P6).

Cell migration assay. Migration was performed using two chambers Ibidi inserts (Ibidi GmbH, Martinsried, Germany). One chamber was filled with 4400 MPCs in Ham F12 growth medium. The other chamber was seeded with 4400 HDMECs in growth ECGMV2. Cells were expanded for 3 days. Then, the silicone walls of the device were removed and cells were cultured in advanced RPMI medium containing 0.5% FBS. The gap between the two cell types was imaged at time 0 and 24 h. The distance covered by each cell was measured using Image J software (http://imagej.nih.gov/ij/).

HDMEC proliferation. HDMECs were seeded in 12-well plates onto collagen-coated glass coverslips at 3500 cells/cm^2 and cultured for 72 h with ECGMV2. Cells were incubated with or without MPC-conditioned medium for further 36 h. Conditioned media were obtained by incubating MPCs at 7000 cells/cm^2 for 24 h in advanced RPMI 1640 medium (Gibco, Life Technologies, Grand Island, NY) containing 0.5% FBS. HDMEC were labeled with anti-Ki67 1/200 (CP249; Biocare Medical, Pike Lane Concord, CA) primary antibodies revealed by Cy3-conjugated secondary antibodies. Approximately 10 pictures (x10 magnification) were taken from each experiment, representing about 1000-3000 cells per condition per experiment.

Fibrin gel bead angiogenesis assay. Three-dimensional fibrin gel assays were carried out as previously described (29). HDMECs were expended in growth ECGMV2, then they were seeded with gelatin-coated Cytodex 3 microcarriers (Amersham Pharmacia Biotech, Piscataway, NJ) at a concentration of 400 HDMECs per bead in 2 ml of ECGMV2 free medium (preparation was gently shaken every 15 min for 2 h, then every 30 min for 2 h). Beads with cells were transferred into a 75 cm^2 tissue culture flask and left for 24 h in 10 ml of growth ECGMV2. The following day, fibrin gels were prepared as bovine fibrinogen (2.5 mg/ml; Sigma-Aldrich, St. Louis, MO) dissolved in ECGMV2, with aprotinin (0.002 mg/ml; Sigma-Aldrich). Beads with cells were resuspended and 150 µl of fibrinogen/bead solution was added to 10 µl of 10 U/ml thrombin solution (Sigma-Aldrich) in one well of 8-well tissue culture plate (Ibidi GmbH). Fibrinogen/bead solution was allowed to clot for 5 min at room temperature and then at 37°C for 10 min. MPCs were expended in HAM F12 medium for two days before seeding on top of the gel (20000 cells/ well) in 150 µl of EndoGro medium (SCME-BM+Mix SCME-002; Millipore). The EndoGro medium was changed every other day. Bead assays were monitored for 6 days. Pictures of beads were captured on a Zeiss microscope with a 10X objective and analyzed with ImageJ software (http://imagej.nih.gov/ij/). Sprout lengths, sprout/bead ratio and % of lumenized sprouts were measured on at least 25 beads for each condition.

Angiogenesis array. MPCs obtained from normal, JDM and DMD patients, as well as from normal MPCs that have received various treatments were analyzed to determine their angiogenic signature. Normal MPCs were treated for 24 h with 20 ng/ml IFN-β (Peprotech, Neuilly sur Seine, France). To mimic hypoxic/ischemic environment, MPCs were incubated for 24 h in either low glucose DMEM or DMEM containing no glucose (Gibco, Life Technologies, Grand Island, NY), in hypoxic GenBag microaer (3% oxygen) chambers (Biomerieux SA, Marcy l'étoile, France). Cells were collected and proteins were extracted.

Protein concentrations were determined by the BCA assay. Equal amounts of MPC protein samples were processed on membranes printed with 43 antibodies against proteins related to angiogenesis (Human angiogenesis array C1000, Ray Biotech, Norcross, USA) according to the manufacturer instructions. Pictures were taken with a ChemiDoc MP Biorad and the pixel density was analyzed for each spot with ImageJ software (http://imagej.nih.gov/ij/). Analysis and normalization was performed according to the manufacturer instructions.

Transcriptomic analysis of MPCs and ECs. Fresh muscle biopsies (n=3 for each condition, ie JDM, DMD and normal muscle) weighing 100-900 mg, were finely minced, then digested for 30 min at 37°C under continuous agitation in 10 ml solution of 1 mg/ml collagenase B (Roche Diagnostics GmbH) and 2,4 U/ml dispase 2 (Roche Diagnostics GmbH) per gram of tissue. The digested tissue was pelleted and resuspended in growth ECGMV2 medium and then passed through 100 µm and 70 µm strainers to obtain a single cell suspension. Cells were collected in PBS containing 5% SVF and were incubated with a mouse anti-human CD31-FITC (eBioscience) and a mouse anti-human CD56-APC (BD Biosciences) for 45 min. Cells were also labelled with 1 µM propidium iodide (Sigma-Aldrich, St. Louis, MO) to exclude dead cells from the analysis. Cells were sorted using a FACS Aria III (Becton Dickinson) and immediately treated with Trizol reagent (Life Technologies, Inc.) to extract RNA. After validation of the RNA quality with Bioanalyzer 2100 (using Agilent RNA6000 nano chip kit), 125 pg of total RNA was reverse transcribed following the Ovation Pico WTA System V2 (Nugen). Briefly, the resulting double strand cDNA was used for amplification based on SPIA technology. After purification according to Nugen protocol, 3 µg of Sens Target DNA were fragmented and biotin labelled using Encore Biotin Module kit (Nugen). After control of fragmentation using Bioanalyzer 2100, cDNA was then hybridized to GeneChip® Human Gene 2.0 ST (Affymetrix) at 45°C for 17 h. After hybridization, chips were washed on the fluidic station FS450 following specific protocols (Affymetrix) and scanned using the

GCS3000 7G. The scanned images were then analyzed with Expression Console software (Affymetrix) to obtain raw data (cel files) and metrics for Quality Controls. Raw data were normalized using the Robust Multichip Algorithm (RMA) in Bioconductor R (30). Then all quality controls and statistics were performed using Partek GS ® (version 6.6 Copyright © 2012 Partek Inc., St. Louis, MO, USA). A hierarchical clustering (Pearson's dissimilarity and average linkage) and Principal Composant Analysis as unsupervised exploratory data analysis were first made. This multivariate technical aimed at controlling data from experimental bias or outlier samples. To find differentially expressed genes, a two way with interaction analysis of variance (ANOVA) was applied for each gene as well as pair wise Tukey's post hoc tests between groups (CD31 vs. CD56 and Normal vs. DMD vs JDM). Then, p-values and fold changes were used to filter and select differentially expressed genes. The functional analysis (interactions, pathways and functional enrichment analysis) were carried out through the use of IPA (Ingenuity® Systems, USA, www.ingenuity.com), Pathway Studio (Ariadne Genomics, http://www.elsevier.com/online-tools/pathway-studio) and DAVID (http://david.abcc.ncifcrf.gov/home.jsp) (31). All data obtained by microarray analysis have been submitted on GEO NCBI site.

Statistics. All experiments were performed at least three times using independent MPC primary cultures. Data are expressed as mean ±SEM. The data were analyzed by t test, non parametric Mann–Whitney u test and ANOVA. *p* value less than 0.05 was considered as statistically significant (GraphPad Prism 5.0).

RESULTS

JDM and DMD-derived MPCs attract ECs

EC/MPC cell migration toward each other was analyzed in a double chamber device (Fig.1A). Controls included migration of the cells towards the same cell type (e.g. ECs towards ECs and

MPCs towards MPCs). MPCs issued from a normal muscle neither showed significant chemotaxis towards ECs nor attracted ECs (Fig.1B). JDM-derived MPCs strongly attracted ECs (+90% $p<0.05$) while they did not significantly migrate towards ECs (Fig. 1C). On the opposite, DMD-derived MPCs showed strong interactions with ECs since ECs migrated towards DMD-derived MPCs (+137%, $p<0.01$) and DMD-derived MPCs also migrated towards ECs (+47%, $p<0.05$) (Fig.1D). These results show specific EC migration by MPCs-derived chemoattractants in JDM while in DMD both ECs and MPCs were bidirectionally attracted.

DMD and JDM-derived MPCs induce EC proliferation

EC proliferation was assessed by Ki67 immunostaining (Fig.2A) after incubation with MPC-conditioned medium. MPCs derived from normal skeletal muscle did not induce EC proliferation (Fig.2B). On the contrary, JDM-derived MPCs significantly stimulated EC proliferation (+27%, $p<0.05$) (Fig.2C), as did also DMD-derived MPCs (+63%, $p<0.01$) (Fig.2D). These results indicate that MPCs in diseased muscle delivered specific effectors that induced EC proliferation.

JDM and DMD-derived MPCs display proangiogenic activity but only JDM-derived MPCs support the formation of functional vessel-like structures

To investigate and to compare the potential role of JDM- and DMD-derived MPCs to promote vessel formation, a three-dimensional angiogenic model was used, in which ECs sprout in a fibrin gel (29). MPCs were layered on top of the gel allowing the evaluation of cell angiogenic potential by providing soluble factors. This model closely recapitulates the key early stages of angiogenesis. Importantly, the formed vessels display patent intercellular lumens surrounded by polarized ECs indicative of maturation of the structure resembling functional vessels (Fig.3A). As compared with MPCs derived from normal muscle (Ctl), JDM- and DMD-derived MPCs significantly increased sprout length formed from the surface

of the beads at day 6 (+28% p<0,05, +48% p<0,05, respectively) (Fig.3B). While the number of sprouts per bead did not differ (Fig.3C), the % of lumenized sprouts differed in the two pathologies. JDM-derived MPCs induced much more vessel sprouts with lumen as compared with control (+73% p=0,06). Inversely, sprouts induced by DMD-derived MPCs were poorly lumenized, and significantly less than those induced by control MPCs (-27% p<0.05) (Fig.3D). These results show that JDM-derived MPCs displayed a high proangiogenic activity that seemed to be efficient since vessel-like structures underwent lumenization. On the contrary, DMD-derived MPCs secreted factors enhancing EC sprouting, but with very low maturation/lumenization efficiency. These functional results indicate strong differences between MPCs issued from JDM and DMD muscle and suggest a differential secretion of angiogenic factors.

Angiogenic signature of normal, JDM and DMD-derived MCPs

To define directly the angiogenic signature of JMD and DMD-derived MPCs, the relative levels of 43 angiogenesis-related proteins were assessed using an antibody array (Fig.4A). Statistical analysis showed that JDM-derived MPCs differentially expressed these proteins as compared with control MPCs (p<0.01) and with DMD-derived MPCs (p<0.001) while these later were not significantly different from the control MPCs (Fig.4B and C). Among 30 proteins upregulated in JDM-derived MPCs, 56% were also upregulated in DMD (although at a much lesser extent) while 43% were specifically upregulated in JDM-derived MPCs. Particularly, JDM-derived MPCs exhibit drastic increase in IL-6 and type 1 IFNs inducible cytokines levels including monocyte chemo attractant protein-1(MCP-1/CCL2) compared to control and DMD-derived MPCs (Fig 4B). These results suggest that muscle remodeling is associated with an angiogenic response in both pathologies, but with a much larger magnitude in JDM as compared with DMD.

Since DM has been associated with systemic and muscle production of IFN-β (33) as well as ischemic processes (34), we attempted to reproduce these conditions and analyzed the specific MPC response (Fig.5). Upon IFN-β treatment, the angiogenic signature of MPCs partially mimicked that of JDM-derived MPCs (Fig.5B *vs* A). Indeed, 85% of the upregulated proteins in IFN treated cells were also upregulated in JDM-derived MPCs *vs.* 50% in DMD-derived MPCs. Particularly, MCP-1/CCL2 chemokine was strongly upregulated as it was for JDM-derived MPCs.

Culturing MPCs in hypoxic conditions as well as in glucose-free medium under hypoxia to mimic ischemia also partially phenocopied the JDM-MPC derived signature, although to a lesser extent (Fig.5C and D). Among the upregulated proteins in these conditions, 59 and 65% were found to be also upregulated in JDM-derived MPCs for hypoxia and ischemia conditions, respectively, *vs.* 26 and 27% upregulated in DMD-derived MPCs. Particularly, the strong upregulation of IL-8, PLGF, EGF, leptin, THPO and CC-chemokines (MCP3, MCP4) was observed in both conditions ($p<0.05$ and $p<0.01$) for hypoxia and ischemia conditions, respectively, as it was for JDM-derived MPCs ($p<0.05$).

Transcriptomic analysis of MPCs and ECs isolated from human normal, JDM and DMD muscles

Whole variation in gene expression differed according to the pathology. Table 1 shows that in JDM patients, most gene variations occurred in ECs (+71% as compared with MPCs) (Table 1A) while, inversely, in DMD patients, most gene variations occurred in MPCs (+128% as compared with ECs, Table 1B), in keeping with a fundamental role of vessel injury in JDM.

Regarding ECs, a majority of genes were downregulated in both pathologies. Gene ontology (GO) analysis showed that similar families of genes were downregulated including cell migration, vessel development, intracellular signaling and intracellular trafficking (Tables 2C

and D and G and H), suggesting strong remodeling of the vessels in both pathologies. However, the number of upregulated genes in JDM-derived ECs was much higher than in DMD (Table 1) and were specifically enriched for genes associated with inflammation, metabolism, transcription and cell cycle (Table 2B *vs* 2F). Among the 30 genes the most upregulated in JDM-derived ECs, 25% were genes inducible by type1 IFNs and 10% belonged to the S100/Myeloid related protein (MRP) family genes (*MRP8/14* also known as *S100A8/A9*) known to induce a thrombogenic and inflammatory responses in endothelial cells (Table 2A) (35). Very interestingly, the most upregulated genes in JDM-derived ECs are the IFN inducible *CXCL10/IP10* (fold> x100) *and CXCL11/I-TAC* (fold x40) known to inhibit angiogenesis in human (36,37). Comparison of genes differentially expressed by ECs between the two pathologies confirmed a specific inflammatory signature of JDM-derived ECs (Table 2I).

Concerning MPCs, the number of upregulated genes was much higher in DMD than in JDM (Table 1). In DMD, upregulated genes were consistent with unbalanced muscle homeostasis (neurological system process, ion homeostasis, intracellular signaling, notably G-protein signaling). Moreover a lot of upregulated genes were enriched for numerous GO categories linked to cell interaction with the environment (Table 3E and F). In JDM, upregulated genes were specifically enriched with GO categories of inflammation, metabolism, cell proliferation (Table 3B), indicating strong differences between MPCs in the two pathologies. Inversely, in both pathologies, downregulated genes were enriched for similar GO categories (including skeletal muscle development, morphogenesis…) (Table 3D, 3H) indicative of muscle remodeling. When analyzing the 30 most upregulated genes in JDM-derived MPCs a strong IFN signature was observed with at least 15/30 of the most upregulated genes being IFN inducible (Table 3A). Particularly upregulation of *IF27, ISG15, IFI44L* (fold change>X30) described as specific for an "IFN signature" was identified (38). This was not observed in

DMD-derived MPCs (Table 3E). Interestingly, when comparing the expression of genes of MPCs in the two pathologies, JDM-derived MPCs were characterized by an upregulation of genes associated with inflammation including a strong IFN signature, large metabolic (protein and RNA) regulation, and morphogenesis including vessel development and cell proliferation (Table 3I).

Altogether, these data are consistent with a central primary vasculopathy in JDM with a strong and specific response to an inflammatory environment. Both JDM-derived MPCs and ECs exhibited a preponderant, however not similar IFN response. JDM-derived MPCs presented a so called "IFN signature" and ECs upregulated genes involved in the regulation of angiogenesis likely also mediated by IFN. Particularly, the strong upregulation of genes associated with inhibition of angiogenesis or ECs inflammatory response is relevant for JDM pathophysiology. On the contrary, DMD cells presented an unbalanced homeostasis with deregulation of several processes including muscle and vessel development with attempts to recover neuromuscular homeostasis by MPCs.

DISCUSSION

Although highly vascularized, the importance of vessel remodeling and plasticity has been poorly investigated in both normal muscle regeneration and myopathic context. While it is known at the tissue level that myogenesis and angiogenesis take place concomitantly in regenerating muscle (39), our previous investigations showed *in vitro* that ECs and MPCs specifically and bidirectionally interact to promote both myogenesis and angiogenesis (4). The aim of the present study was to investigate the interactions between ECs and MPCs isolated from human myopathies, by analyzing two pathologic conditions that could be considered as paradigmatic situations of vessel plasticity. Our results show that MPCs act

differently on ECs in JDM and DMD, suggesting that vessel plasticity takes part of tissue remodeling in these myopathies.

Concerning DMD, we demonstrated *in vitro* that DMD-derived MPCs and ECs were strongly attracted towards each other. Furthermore, MPCs induced EC proliferation, as well as the formation of vessel-like structures. However, this apparent strong proangiogenic effect of DMD-derived MPCs is associated with a failure to finally support the lumen formation of these neo-vessels, suggesting a defect in the maturation of the vessels, rendering them not functional. In recent years, interest in DMD vascular network has increased with primary focus on vasculature-related therapeutic strategies (40). The evidence of vascular involvement in DMD is based on the observation of "grouped necrotic fibers" in muscles of DMD patients, suggesting local failure in capillary blood supply and muscle ischemic necrosis (41). Furthermore, the dystrophin deficiency in vascular smooth muscle cells (42) and the absence of nitric oxide synthase (NOS) from the sarcolemma have indicated that DMD muscle is subjected to impaired blood flow (20). Recent studies carried out in DMD patients confronted blood vessel alteration with tissue fibrosis. They suggested that endomysial fibrosis causes an increase in capillary-to-myofiber distance, which impairs both muscle fiber mechanical function and gas exchanges (25). Collectively, these results suggest complex interactions between ECs and MPCs in DMD, which is sustained by the molecular data presented here, showing a nonspecific dysregulation (apart from muscle direct associated defects) but a plethora of dysregulation of genes involved in MPC interaction with their environment, indicative of a strongly unbalanced homeostasis in this disease and relevant for a progressive exhaustion of the muscle function, non-controlled by vessels.

JDM is characterized by a transient loss of vessels, followed by recovery and return to muscle homeostasis in most of the patients. *In vitro* JDM-derived MPCs displayed a strong proangiogenic activity on ECs: they attracted ECs, stimulated EC proliferation and favored

the formation of vessel-like structures with lumen, indicative of maturation. These effects were due to the secretion of specific angiogenic soluble factors by JDM-derived MPCs, likely among the one detected with the antibody array. Indeed, protein analysis indicated a strong pro-angiogenic signature of MPCs including drastic increase in MCP-1/CCL2 (+225%) and IL-6 (+800%) levels. The role of MCP-1 and IL-6 in promoting angiogenesis is well established particularly in the cancer research field (43).

JDM myopathology combines inflammation, myofiber alterations and microvascular changes. Abnormal capillary morphology and capillary loss is an early manifestation of DM, often seen prior to inflammatory infiltrates (15). Capillary obliteration and arterial lumen occlusion are supposed to cause the swelling of ECs, capillary necrosis which results in focal capillary drop out, perivascular inflammation, and muscle ischemia (13,34). Despite increasing attention paid to microcirculatory changes, the pathophysiological mechanism of capillary depletion in DM remains uncertain (44). The transcriptomic analysis of ECs and MPCs isolated from JDM muscle fitted with a central role of the vessel pathology and a direct involvement of MPCs on vessel remodeling through a strong and specific inflammatory response to finally restore the vascular bed and thus the muscle function. We showed that ECs display an anti-angiogenic, and apoptotic response. Indeed, *CXCL10/IP10*, *S100A8/MRP8*, *S100A9*/*MRP14* are strongly upregulated and genes involved in vessels development are downregulated in JDM-derived ECs. Very recently, CXCL10/IP10 and MRP proteins were identified as novel markers of active JDM (45,46). IFN-inducible CXCL10/IP10 protein is a member of the CXC chemokine family and binds to the ubiquitous CXCR3 chemokine receptor. CXCL10/IP10 can limit new vessel growth by inhibiting EC migration, and can induce involution of new vessels by triggering EC death (36,37). Furthermore, the influence of unbalanced MRP8/14 (known as endogenous Toll-like receptor 4 agonist) production by activated ECs of the microvascular circulation in JDM could confer thrombogenic and apoptotic properties to ECs (47).

Altogether our results strongly suggest a vascular injury via an autocrine secretion of anti-angiogenic factors and a further enhancement of the inflammatory response. Recent peripheral blood and whole muscle transcriptomic studies have identified that type1 IFNs inducible genes contribute to JDM disease activity suggesting a mechanism of myofiber and capillary injury driven by type 1 IFNs (48). Detection of IFN stimulated 15 (ISG-15) protein, an ubiquitin-like modifier which binds to various proteins, in the regions of DM pathologic activity such as perifascicular myofibers and capillaries, supports the idea of a related IFN myo-angio-toxicity (49). However, it was demonstrated recently that human ISG15 is a key negative regulator of IFN-α/β immunity, thereby preventing auto-inflammatory consequences of uncontrolled IFN-α/β amplification (50) and that ISG15 silencing does not reverse type1-IFN mediated toxicity, providing evidence against ISG15 being a major factor mediating the myotoxic effects of type1 IFNs (51). We showed here that JDM-derived MPCs exhibit a specific IFN signature including ISG15 upregulation confirming its main role in JDM pathophysiology.

Whatever the sequence of pathogenic events, we demonstrate that the vessel pathology is fundamental in JDM. MPCs, through an inflammatory and immune response including a striking type1 IFNs signature, orchestrate an angiogenic response by the secretion of angiogenic factors, thus directly participate in the neoangiogenesis process. The IFN-related changes alone cannot easily explain the characteristic vascular and muscle fiber pathology in DM and an additional role of ischemia-reperfusion process as a primary or auxiliary pathogenic event has been also proposed (44). By our approach allowing the delineation of specific role of MPCs isolated from JDM muscle, we showed a specific cytokine secretion by MPCs including IFN inducible proteins such as MCP-1 or others cytokines including IL-6. IFN-β treatment as well as hypoxia/ischemia preconditioning of normal MPCs partially mimicked the angiogenic JDM signature and suggested a combination of the two mechanisms

in the pathophysiology of JDM. Particularly, we showed that IFN-β treatment of normal MPCs significantly induced CC-chemokines secretion including MCP-1. Myoblasts are known to produce MCP-1 and IL-6 (52) likely via a MRP8/14 (S100A8/S100A9)-dependent pathway (46). As we showed that this pathway was strongly upregulated in ECs, it could be suggested that MRP8/14 may trigger the secretion of proangiogenic cytokines by MPCs including type1 IFNs regulated chemokines and IL-6. The coordinated dysregulation of type1-IFNs signaling and IL-6 production may further promote the neoangiogenesis and sustain the inflammatory response (53).

In conclusion, our data reveal different mechanisms underlying vessel remodeling using two paradigmatic models of human myopathies. In DMD, our functional data suggest the establishment of an anarchic, although strong, EC stimulation, leading to the formation of nonfunctional vessels. Molecular analysis in these primarily myofiber disease suggests that EC dysfunction is a consequence of the attempts of MPCs to rebuild the muscle main function, i.e. contraction, through the expression of genes involved in neuromuscular and ion homeostasis. In JDM, MPCs fully participate in vessel reconstruction, through response to inflammatory signal including type1-IFN signaling, leading to the expression of a specific MPC IFN signature, triggering extensive gene reprogrammation in ECs, finally favorable to angiogenesis.

REFERENCES

1: Tozer S, Bonnin MA, Relaix F, Di Savino S, Garcia-Villalba P, Coumailleau P, et al. Involvement of vessels and PDGFB in muscle splitting during chick limb development. Development 2007;134:2579–91.

2: Egginton, S. Physiological factors influencing capillary growth: Physiological angiogenesis. Acta Physiol 2011;202, 225–39.

3: Abou-Khalil R, Le Grand F, Pallafacchina G, Valable S, Authier FJ, Rudnicki MA, et al. Autocrine and paracrine angiopoietin 1/Tie-2 signaling promotes muscle satellite cell self-renewal. Cell Stem Cell 2009;5:298-309.

4: Christov C, Chretien F, Abou-Khalil R, Bassez G, Vallet G, Authier FJ, et al. Muscle satellite cells and endothelial cells: close neighbors and privileged partners. Mol Biol Cell 2007;18:1397-409.

5: Scholz D, Thomas S, Sass S, Podzuweit T. Angiogenesis and myogenesis as two facets of inflammatory post-ischemic tissue regeneration. Mol Cell Biochem 2003;246:57-67.

6: Arsic N, Zacchigna S, Zentilin L, Ramirez-Correa G, Pattarini L, Salvi A, et al. Vascular endothelial growth factor stimulates skeletal muscle regeneration in vivo. Mol Ther 2004;10:844-54.

7: Borselli C, Storrie H, Benesch-Lee F, Shvartsman D, Cezar C, Lichtman JW, et al. Functional muscle regeneration with combined delivery of angiogenesis and myogenesis factors. Proc Natl Acad Sci USA 2010;107:3287-92.

8: Relaix F, Zammit PS. Satellite cells are essential for skeletal muscle regeneration: the cell on the edge returns centre stage. Development 2012;139:2845-56.

9: Mounier R, Chrétien F, Chazaud B. Blood vessels and the satellite cell niche. Curr Top Dev Biol 2011;96:121-38.

10: Flann KL, Rathbone CR, Cole LC, Liu X, Allen RE, Rhoads RP. Hypoxia simultaneously alters satellite cell-mediated angiogenesis and hepatocyte growth factor expression. J Cell Physiol 2014;229:572-9.

11: Rhoads RP, Flann KL, Cardinal TR, Rathbone CR, Liu X, Allen RE. Satellite cells isolated from aged or dystrophic muscle exhibit a reduced capacity to promote angiogenesis in vitro. Biochem Biophys Res Commun 2013;440:399-404.

12: Carpenter S, Karpati G, Rothman S, Watters G. The childhood type of dermatomyositis. Neurology 1976;26:952-62.

13: Crowe WE, Bove KE, Levinson JE, Hilton PK. Clinical and pathogenetic implications of histopathology in childhood polydermatomyositis. Arthritis Rheum 1982;25:126-39.

14: Kissel JT, Mendell JR, Rammohan KW. Microvascular deposition of complement membrane attack complex in dermatomyositis. N Engl J Med 1986;314:329-34.

15: Emslie-Smith AM, Engel AG. Microvascular changes in early and advanced dermatomyositis: a quantitative study. Ann Neurol 1990;27:343-56.

16: Feldman BM, Rider LG, Reed AM, Pachman LM. Juvenile dermatomyositis and other idiopathic inflammatory myopathies of childhood. Lancet 2008;371:2201-12.

17: Banker BQ. Dermatomyostis of childhood, ultrastructural alterations of muscle and intramuscular blood vessels. J Neuropathol Exp Neurol 1975;34:46-75.

18: Monaco AP, Bertelson CJ, Colletti-Feener C, Kunkel LM. Localization and cloning of Xp21 deletion breakpoints involved in muscular dystrophy. Hum Genet 1987;75:221-7.

19: Sander M, Chavoshan B, Harris SA, Iannaccone ST, Stull JT, Thomas GD, et al. Functional muscle ischemia in neuronal nitric oxide synthase-deficient skeletal muscle of children with Duchenne muscular dystrophy. Proc Natl Acad Sci USA 2000;97:13818-23.

20: Loufrani L, Levy BI, Henrion D. Defect in microvascular adaptation to chronic changes in blood flow in mice lacking the gene encoding for dystrophin. Circ Res 2002;91:1183-9.

21: Ito K, Kimura S, Ozasa S, Matsukura M, Ikezawa M, Yoshioka K, et al. Smooth muscle-specific dystrophin expression improves aberrant vasoregulation in mdx mice. Hum Mol Genet 2006;15:2266-75.

22: Bagher P, Duan D, Segal SS. Evidence for impaired neurovascular transmission in a murine model of Duchenne muscular dystrophy. J Appl Physiol 2011;110:601-9.

23: Froehner SC, Reed SM, Anderson KN, Huang PL, Percival JM. Loss of nNOS inhibits compensatory muscle hypertrophy and exacerbates inflammation and eccentric contraction-induced damage in mdx mice. Hum Mol Genet 2015;24:492-505.

24: Miike T, Sugino S, Ohtani Y, Taku K, Yoshioka K. Vascular endothelial cell injury and platelet embolism in Duchenne muscular dystrophy at the preclinical stage. J Neurol Sci 1987;82:67-80.

25: Desguerre I, Mayer M, Leturcq F, Barbet JP, Gherardi RK, Christov C. Endomysial fibrosis in Duchenne muscular dystrophy: a marker of poor outcome associated with macrophage alternative activation. J Neuropathol Exp Neurol 2009;68:762-73.

26: Nguyen F, Guigand L, Goubault-Lleroux I, Wyers M, Cherel Y. Microvessel density in muscles of dogs with golden retriever muscular dystrophy. Neuromusc Disord 2005;15:154-

27: Brown VE, Pilkington CA, Feldman BM, Davidson JE; Network for Juvenile Dermatomyositis, Paediatric Rheumatology European Society (PReS). An international consensus survey of the diagnostic criteria for juvenile dermatomyositis (JDM). Rheumatology (Oxford). 2006;45:990-3.

28: Chazaud B, Sonnet C, Lafuste P, Bassez G, Rimaniol AC, Poron F, et al. Satellite cells attract monocytes and use macrophages as a support to escape apoptosis and enhance muscle growth. J Cell Biol 2003;163:1133-43.

29: Nakatsu MN, Hughes CC. An optimized three-dimensional in vitro model for the analysis of angiogenesis. Methods Enzymol 2008;443:65-82.

30: Bolstad BM, Irizarry RA, Astrand M, Speed .P. A Comparison of Normalization Methods for High Density Oligonucleotide Array Data Based on Bias and Variance. Bioinformatics 2003;19:185-193.

31: Huang da W, Sherman BT, Lempicki RA. Bioinformatics enrichment tools: paths toward the comprehensive functional analysis of large gene lists. Nucleic Acids Res 2009;37:1-13.

32: Huang da W, Sherman BT, Lempicki RA. Systematic and integrative analysis of large gene lists using DAVID bioinformatics resources. Nat Protoc 2009;4:44-57.

33: Liu Liao AP, Salajegheh M, Nazareno R, Kagan JC, Jubin RG, Greenberg SA. Interferon β is associated with type 1 interferon-inducible gene expression in dermatomyositis. Ann Rheum Dis. 2011;70:831-6.

34: Miles L, Bove KE, Lovell D, Wargula JC, Bukulmez H, Shao M, et al. Predictability of the clinical course of juvenile dermatomyositis based on initial muscle biopsy: a retrospective study of 72 patients. Arthritis Rheum 2007;57:1183–91.

35: Viemann D, Strey A, Janning A, Jurk K, Klimmek K, Vogl T, et al. Myeloid-related proteins 8 and 14 induce a specific inflammatory response in human microvascular endothelial cells. Blood. 2005 Apr 1;105(7):2955-62.

36: Bodnar RJ, Yates CC, Rodgers ME, Du X, Wells A. IP-10 induces dissociation of newly formed blood vessels. J Cell Sci 2009;122:2064-77.

37: Yates-Binder CC, Rodgers M, Jaynes J, Wells A, Bodnar RJ, Turner T. An IP-10 (CXCL10)-derived peptide inhibits angiogenesis. PLoS One 2012;7:e40812.

38: Rice GI, Forte GM, Szynkiewicz M, Chase DS, Aeby A, Abdel-Hamid MS et al. Assessment of interferon-related biomarkers in Aicardi-Goutières syndrome associated with mutations in TREX1, RNASEH2A, RNASEH2B, RNASEH2C, SAMHD1, and ADAR: a case-control study. Lancet Neurol 2013;12:1159-69.

39: Roberts P, McGeachie JK. Endothelial cell activation during angiogenesis in freely transplanted skeletal muscles in mice and its relationship to the onset of myogenesis. J Anat. 1990;169:197-207.

40: Ennen JP, Verma M, Asakura A. Vascular-targeted therapies for Duchenne muscular dystrophy. Skelet Muscle. 2013;3:9.

41: Engel WK, Hawley RJ. Focal lesions of muscle in peripheral vascular disease. J Neurol. 1977 Jun 13;215(3):161-8.

42: Miyatake M, Miike T, Zhao J, Yoshioka K, Uchino M, Usuku G. Possible systemic smooth muscle layer dysfunction due to a deficiency of dystrophin in Duchenne muscular dystrophy. J Neurol Sci. 1989;93:11-7.

43: Bonapace L, Coissieux MM, Wyckoff J, Mertz KD, Varga Z, Junt T, et al. Cessation of CCL2 inhibition accelerates breast cancer metastasis by promoting angiogenesis. Nature. 2014;515:130-3.

44: Gitiaux C, Kostallari E, Lafuste P, Authier FJ, Christov C, Gherardi RK. Whole microvascular unit deletions in dermatomyositis. Ann Rheum Dis 2013. 72, 445-52.

45: Bellutti Enders F, van Wijk F, Scholman R, Hofer M, Prakken BJ, van Royen-Kerkhof A, et al. Correlation of CXCL10, tumor necrosis factor receptor type II, and galectin 9 with disease activity in juvenile dermatomyositis. Arthritis Rheum 2014;66:2281-9.

46: Nistala K, Varsani H, Wittkowski H, Vogl T, Krol P, Shah V, et al. Myeloid related protein induces muscle derived inflammatory mediators in juvenile dermatomyositis. Arthritis Res Ther 2013;15:R131.

47: Viemann D, Barczyk K, Vogl T, Fischer U, Sunderkötter C, Schulze-Osthoff K, et al. MRP8/MRP14 impairs endothelial integrity and induces a caspase-dependent and -independent cell death program. Blood 2007;109:2453-60.

48: Tezak Z, Hoffman EP, Lutz JL, Fedczyna TO, Stephan D, Bremer EG, et al. Gene expression profiling in DQA1*0501+ children with untreated dermatomyositis: a novel model of pathogenesis. J Immunol 2002;168:4154-63.

49: Salajegheh M, Kong SW, Pinkus JL, Walsh RJ, Liao A, Nazareno R, et al. Interferon-stimulated gene 15 (ISG15) conjugates proteins in dermatomyositis muscle with perifascicular atrophy. Ann Neurol 2010;67:53-63.

50: Zhang X, Bogunovic D, Payelle-Brogard B, Francois-Newton V, Speer SD, Yuan C, Volpi S, Li Z, et al. Human intracellular ISG15 prevents interferon-α/β over-amplification and auto-inflammation. Nature 2015;517:89-93.

51: Franzi S, Salajegheh M, Nazareno R, Greenberg SA. Type 1 interferons inhibit myotube formation independently of upregulation of interferon-stimulated gene 15. PLoS One 2013;8:e65362.

52: De Rossi M, Bernasconi P, Baggi F, de Waal Malefyt R, Mantegazza R. Cytokines and chemokines are both expressed by human myoblasts: possible relevance for the immune pathogenesis of muscle inflammation. Int Immunol 2000;12:1329-35.

53: Bilgic H, Ytterberg SR, Amin S, McNallan KT, Wilson JC, Koeuth T,et al. Interleukin-6 and type I interferon-regulated genes and chemokines mark disease activity in dermatomyositis. Arthritis Rheum 2009;60:3436-46.

FIGURE LEGEND

Figure 1: Effects of MPCs on EC migration. (A) MPCs and ECs were cultured in two-chamber devices, so the two cell types faced each other, allowing migration toward each other over a 24 h period. Pictures were taken at 0 and 24 h. (A) Virtual line was drawn on the picture at the cell front at time 0 h and copied to the picture at time 24 h. Individual cell migration was calculated from this line with ImageJ software. (B,C,D) Individual cell migration of ECs towards normal MPCs (left panel) and of MPCs towards ECs (right panel) for normal muscle-derived MPCs (B), JDM-derived MPCs (C) and DMD-derived MPCs (D). Results are means +/- SEM of 4 independent experiments. Indicated p values: * $p< 0.05$; **$p<0.01$.

Figure 2: Effects of MPCs on EC proliferation. Proliferation of ECs cultured alone (None) or with MPC-derived conditioned medium (CM) assessed by ki67 staining (red) against Hoechst staining (blue) (A). MPCs were derived from normal (B), JDM (C) and DMD (D) muscle. Results are means +/- SEM of 4 independent experiments. Indicated p values: * $p< 0.05$; **$p<0.01$.

Figure 3: Effects of MPCs on angiogenesis. MPCs derived from normal (A, white bars in D,E,F), JDM (B, blue bars in D,E,F), DMD (C, red bars in D,E,F) were laid on top of fibrin gels containing ECs cultured on collagen-coated cytodex beads and the formation of vessel-like structures is observed 6 days later. These sprouts may contain (arrows) or not (arrowheads) lumen (A-C). The sprout length (expressed in µm) (D), the number of sprout/bead (E) and the % of lumenized sprouts (F) were measured. Results are means +/- SEM of 4 independent experiments. Indicated p values: * $p< 0.05$; ** $p<0.01$.

Figure 4: Angiogenic signature of JDM and DMD-derived MPCs. Protein extracts from MPCs were tested on antibodies arrays (example in A) and the signal obtained was analyzed and expressed in fold changes of protein expression in JDM-derived MPCs (B) and DMD-derived MPCs (C) as compared with MPCs issued from normal age-matched muscle. Results are means +/- SEM of 3 independent experiments.

Figure 5: IFN-treatment, hypoxia and ischemia partially mimicked angiogenic signature of JDM-derived MPCs. In (A) results obtained in Fig.4B, i.e. angiogenic signature of JDM-derived MPCs, were reported for an easier comparison with signature of MPCs treated with β-IFN (B), MPCs incubated in hypoxic condition (C), MPCs incubated in ischemic condition (D). Results are expressed in fold changes as compared with untreated MPCs and are means +/- SEM of 3 independent experiments.

Table 1

A- Differentially expressed genes in ECs (CD31+ cells)

Disease	Total	up	down
JDM (vs. control)	1871	919	952
DMD (vs. Control)	1126	414	712
DMD vs JDM	726	271	455

B- Differentially expressed genes in MPCs (CD56+ cells)

Disease	Total	up	down
JDM (vs. control)	1089	566	523
DMD (vs. Control)	2566	1483	1083
DMD vs JDM	1478	806	672

Table 2A - List of the 30 genes with the highest fold changes in JDM-derived ECs (vs. control)
(IFNs inducible gene are highlighted in yellow, S100 (MRP) genes are highlighted in green)

Fold change	Gene symbol	Gene title
125.499	CXCL10	chemokine (C-X-C motif) ligand 10
41.5768	CXCL11	chemokine (C-X-C motif) ligand 11
36.0173	S100A8	S100 calcium binding protein A8
28.7486	IGJ	immunoglobulin J polypeptide
27.0824	S100A9	S100 calcium binding protein A9
25.3322	S100A12	S100 calcium binding protein A12
19.0843	MNDA	myeloid cell nuclear differentiation antigen
18.782	SIGLEC14	sialic acid binding Ig-like lectin 14 (Receptor Ig)
17.5002	RNASE2	ribonuclease, RNase A family, 2
17.1711	PLAC8	placenta-specific 8 (enhance cancer progression How ?)
16.8426	MX2	MX dynamin-like GTPase 2
14.8098	SCIMP	SLP adaptor and CSK interacting membrane protein
13.5943	LILRA6	leukocyte immunoglobulin-like receptor, subfamily A, member 6
13.541	OAS1	2'-5'-oligoadenylate synthetase 1, 40/46kDa
13.2041	DYNLT1	dynein, light chain, Tctex-type 1 (role dans hypoxie)
12.6756	GZMB	granzyme B (increase vasc permeability)
11.961	THBS1	thrombospondin 1 (inh angiogenesis)
11.8099	EREG	Epiregulin (famille EGF regulate angiogenesis)
11.8051	ISG20	interferon stimulated exonuclease gene 20kDa
11.532	ARHGAP15	Rho GTPase activating protein 15
11.1012	SELL	selectin L
10.9743	ISG15	ISG15 ubiquitin-like modifier
10.5062	LGALS2	lectin, galactoside-binding, soluble, 2 (angiogenesis via chem.)
9.96193	MT1F	metallothionein 1F
9.95969	C15orf48	chromosome 15 open reading frame 48
9.86885	IFIT2	interferon-induced protein with tetratricopeptide repeats 2
9.76117	CD38	CD38 molecule
9.55858	IL1RN	interleukin 1 receptor antagonist
9.46691	VCAN	versican
8.87269	FASTKD5	FAST kinase domain 5

Table 2B

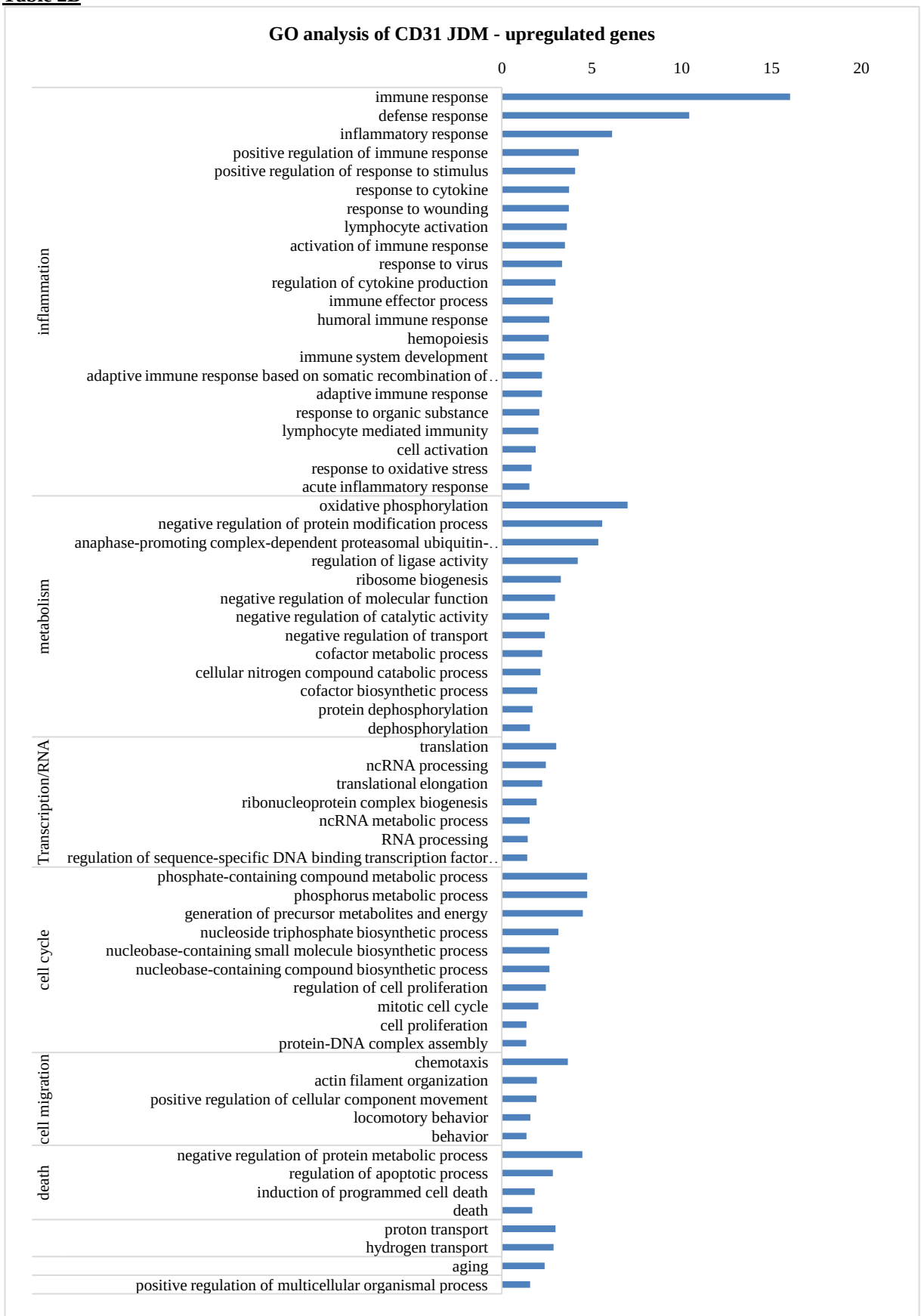
GO analysis of CD31 JDM - upregulated genes
0
5
10
15
20
inflammation
immune response
defense response
inflammatory response
positive regulation of immune response
positive regulation of response to stimulus
response to cytokine
response to wounding
lymphocyte activation
activation of immune response
response to virus
regulation of cytokine production
immune effector process
humoral immune response
hemopoiesis
immune system development
adaptive immune response based on somatic recombination of…
adaptive immune response
response to organic substance
lymphocyte mediated immunity
cell activation
response to oxidative stress
acute inflammatory response
metabolism
oxidative phosphorylation
negative regulation of protein modification process
anaphase-promoting complex-dependent proteasomal ubiquitin-…
regulation of ligase activity
ribosome biogenesis
negative regulation of molecular function
negative regulation of catalytic activity
negative regulation of transport
cofactor metabolic process
cellular nitrogen compound catabolic process
cofactor biosynthetic process
protein dephosphorylation
dephosphorylation
Transcription/RNA
translation
ncRNA processing
translational elongation
ribonucleoprotein complex biogenesis
ncRNA metabolic process
RNA processing
regulation of sequence-specific DNA binding transcription factor…
cell cycle
phosphate-containing compound metabolic process
phosphorus metabolic process
generation of precursor metabolites and energy
nucleoside triphosphate biosynthetic process
nucleobase-containing small molecule biosynthetic process
nucleobase-containing compound biosynthetic process
regulation of cell proliferation
mitotic cell cycle
cell proliferation
protein-DNA complex assembly
cell migration
chemotaxis
actin filament organization
positive regulation of cellular component movement
locomotory behavior
behavior
death
negative regulation of protein metabolic process
regulation of apoptotic process
induction of programmed cell death
death
proton transport
hydrogen transport
aging
positive regulation of multicellular organismal process

Table 2C - List of the 30 genes with the lowest fold changes in JDM-derived ECs (vs. control)

Fold change	Gene symbol	Gene title
-26.2681	CSRP2	cysteine and glycine-rich protein 2
-23.6704	INMT	indolethylamine N-methyltransferase
-20.3957	ANXA3	annexin A3
-19.7264	LYVE1	lymphatic vessel endothelial hyaluronan receptor 1
-19.3381	TEK	TEK tyrosine kinase, endothelial
-16.1883	TSPAN18	tetraspanin 18
-15.8275	DPRX	divergent-paired related homeobox
-15.0754	ITGA1	integrin, alpha 1
-14.9145	ANO2	anoctamin 2, calcium activated chloride channel
-13.7978	LOC101928558	serine/arginine repetitive matrix protein 2-like
-13.246	TSPAN7	tetraspanin 7
-12.6833	HMCN1	hemicentin 1
-12.6824	F8	coagulation factor VIII, procoagulant component
-12.5781	HIST1H4A	histone cluster 1, H4a
-11.835	NBPF1	neuroblastoma breakpoint family, member 1
-11.6503	TIMP4	TIMP metallopeptidase inhibitor 4
-11.4063	ST6GALNAC3	ST6-N-acetylgalactosaminide alpha-2,6-sialyltransferase 3
-11.3872	EFNB2	ephrin-B2
-11.1272	NDNF	neuron-derived neurotrophic factor
-10.5234	FMO2	flavin containing monooxygenase 2 (non-functional)
-10.488	SELE	selectin E
-10.446	PKD1L1	polycystic kidney disease 1 like 1
-10.3579	C10orf10	chromosome 10 open reading frame 10
-10.2334	PTPRB	protein tyrosine phosphatase, receptor type, B
-9.97321	RASGRF2	Ras protein-specific guanine nucleotide-releasing factor 2
-9.86673	GJA1	gap junction protein, alpha 1, 43kDa
-9.71341	MLLT4	myeloid/lymphoid or mixed-lineage leukemia translocated 4
-9.62486	CCDC68	coiled-coil domain containing 68
-9.608	HLA-DRB5	major histocompatibility complex, class II, DR beta 5
-9.2784	PLCB4	phospholipase C, beta 4

Table 2D

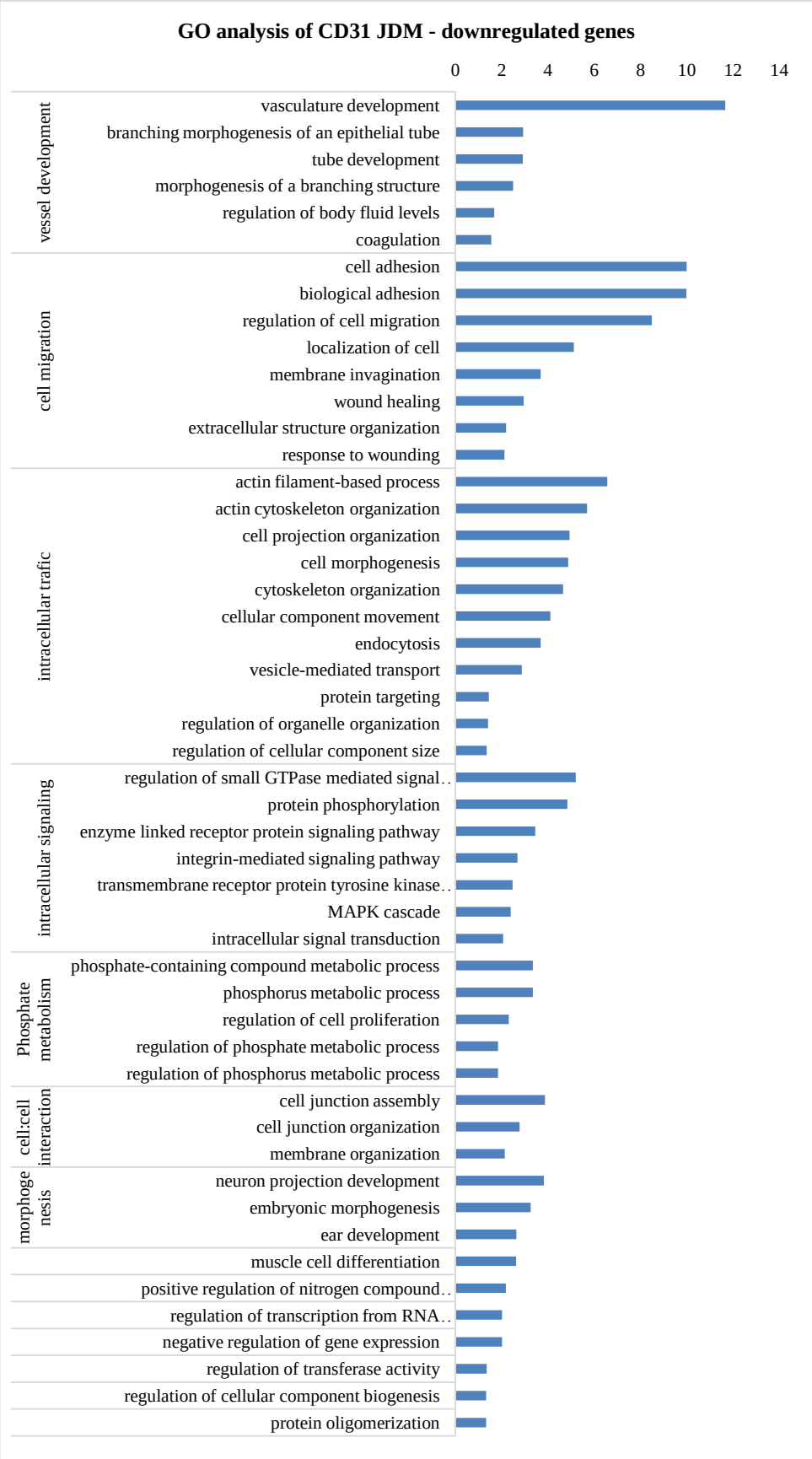
GO analysis of CD31 JDM - downregulated genes
0
2
4
6
8
10
12
14
vessel development
vasculature development
branching morphogenesis of an epithelial tube
tube development
morphogenesis of a branching structure
regulation of body fluid levels
coagulation
cell migration
cell adhesion
biological adhesion
regulation of cell migration
localization of cell
membrane invagination
wound healing
extracellular structure organization
response to wounding
intracellular trafic
actin filament-based process
actin cytoskeleton organization
cell projection organization
cell morphogenesis
cytoskeleton organization
cellular component movement
endocytosis
vesicle-mediated transport
protein targeting
regulation of organelle organization
regulation of cellular component size
intracellular signaling
regulation of small GTPase mediated signal..
protein phosphorylation
enzyme linked receptor protein signaling pathway
integrin-mediated signaling pathway
transmembrane receptor protein tyrosine kinase..
MAPK cascade
intracellular signal transduction
Phosphate metabolism
phosphate-containing compound metabolic process
phosphorus metabolic process
regulation of cell proliferation
regulation of phosphate metabolic process
regulation of phosphorus metabolic process
cell:cell interaction
cell junction assembly
cell junction organization
membrane organization
morphogenesis
neuron projection development
embryonic morphogenesis
ear development
muscle cell differentiation
positive regulation of nitrogen compound..
regulation of transcription from RNA..
negative regulation of gene expression
regulation of transferase activity
regulation of cellular component biogenesis
protein oligomerization

Table 2E - List of the 30 genes with the highest fold changes in DMD-derived ECs (vs. control)

Fold change	Gene symbol	Gene title
15.4171	P2RY10	purinergic receptor P2Y, G-protein coupled, 10
14.9884	SPP1	secreted phosphoprotein 1
14.4238	CCL18	chemokine (C-C motif) ligand 18 (pulmonary and activation-regulated)
12.8532	APOC1	apolipoprotein C-I
12.2057	FCGR2B	Fc fragment of IgG, low affinity IIb, receptor (CD32)
11.5088	GPNMB	glycoprotein (transmembrane) nmb
7.83498	SLAMF6	SLAM family member 6
7.13915	CD69	CD69 molecule
7.12287	RGS10	regulator of G-protein signaling 10
6.90812	CD3G	CD3g molecule, gamma (CD3-TCR complex)
6.88653	SLC38A1	solute carrier family 38, member 1
6.88481	ARHGAP15	Rho GTPase activating protein 15
6.30791	XCL1	chemokine (C motif) ligand 1
6.01568	DOCK10	dedicator of cytokinesis 10
5.75725	ITK	IL2-inducible T-cell kinase
5.64701	IL10RA	interleukin 10 receptor, alpha
5.60299	SIT1	signaling threshold regulating transmembrane adaptor 1
5.52419	AOAH	acyloxyacyl hydrolase (neutrophil)
5.48817	ITGA4	integrin, alpha 4 (antigen CD49D, alpha 4 subunit of VLA-4 receptor)
5.10459	PTRHD1	peptidyl-tRNA hydrolase domain containing 1
5.05084	TC2N	tandem C2 domains, nuclear
4.93088	AMICA1	adhesion molecule, interacts with CXADR antigen 1
4.77597	MNDA	myeloid cell nuclear differentiation antigen
4.65219	CD3D	CD3d molecule, delta (CD3-TCR complex)
4.53398	RAB8B	RAB8B, member RAS oncogene family
4.4154	GZMH	granzyme H (cathepsin G-like 2, protein h-CCPX)
4.39804	APOE	apolipoprotein E
4.34423	KLHL41	kelch-like family member 41
4.34173	RPS21	ribosomal protein S21
4.33738	CPVL	carboxypeptidase, vitellogenic-like

Table 2F

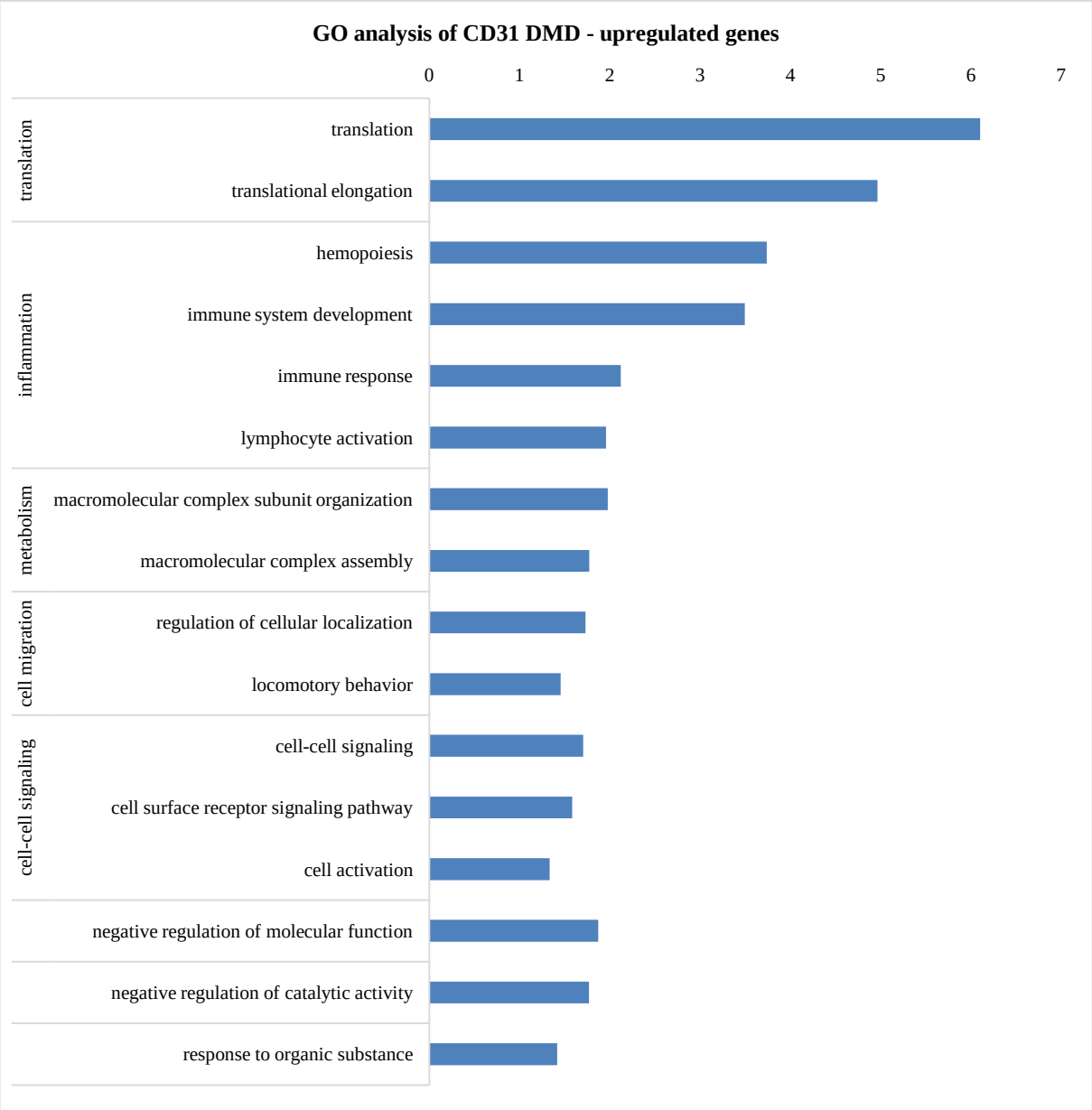
GO analysis of CD31 DMD - upregulated genes
0
1
2
3
4
5
6
7
translation
translation
translational elongation
inflammation
hemopoiesis
immune system development
immune response
lymphocyte activation
metabolism
macromolecular complex subunit organization
macromolecular complex assembly
cell migration
regulation of cellular localization
locomotory behavior
cell-cell signaling
cell-cell signaling
cell surface receptor signaling pathway
cell activation
negative regulation of molecular function
negative regulation of catalytic activity
response to organic substance

Table 2G - List of the 30 genes with the lowest fold changes in DMD-derived ECs (vs. control)

Fold change	Gene symbol	Gene title
-22.4249	ANXA3	annexin A3
-19.3343	DPRX	divergent-paired related homeobox
-17.4519	CSRP2	cysteine and glycine-rich protein 2
-12.1046	HLA-DRB5	major histocompatibility complex, class II, DR beta 5
-10.9958	ZNF417	zinc finger protein 417
-10.8707	DOC2B	double C2-like domains, beta
-9.84301	TSPAN18	tetraspanin 18
-9.77306	PLCB4	phospholipase C, beta 4
-9.6277	CYP4F12	cytochrome P450, family 4, subfamily F, polypeptide 12
-9.57188	ZNF721	zinc finger protein 721
-9.53323	HIST1H4A	histone cluster 1, H4a
-9.14744	TEK	TEK tyrosine kinase, endothelial
-8.77429	TIMP4	TIMP metallopeptidase inhibitor 4
-8.18946	GIMAP8	GTPase, IMAP family member 8
-7.63852	ANO2	anoctamin 2, calcium activated chloride channel
-7.436	ST6GALNAC3	ST6 -N-acetylgalactosaminide alpha-2,6-sialyltransferase 3
-7.30309	C10orf10	chromosome 10 open reading frame 10
-7.24945	EPB41L2	erythrocyte membrane protein band 4.1-like 2
-7.1899	CEACAM1	carcinoembryonic antigen-related cell adhesion molecule 1 (biliary glycoprotein)
-7.12119	CCL8	chemokine (C-C motif) ligand 8
-7.04312	OR51E1	olfactory receptor, family 51, subfamily E, member 1
-6.93712	EPB41L4A	erythrocyte membrane protein band 4.1 like 4A
-6.81852	LRRC32	leucine rich repeat containing 32
-6.76468	LPL	lipoprotein lipase
-6.65484	RASGRF2	Ras protein-specific guanine nucleotide-releasing factor 2
-6.64942	TSPAN13	tetraspanin 13
-6.62254	EML1	echinoderm microtubule associated protein like 1
-6.61729	MECOM	MDS1 and EVI1 complex locus
-6.60275	TUSC3	tumor suppressor candidate 3
-6.56929	IDO1	indoleamine 2,3-dioxygenase 1

Table 2H

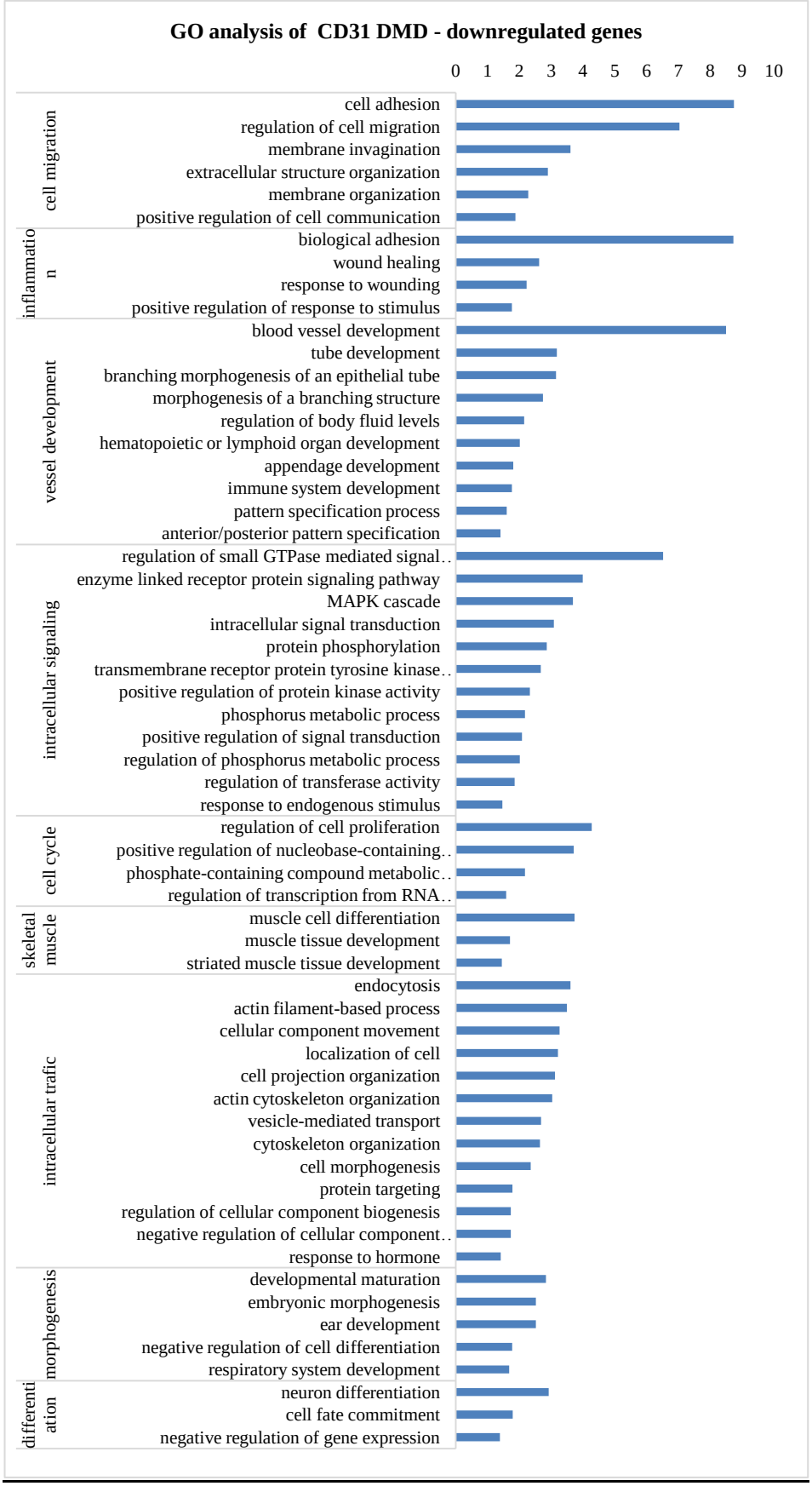
GO analysis of CD31 DMD - downregulated genes
0 1 2 3 4 5 6 7 8 9 10
cell migration
cell adhesion
regulation of cell migration
membrane invagination
extracellular structure organization
membrane organization
positive regulation of cell communication
inflammation
biological adhesion
wound healing
response to wounding
positive regulation of response to stimulus
vessel development
blood vessel development
tube development
branching morphogenesis of an epithelial tube
morphogenesis of a branching structure
regulation of body fluid levels
hematopoietic or lymphoid organ development
appendage development
immune system development
pattern specification process
anterior/posterior pattern specification
intracellular signaling
regulation of small GTPase mediated signal..
enzyme linked receptor protein signaling pathway
MAPK cascade
intracellular signal transduction
protein phosphorylation
transmembrane receptor protein tyrosine kinase..
positive regulation of protein kinase activity
phosphorus metabolic process
positive regulation of signal transduction
regulation of phosphorus metabolic process
regulation of transferase activity
response to endogenous stimulus
cell cycle
regulation of cell proliferation
positive regulation of nucleobase-containing..
phosphate-containing compound metabolic..
regulation of transcription from RNA..
skeletal muscle
muscle cell differentiation
muscle tissue development
striated muscle tissue development
intracellular trafic
endocytosis
actin filament-based process
cellular component movement
localization of cell
cell projection organization
actin cytoskeleton organization
vesicle-mediated transport
cytoskeleton organization
cell morphogenesis
protein targeting
regulation of cellular component biogenesis
negative regulation of cellular component..
response to hormone
morphogenesis
developmental maturation
embryonic morphogenesis
ear development
negative regulation of cell differentiation
respiratory system development
differentiation
neuron differentiation
cell fate commitment
negative regulation of gene expression

Table 2I

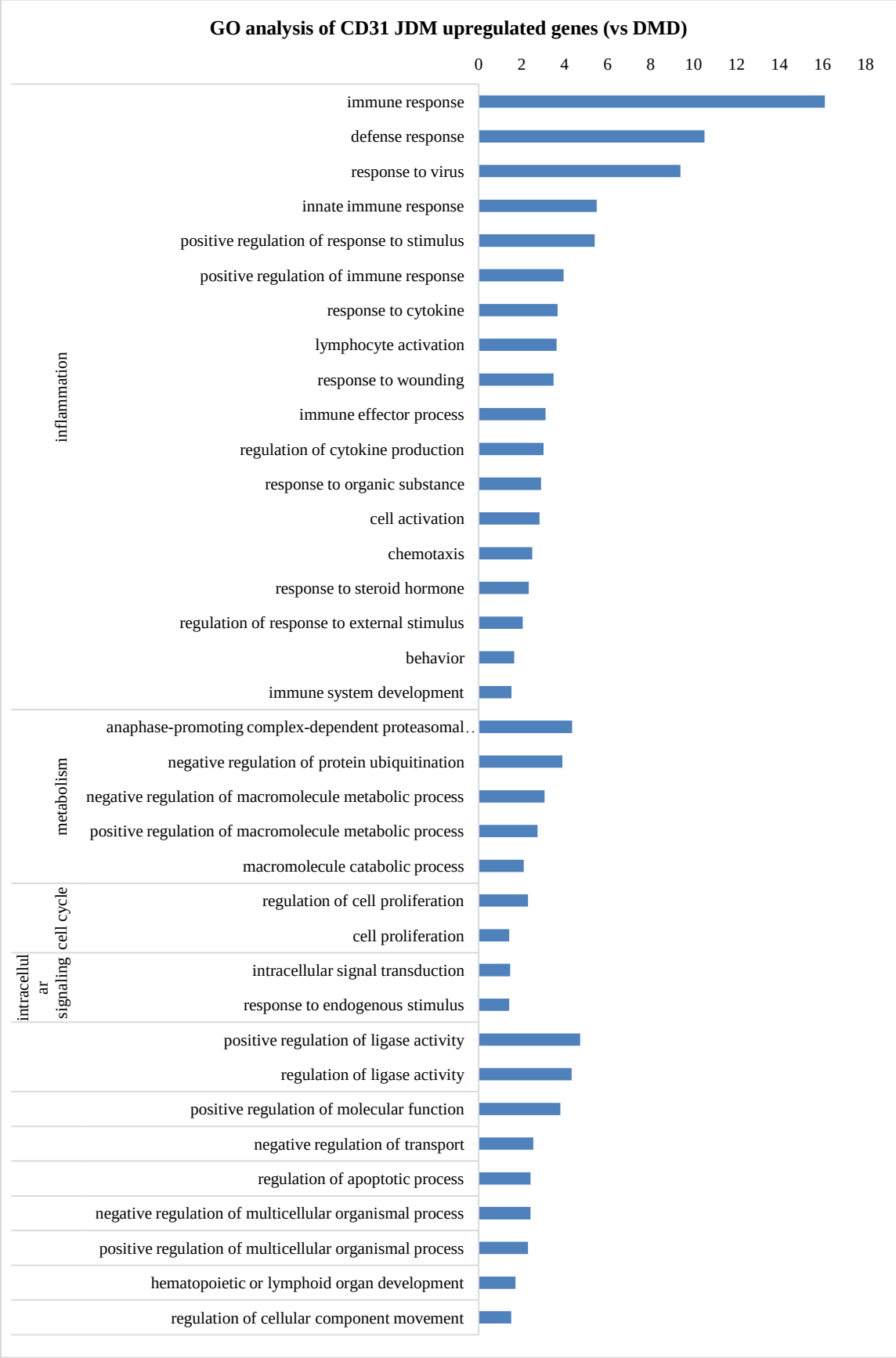
GO analysis of CD31 JDM upregulated genes (vs DMD)
0
2
4
6
8
10
12
14
16
18
inflammation
immune response
defense response
response to virus
innate immune response
positive regulation of response to stimulus
positive regulation of immune response
response to cytokine
lymphocyte activation
response to wounding
immune effector process
regulation of cytokine production
response to organic substance
cell activation
chemotaxis
response to steroid hormone
regulation of response to external stimulus
behavior
immune system development
metabolism
anaphase-promoting complex-dependent proteasomal..
negative regulation of protein ubiquitination
negative regulation of macromolecule metabolic process
positive regulation of macromolecule metabolic process
macromolecule catabolic process
cell cycle
regulation of cell proliferation
cell proliferation
intracellular signaling
intracellular signal transduction
response to endogenous stimulus
positive regulation of ligase activity
regulation of ligase activity
positive regulation of molecular function
negative regulation of transport
regulation of apoptotic process
negative regulation of multicellular organismal process
positive regulation of multicellular organismal process
hematopoietic or lymphoid organ development
regulation of cellular component movement

Table 3A - list of the 30 genes with the highest fold changes in JDM-derived MPCs (vs. control)
(IFNs inducible genes and genes included in the so called IFN signature (Rice et al., are highlighted in yellow and green respectively)

Fold Change	Gene symbol	Gene title
53.7161	IFI27	interferon, alpha-inducible protein 27
42.1068	ISG15	ISG15 ubiquitin-like modifier
29.9415	IFI44L	interferon-induced protein 44-like
27.8822	OAS1	2'-5'-oligoadenylate synthetase 1, 40/46kDa
27.6111	MX1	MX dynamin-like GTPase 1
24.4096	MX2	MX dynamin-like GTPase 2
21.6658	OAS3	2'-5'-oligoadenylate synthetase 3, 100kDa
20.0162	IFIH1	interferon induced with helicase C domain 1
19.8526	IFIT3	interferon-induced protein with tetratricopeptide repeats 3
18.8475	IFI44	interferon-induced protein 44
17.115	RSAD2	radical S-adenosyl methionine domain containing 2
16.5991	HERC6	HECT and RLD domain containing E3 ubiquitin protein ligase 6
15.8558	HERC5	HECT and RLD domain containing E3 ubiquitin protein ligase 5
14.4781	CD69	CD69 molecule
13.1432	IFIT2	interferon-induced protein with tetratricopeptide repeats 2
12.2424	SAMD9	sterile alpha motif domain containing 9
11.6855	RGS1	regulator of G-protein signaling 1
10.6407	ALOX5AP	arachidonate 5-lipoxygenase-activating protein
9.96747	FCER1G	Fc fragment of IgE, high affinity I, receptor for; gamma polypeptide
9.74833	PARP14	poly (ADP-ribose) polymerase family, member 14
9.73694	LOC101927910	keratin-associated protein 5-5-like
9.66827	IFIT1	interferon-induced protein with tetratricopeptide repeats 1
9.52508	OAS2	2'-5'-oligoadenylate synthetase 2, 69/71kDa
9.19794	IFI6	interferon, alpha-inducible protein 6
8.71974	NMI	N-myc (and STAT) interactor
8.34035	C1S	complement component 1, s subcomponent
8.22904	TNFSF10	tumor necrosis factor (ligand) superfamily, member 10
8.22507	C3	complement component 3
8.17584	CXCL2	chemokine (C motif) ligand 2
7.84861	FXYD5	FXYD domain containing ion transport regulator 5

Table 3B

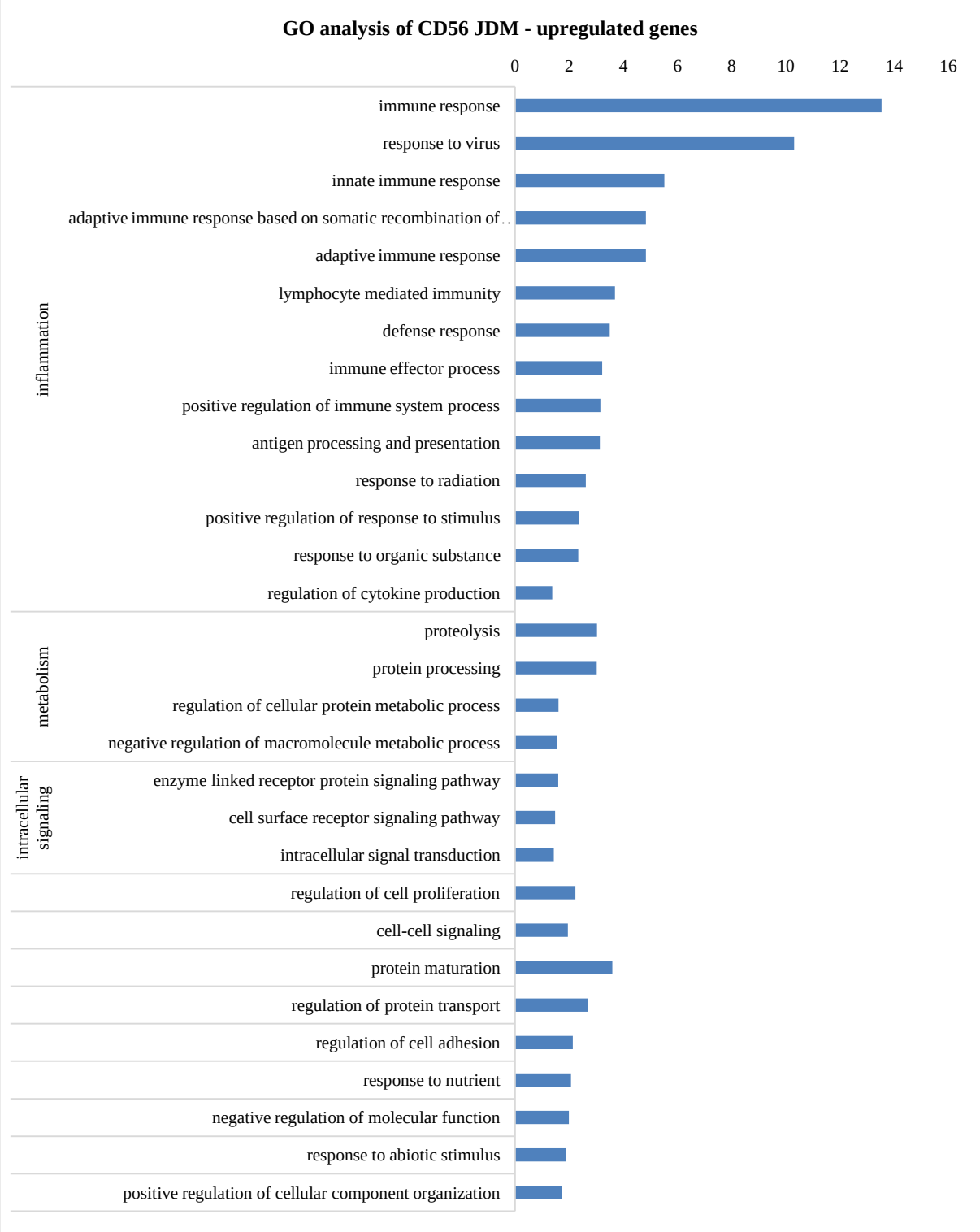
GO analysis of CD56 JDM - upregulated genes
0
2
4
6
8
10
12
14
16
inflammation
immune response
response to virus
innate immune response
adaptive immune response based on somatic recombination of..
adaptive immune response
lymphocyte mediated immunity
defense response
immune effector process
positive regulation of immune system process
antigen processing and presentation
response to radiation
positive regulation of response to stimulus
response to organic substance
regulation of cytokine production
metabolism
proteolysis
protein processing
regulation of cellular protein metabolic process
negative regulation of macromolecule metabolic process
intracellular signaling
enzyme linked receptor protein signaling pathway
cell surface receptor signaling pathway
intracellular signal transduction
regulation of cell proliferation
cell-cell signaling
protein maturation
regulation of protein transport
regulation of cell adhesion
response to nutrient
negative regulation of molecular function
response to abiotic stimulus
positive regulation of cellular component organization

Table 3C - list of the 30 genes with the lowest fold changes in JDM-derived MPCs (vs. control)

Fold change	Gene symbol	Gene title
-31.8471	BEX1	brain expressed, X-linked 1
-12.0442	MYOT	myotilin
-10.2404	HIST1H4B	histone cluster 1, H4b
-10.214	MB	myoglobin
-9.95018	HOXC6	homeobox C6
-9.23722	XIRP2	xin actin-binding repeat containing 2
-9.14455	PGAM2	phosphoglycerate mutase 2 (muscle)
-8.98452	MAL	mal, T-cell differentiation protein
-8.94552	MYBPC1	myosin binding protein C, slow type
-8.48273	HSPB6	heat shock protein, alpha-crystallin-related, B6
-8.3078	PLN	phospholamban
-8.18731	CKM	creatine kinase, muscle
-7.90114	NUS1	nuclear undecaprenyl pyrophosphate synthase 1 homolog (S. cerevisiae)
-7.37785	SLC16A4	solute carrier family 16, member 4
-6.71425	ZNF417	zinc finger protein 417
-6.65564	FABP3	fatty acid binding protein 3, muscle and heart
-6.60847	CADM1	cell adhesion molecule 1
-6.53786	CSRP3	cysteine and glycine-rich protein 3 (cardiac LIM protein)
-6.25179	HSPB7	heat shock 27kDa protein family, member 7 (cardiovascular)
-6.18863	NDUFB5	NADH dehydrogenase (ubiquinone) 1 beta subcomplex, 5, 16kDa
-5.9559	NRAP	nebulin-related anchoring protein
-5.89214	TNNC1	troponin C type 1 (slow)
-5.80962	EMC2	ER membrane protein complex subunit 2
-5.78669	PYGM	phosphorylase, glycogen, muscle
-5.61033	MYH7	myosin, heavy chain 7, cardiac muscle, beta
-5.43747	MYL2	myosin, light chain 2, regulatory, cardiac, slow
-5.37493	UCHL1	ubiquitin carboxyl-terminal esterase L1 (ubiquitin thiolesterase)
-5.25024	UACA	uveal autoantigen with coiled-coil domains and ankyrin repeats
-5.18213	CEP83	centrosomal protein 83kDa
-5.13299	GM2A	GM2 ganglioside activator

Table 3D

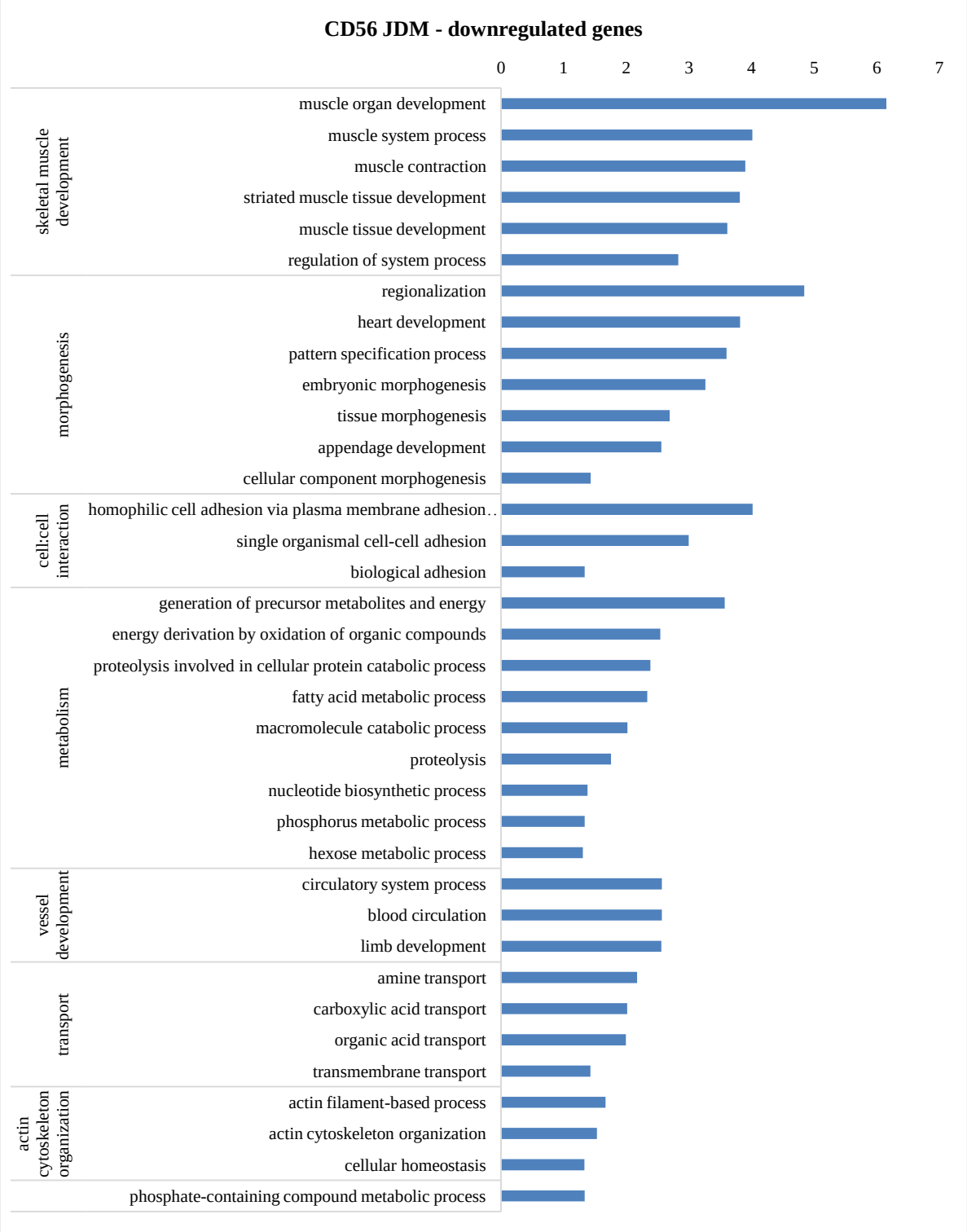
CD56 JDM - downregulated genes
0
1
2
3
4
5
6
7
skeletal muscle development
muscle organ development
muscle system process
muscle contraction
striated muscle tissue development
muscle tissue development
regulation of system process
morphogenesis
regionalization
heart development
pattern specification process
embryonic morphogenesis
tissue morphogenesis
appendage development
cellular component morphogenesis
cell:cell interaction
homophilic cell adhesion via plasma membrane adhesion...
single organismal cell-cell adhesion
biological adhesion
metabolism
generation of precursor metabolites and energy
energy derivation by oxidation of organic compounds
proteolysis involved in cellular protein catabolic process
fatty acid metabolic process
macromolecule catabolic process
proteolysis
nucleotide biosynthetic process
phosphorus metabolic process
hexose metabolic process
vessel development
circulatory system process
blood circulation
limb development
transport
amine transport
carboxylic acid transport
organic acid transport
transmembrane transport
actin cytoskeleton organization
actin filament-based process
actin cytoskeleton organization
cellular homeostasis
phosphate-containing compound metabolic process

Table 3E - list of the 30 genes with the highest fold changes in DMD-derived MPCs (vs. control)

Fold Change	Gene symbol	Gene title
9.15074	FCER1G	Fc fragment of IgE, high affinity I, receptor for; gamma polypeptide
9.03278	FXYD5	FXYD domain containing ion transport regulator 5
8.45184	THY1	Thy-1 cell surface antigen
7.86269	CD69	CD69 molecule
6.63893	RGS1	regulator of G-protein signaling 1
6.37467	LAPTM5	lysosomal protein transmembrane 5
6.27961	KLRB1	killer cell lectin-like receptor subfamily B, member 1
6.03598	C14orf178	chromosome 14 open reading frame 178
5.66	IL2RB	interleukin 2 receptor, beta
5.5682	HIST1H2AI	histone cluster 1, H2ai
4.79903	KLRD1	killer cell lectin-like receptor subfamily D, member 1
4.78607	GZMH	granzyme H (cathepsin G-like 2, protein h-CCPX)
4.60133	SLC2A3	solute carrier family 2 (facilitated glucose transporter), member 3
4.59364	STK10	serine/threonine kinase 10
4.55495	SH3BGRL3	SH3 domain binding glutamate-rich protein like 3
4.40681	SRGN	serglycin
4.37438	KLRC1	killer cell lectin-like receptor subfamily C, member 1
4.15866	CD247	CD247 molecule
4.03522	HIST1H4D	histone cluster 1, H4d
4.02615	CTSW	cathepsin W
3.99454	LCP1	lymphocyte cytosolic protein 1 (L-plastin)
3.99336	OR5P2	olfactory receptor, family 5, subfamily P, member 2
3.95962	CORO1A	coronin, actin binding protein, 1A
3.90255	GMFG	glia maturation factor, gamma
3.89705	C1orf162	chromosome 1 open reading frame 162
3.79751	L1CAM	L1 cell adhesion molecule
3.76154	LCE1F	late cornified envelope 1F
3.7314	PRAMEF26	PRAME family member 26
3.61074	S100A2	S100 calcium binding protein A2
3.48008	LCP2	lymphocyte cytosolic protein 2

Table 3F

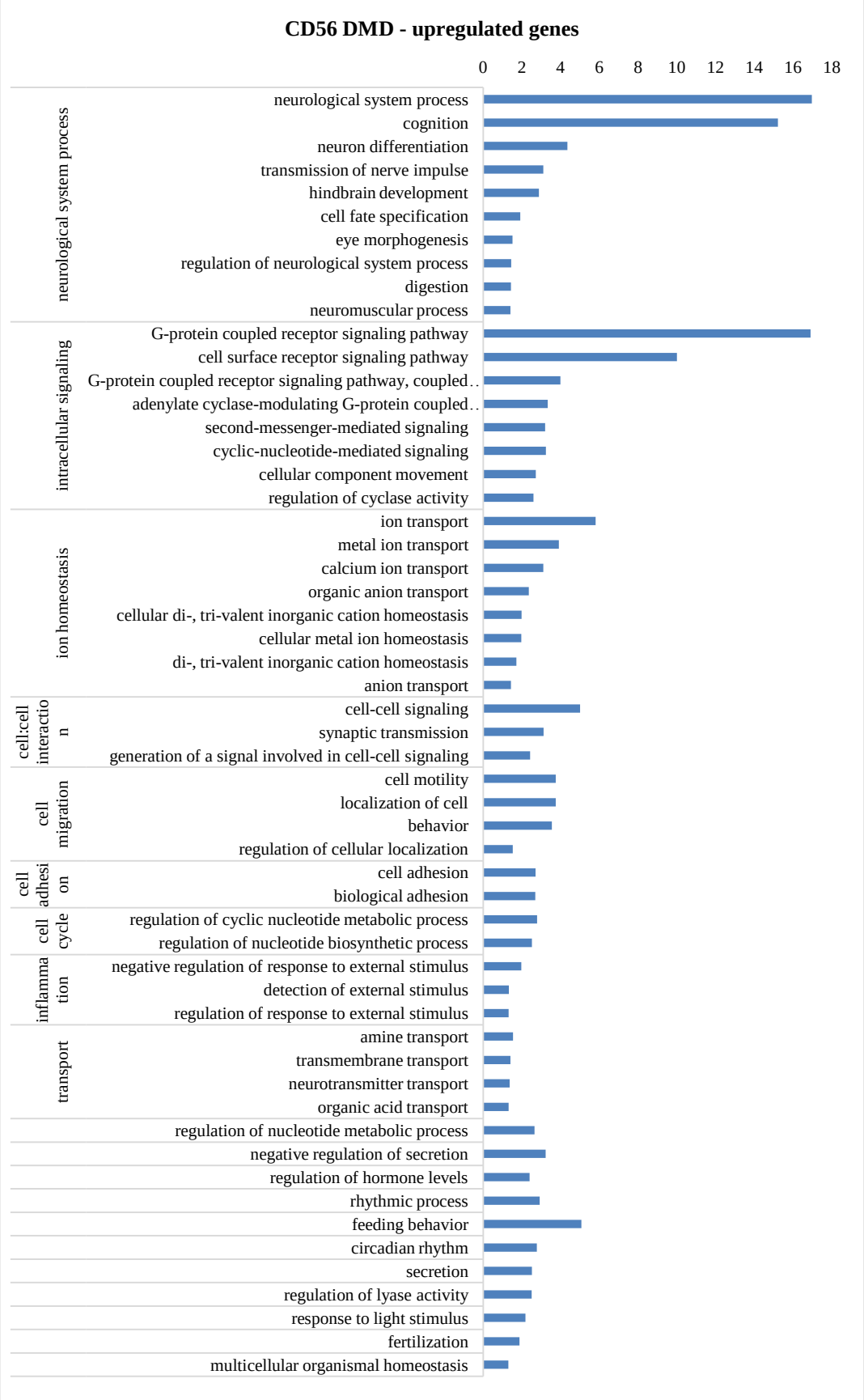
CD56 DMD - upregulated genes
0
2
4
6
8
10
12
14
16
18
neurological system process
neurological system process
cognition
neuron differentiation
transmission of nerve impulse
hindbrain development
cell fate specification
eye morphogenesis
regulation of neurological system process
digestion
neuromuscular process
intracellular signaling
G-protein coupled receptor signaling pathway
cell surface receptor signaling pathway
G-protein coupled receptor signaling pathway, coupled..
adenylate cyclase-modulating G-protein coupled..
second-messenger-mediated signaling
cyclic-nucleotide-mediated signaling
cellular component movement
regulation of cyclase activity
ion homeostasis
ion transport
metal ion transport
calcium ion transport
organic anion transport
cellular di-, tri-valent inorganic cation homeostasis
cellular metal ion homeostasis
di-, tri-valent inorganic cation homeostasis
anion transport
cell:cell interaction
cell-cell signaling
synaptic transmission
generation of a signal involved in cell-cell signaling
cell migration
cell motility
localization of cell
behavior
regulation of cellular localization
cell adhesion
cell adhesion
biological adhesion
cell cycle
regulation of cyclic nucleotide metabolic process
regulation of nucleotide biosynthetic process
inflammation
negative regulation of response to external stimulus
detection of external stimulus
regulation of response to external stimulus
transport
amine transport
transmembrane transport
neurotransmitter transport
organic acid transport
regulation of nucleotide metabolic process
negative regulation of secretion
regulation of hormone levels
rhythmic process
feeding behavior
circadian rhythm
secretion
regulation of lyase activity
response to light stimulus
fertilization
multicellular organismal homeostasis

Table 3G - list of the 30 genes with the lowest fold changes in DMD-derived MPCs

Fold Change	Gene symbol	Gene title
-39.6352	BEX1	brain expressed, X-linked 1
-13.4864	ACSS3	acyl-CoA synthetase short-chain family member 3
-13.1284	GREM1	gremlin 1, DAN family BMP antagonist (-BMP= prolif des sat cell)
-12.8163	MB	myoglobin
-12.3273	MAL	mal, T-cell differentiation protein
-11.7224	TMEM255A	transmembrane protein 255A
-11.5321	PLN	phospholamban
-11.4592	ZIC1	Zic family member 1
-10.9411	PDGFRA	platelet-derived growth factor receptor, alpha polypeptide
-10.37	HSPB6	heat shock protein, alpha-crystallin-related, B6
-10.067	RFTN2	raftlin family member 2
-10.0552	CXCL14	chemokine (C-X-C motif) ligand 14
-9.8912	MYL2	myosin, light chain 2, regulatory, cardiac, slow
-9.81801	DLK1	delta-like 1 homolog (Drosophila)
-9.43691	HOXC6	homeobox C6
-8.72573	NDFIP2	Nedd4 family interacting protein 2
-8.56203	HIST1H4B	histone cluster 1, H4b
-8.26699	XIRP2	xin actin-binding repeat containing 2
-8.23546	SLC16A4	solute carrier family 16, member 4
-8.1084	ABCA8	ATP-binding cassette, sub-family A (ABC1), member 8
-8.00129	PLSCR1	phospholipid scramblase 1
-7.72372	BMP6	bone morphogenetic protein 6
-7.6791	TOMM6	translocase of outer mitochondrial membrane 6 homolog (yeast)
-7.65387	LTBP1	latent transforming growth factor beta binding protein 1
-7.63925	PDK4	pyruvate dehydrogenase kinase, isozyme 4
-7.60921	CALCR	calcitonin receptor
-7.42494	PYGM	phosphorylase, glycogen, muscle
-7.32736	SLC27A6	solute carrier family 27 (fatty acid transporter), member 6
-7.23894	SEMA3C	sema domain, immunoglobulin domain (Ig), short basic domain, secreted, 3C
-7.14162	MYOT	myotilin

Table 3H

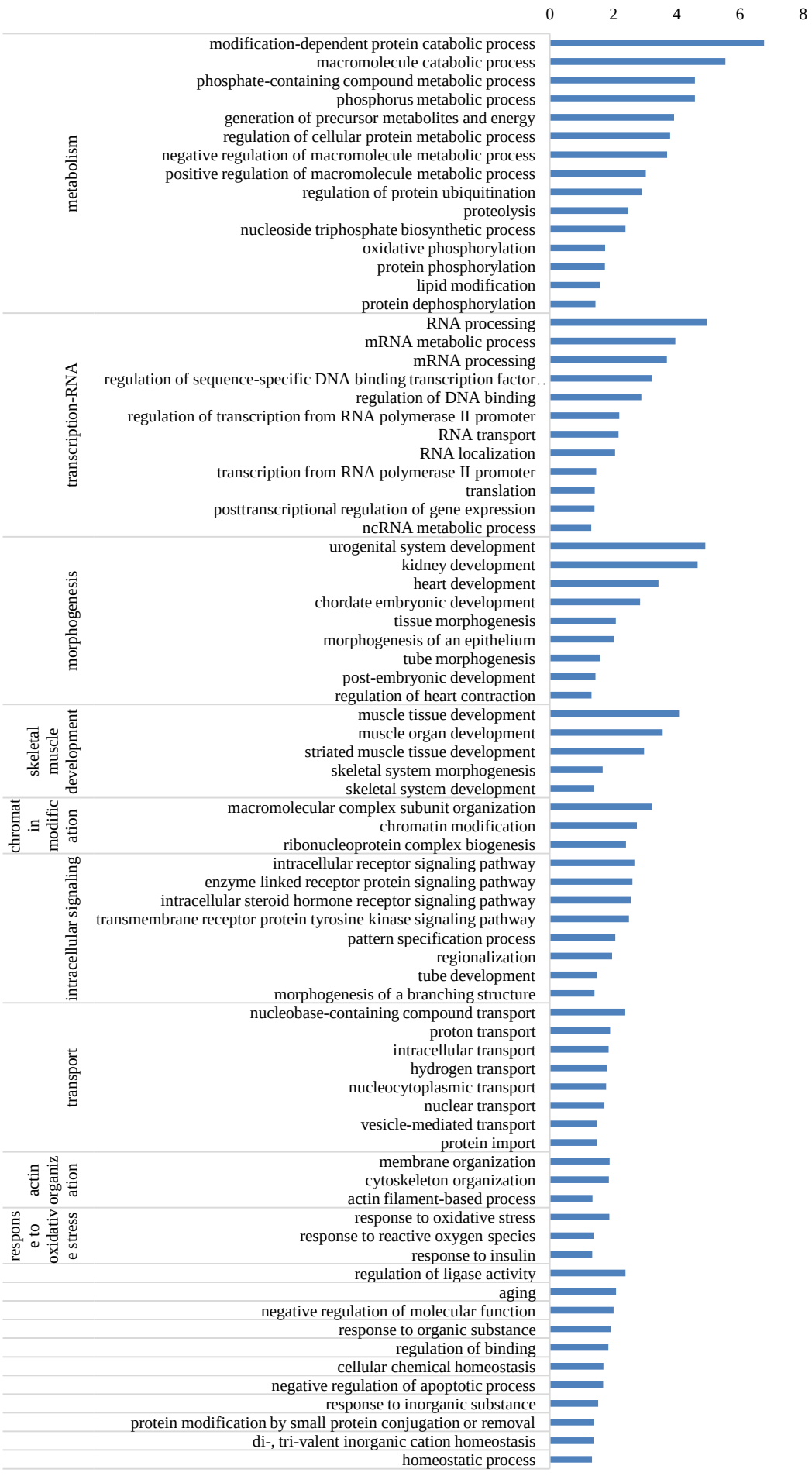
CD56 DMD - downregulated genes
0
2
4
6
8
metabolism
modification-dependent protein catabolic process
macromolecule catabolic process
phosphate-containing compound metabolic process
phosphorus metabolic process
generation of precursor metabolites and energy
regulation of cellular protein metabolic process
negative regulation of macromolecule metabolic process
positive regulation of macromolecule metabolic process
regulation of protein ubiquitination
proteolysis
nucleoside triphosphate biosynthetic process
oxidative phosphorylation
protein phosphorylation
lipid modification
protein dephosphorylation
transcription-RNA
RNA processing
mRNA metabolic process
mRNA processing
regulation of sequence-specific DNA binding transcription factor…
regulation of DNA binding
regulation of transcription from RNA polymerase II promoter
RNA transport
RNA localization
transcription from RNA polymerase II promoter
translation
posttranscriptional regulation of gene expression
ncRNA metabolic process
morphogenesis
urogenital system development
kidney development
heart development
chordate embryonic development
tissue morphogenesis
morphogenesis of an epithelium
tube morphogenesis
post-embryonic development
regulation of heart contraction
skeletal muscle development
muscle tissue development
muscle organ development
striated muscle tissue development
skeletal system morphogenesis
skeletal system development
chromatin modification
macromolecular complex subunit organization
chromatin modification
ribonucleoprotein complex biogenesis
intracellular signaling
intracellular receptor signaling pathway
enzyme linked receptor protein signaling pathway
intracellular steroid hormone receptor signaling pathway
transmembrane receptor protein tyrosine kinase signaling pathway
pattern specification process
regionalization
tube development
morphogenesis of a branching structure
transport
nucleobase-containing compound transport
proton transport
intracellular transport
hydrogen transport
nucleocytoplasmic transport
nuclear transport
vesicle-mediated transport
protein import
actin organization
membrane organization
cytoskeleton organization
actin filament-based process
response to oxidative stress
response to oxidative stress
response to reactive oxygen species
response to insulin
regulation of ligase activity
aging
negative regulation of molecular function
response to organic substance
regulation of binding
cellular chemical homeostasis
negative regulation of apoptotic process
response to inorganic substance
protein modification by small protein conjugation or removal
di-, tri-valent inorganic cation homeostasis
homeostatic process

Table 3I

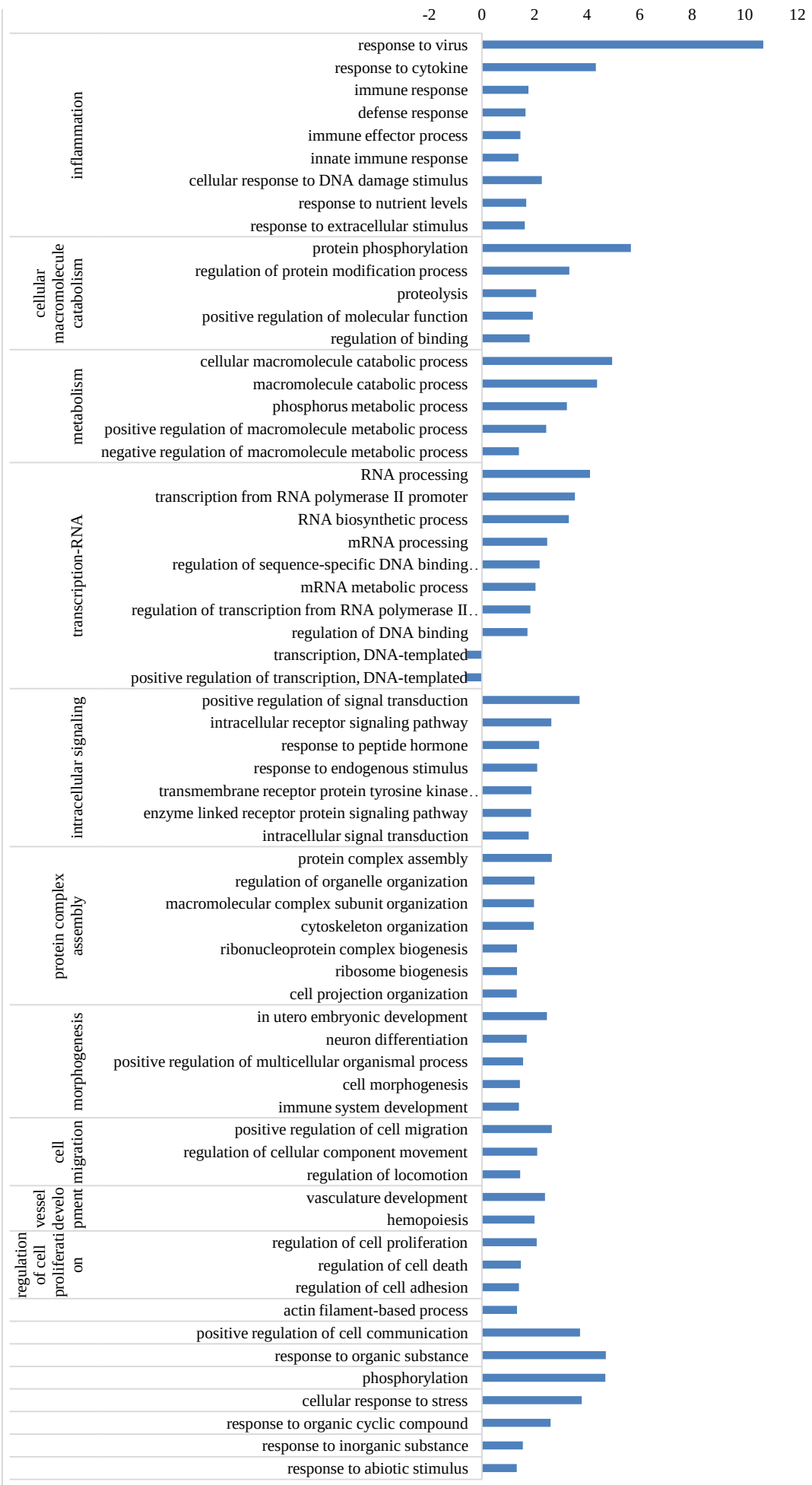
CD56 upregulated in JDM (vs. DMD)
-2
0
2
4
6
8
10
12
inflammation
response to virus
response to cytokine
immune response
defense response
immune effector process
innate immune response
cellular response to DNA damage stimulus
response to nutrient levels
response to extracellular stimulus
cellular macromolecule catabolism
protein phosphorylation
regulation of protein modification process
proteolysis
positive regulation of molecular function
regulation of binding
metabolism
cellular macromolecule catabolic process
macromolecule catabolic process
phosphorus metabolic process
positive regulation of macromolecule metabolic process
negative regulation of macromolecule metabolic process
transcription-RNA
RNA processing
transcription from RNA polymerase II promoter
RNA biosynthetic process
mRNA processing
regulation of sequence-specific DNA binding..
mRNA metabolic process
regulation of transcription from RNA polymerase II..
regulation of DNA binding
transcription, DNA-templated
positive regulation of transcription, DNA-templated
intracellular signaling
positive regulation of signal transduction
intracellular receptor signaling pathway
response to peptide hormone
response to endogenous stimulus
transmembrane receptor protein tyrosine kinase..
enzyme linked receptor protein signaling pathway
intracellular signal transduction
protein complex assembly
protein complex assembly
regulation of organelle organization
macromolecular complex subunit organization
cytoskeleton organization
ribonucleoprotein complex biogenesis
ribosome biogenesis
cell projection organization
morphogenesis
in utero embryonic development
neuron differentiation
positive regulation of multicellular organismal process
cell morphogenesis
immune system development
cell migration
positive regulation of cell migration
regulation of cellular component movement
regulation of locomotion
vessel development
vasculature development
hemopoiesis
regulation of cell proliferation
regulation of cell proliferation
regulation of cell death
regulation of cell adhesion
actin filament-based process
positive regulation of cell communication
response to organic substance
phosphorylation
cellular response to stress
response to organic cyclic compound
response to inorganic substance
response to abiotic stimulus

Figure 1

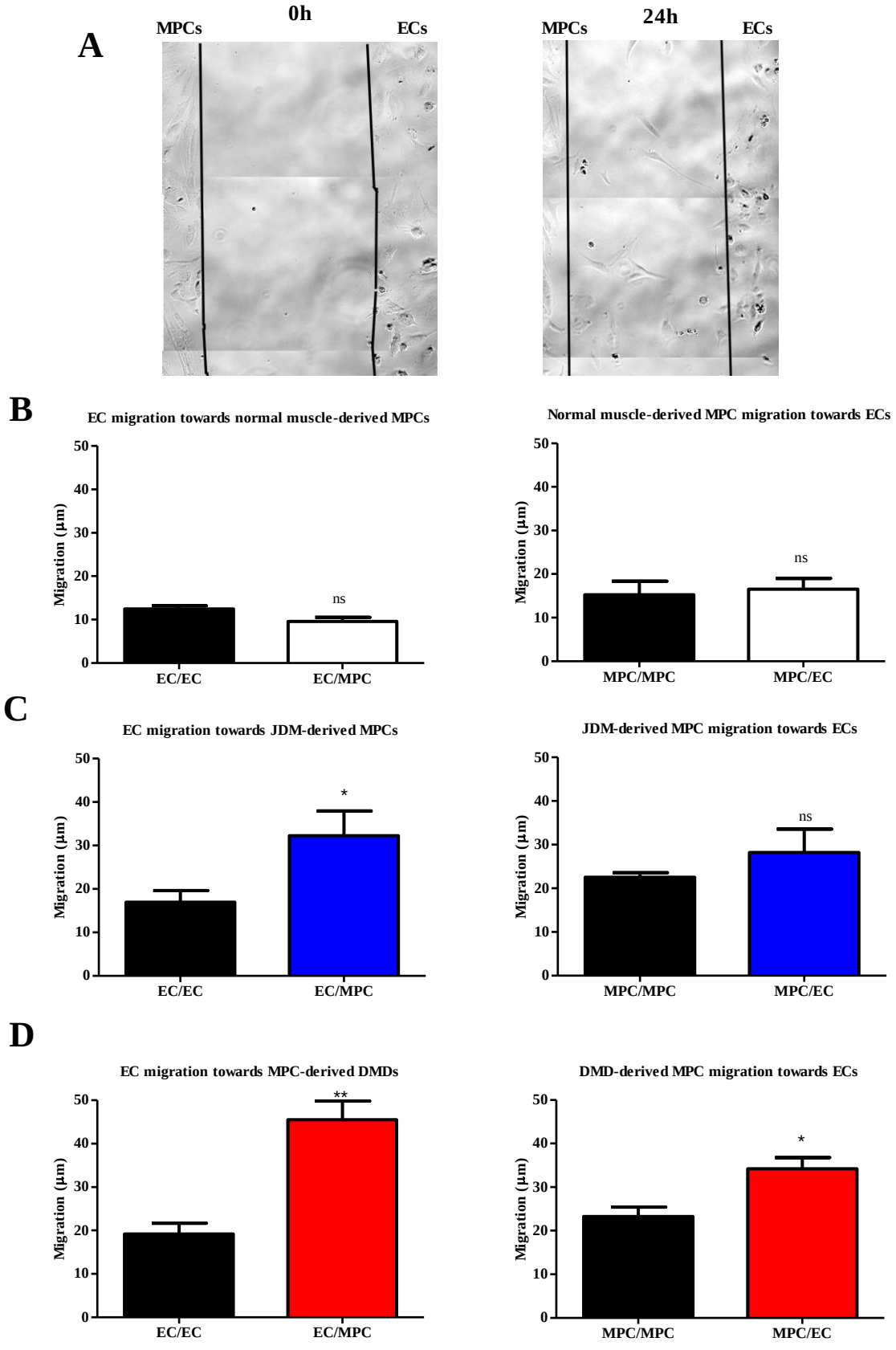

Effects of MPCs on EC migration. (A) MPCs and ECs were cultured in two-chamber devices, so the two cell types faced each other, allowing migration toward each other over a 24 h period. Pictures were taken at 0 and 24 h. (A) Virtual line was drawn on the picture at the cell front at time 0 h and copied to the picture at time 24 h.

Individual cell migration was calculated from this line with ImageJ software. (B,C,D) Individual cell migration of ECs towards normal MPCs (left panel) and of MPCs towards ECs (right panel) for normal muscle-derived MPCs (B), JDM-derived MPCs (C) and DMD-derived MPCs (D). Results are means +/- SEM of 4 independent experiments. Indicated p values: * p< 0.05; **p<0.01.

Figure 2

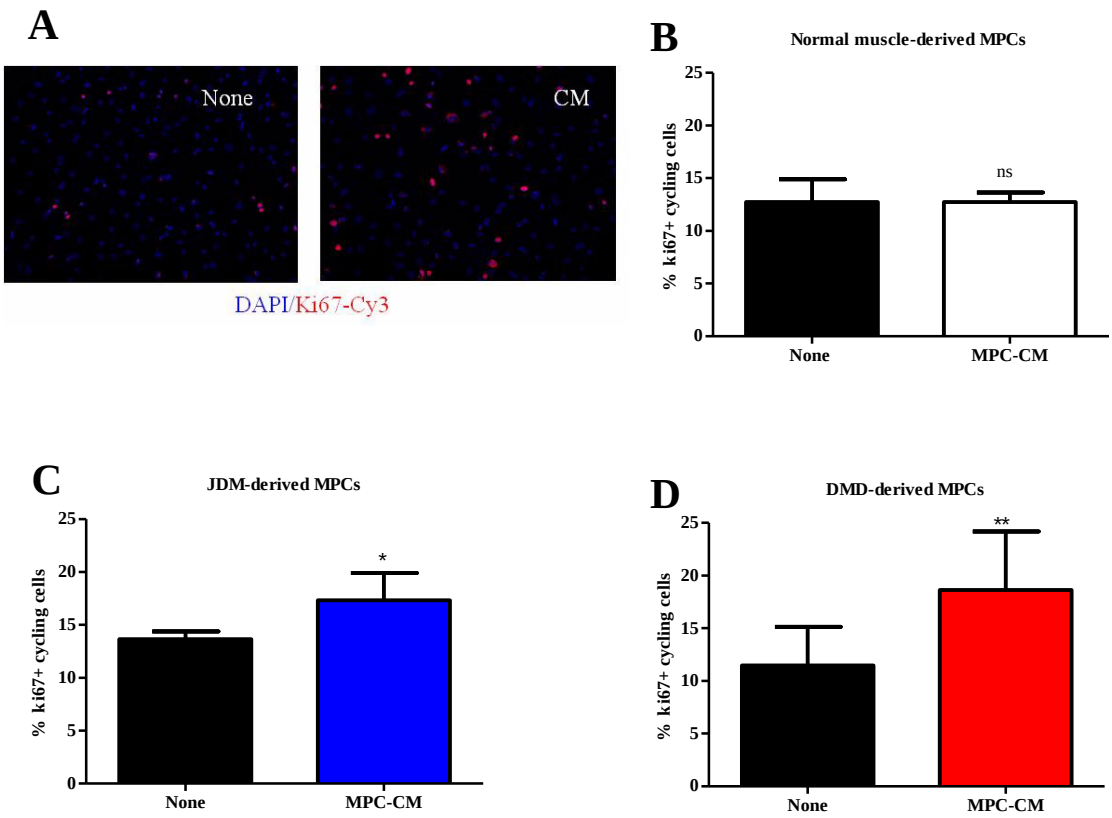

Effects of MPCs on EC proliferation. Proliferation of ECs cultured alone (None) or with MPC-derived conditioned medium (CM) assessed by ki67 staining (red) against Hoechst staining (blue) (A). MPCs were derived from normal (B), JDM (C) and DMD (D) muscle. Results are means +/- SEM of 4 independent experiments. Indicated p values: * p< 0.05; **p<0.01.

Figure 3

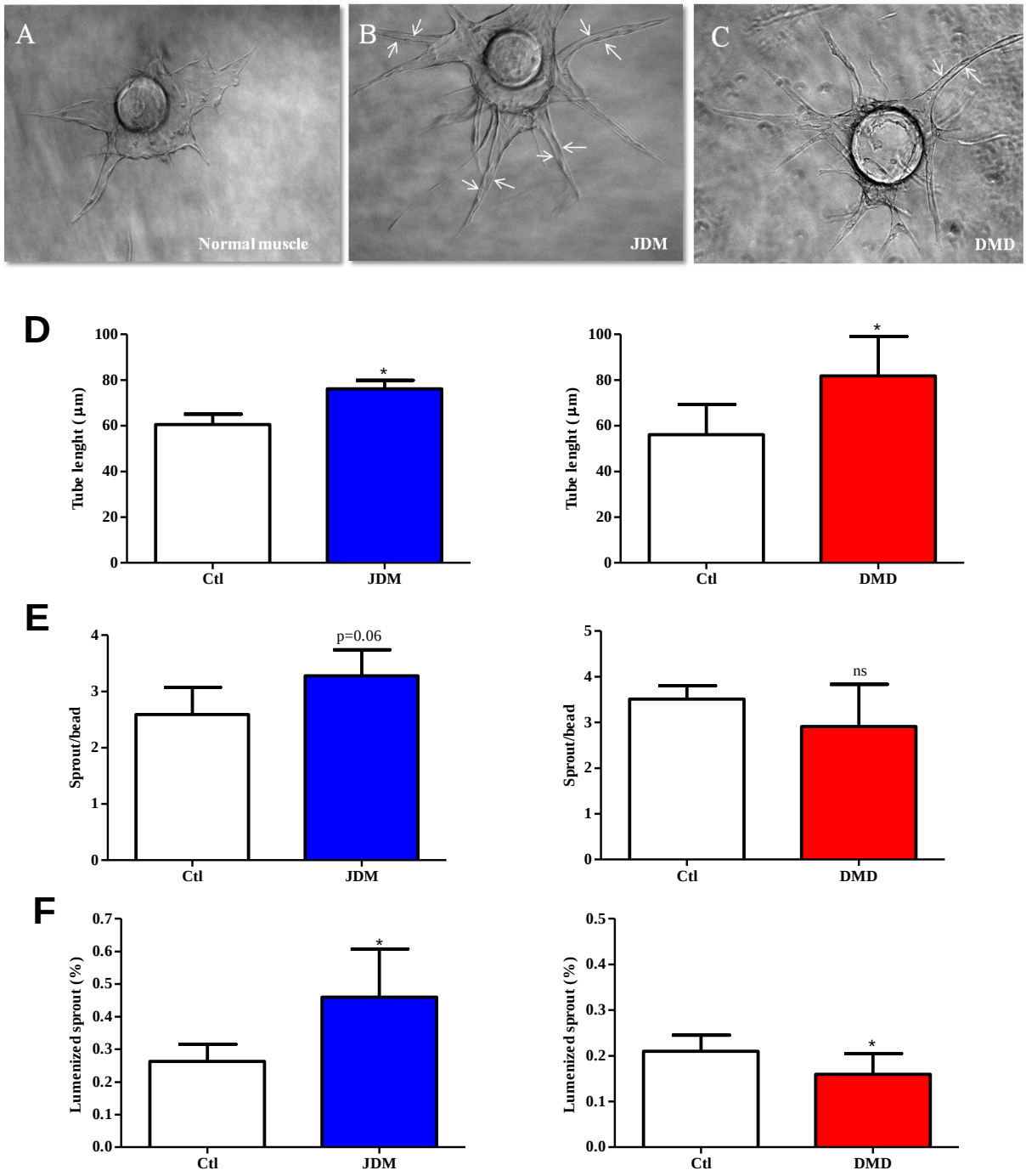

Effects of MPCs on angiogenesis. MPCs derived from normal (A, white bars in D,E,F), JDM (B, blue bars in D,E,F), DMD (C, red bars in D,E,F) were laid on top of fibrin gels containing ECs cultured on collagen-coated cytodex beads and the formation of vessel-like structures is observed 6 days later. These sprouts may contain (arrows) or not (arrowheads) lumen (A-C). The sprout length (expressed in µm) (D), the number of sprout/bead (E) and the % of lumenized sprouts (F) were measured. Results are means +/- SEM of 4 independent experiments. Indicated p values: * p< 0.05; **p<0.01.

Figure 4

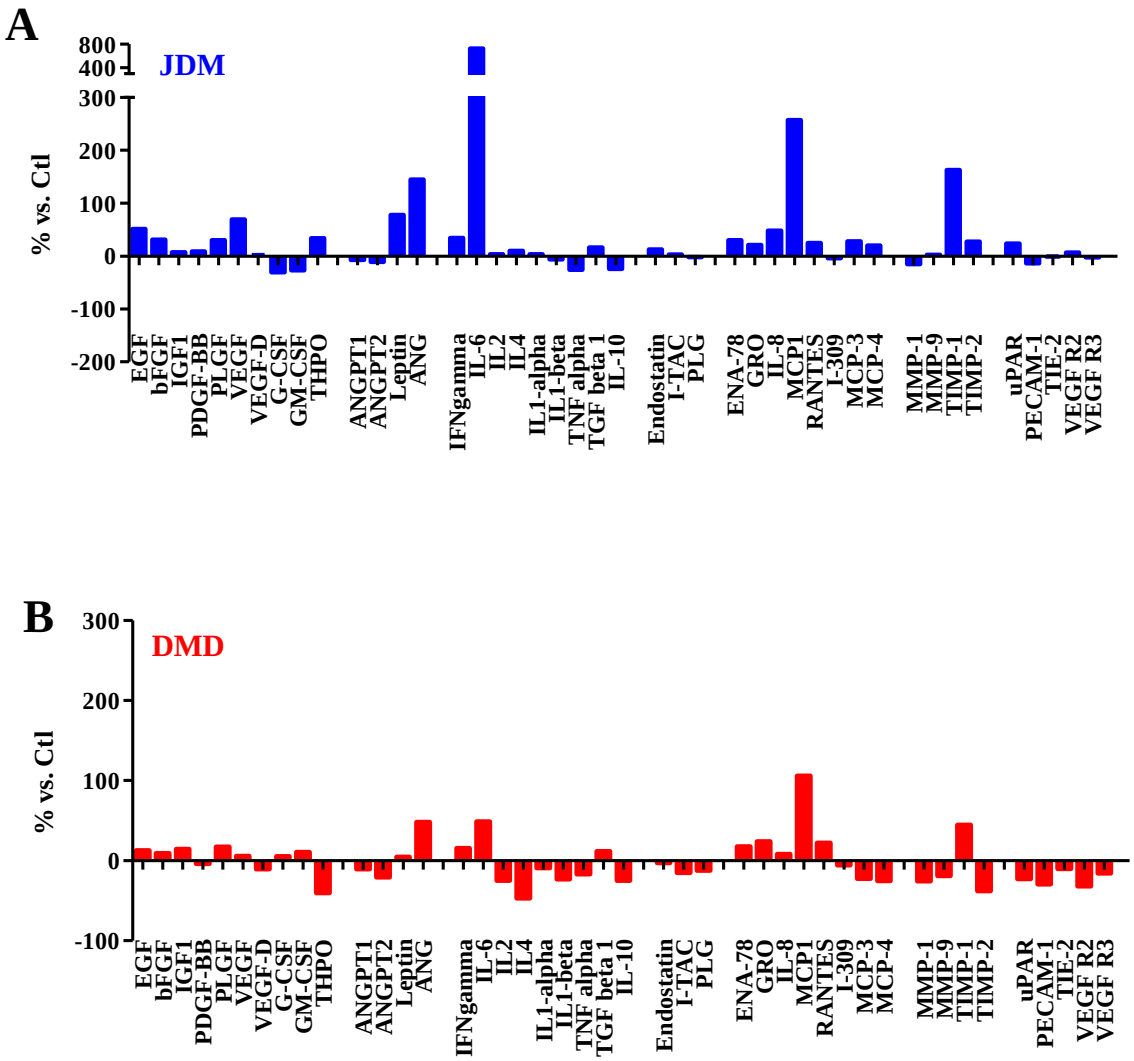

Angiogenic signature of JDM and DMD-derived MPCs. Protein extracts from MPCs were tested on antibodies arrays (example in A) and the signal obtained was analyzed and expressed in fold changes of protein expression in JDM-derived MPCs (B) and DMD-derived MPCs (C) as compared with MPCs issued from normal age-matched muscle. Results are means +/- SEM of 3 independent experiments.

Figure 5

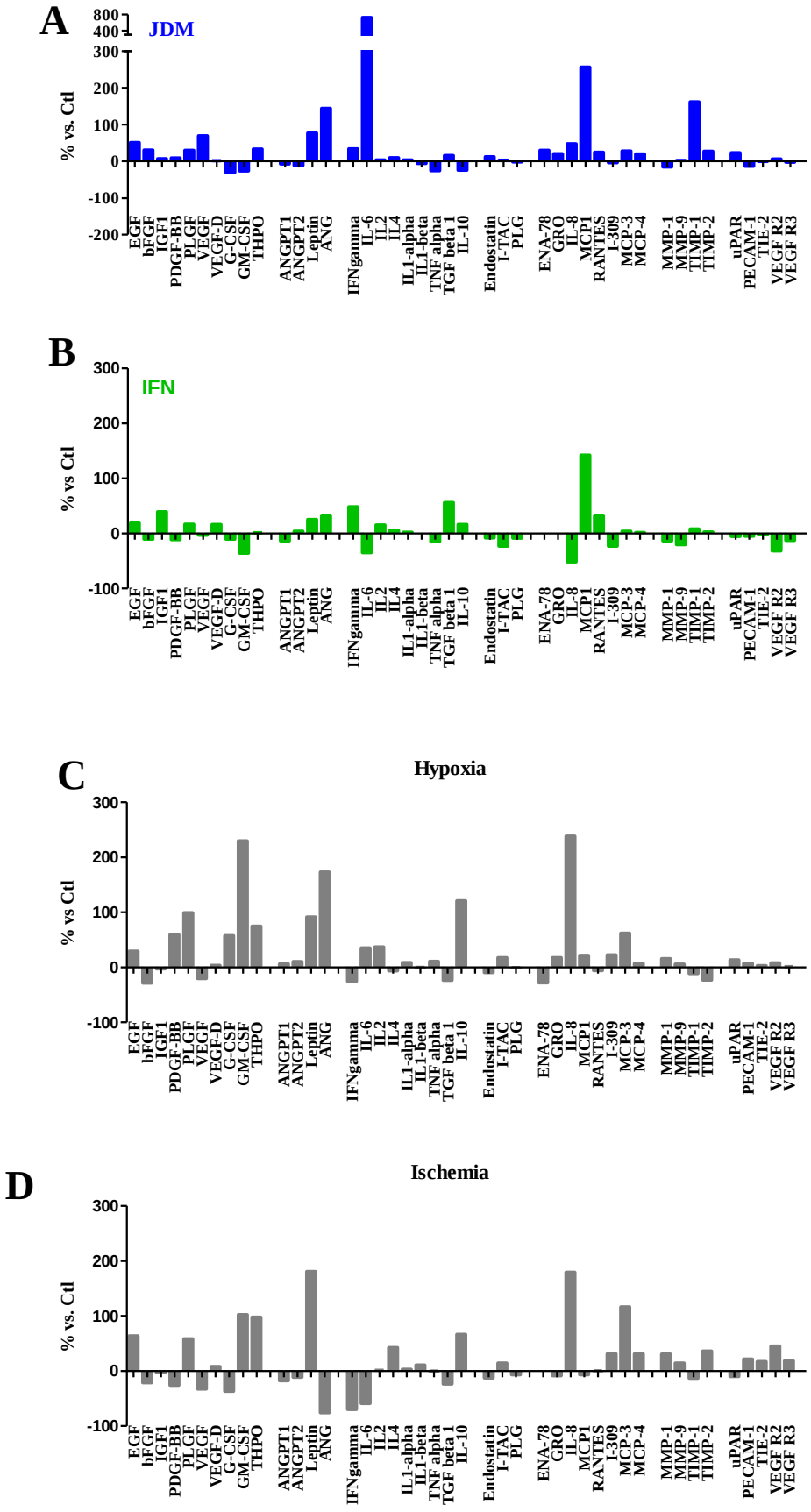
A
JDM
% vs. Ctl
800
400
300
200
100
0
-100
-200
B
IFN
% vs Ctl
300
200
100
0
-100
C
Hypoxia
% vs Ctl
300
200
100
0
-100
D
Ischemia
% vs. Ctl
300
200
100
0
-100
EGF
bFGF
IGF1
PDGF-BB
PLGF
VEGF
VEGF-D
G-CSF
GM-CSF
THPO
ANGPT1
ANGPT2
Leptin
ANG
IFNgamma
IL-6
IL2
IL4
IL1-alpha
IL1-beta
TNF alpha
TGF beta 1
IL-10
Endostatin
I-TAC
PLG
ENA-78
GRO
IL-8
MCP1
RANTES
I-309
MCP-3
MCP-4
MMP-1
MMP-9
TIMP-1
TIMP-2
uPAR
PECAM-1
TIE-2
VEGF R2
VEGF R3

IFN-treatment, hypoxia and ischemia partially mimicked angiogenic signature of JDM-derived MPCs. In (A) results obtained in Fig.4B, i.e. angiogenic signature of JDM-derived MPCs, were reported for an easier comparison with signature of MPCs treated with β-IFN (B), MPCs incubated in hypoxic condition (C), MPCs incubated in ischemic condition (D). Results are expressed in fold changes as compared with untreated MPCs and are means +/- SEM of 3 independent experiments.

CONCLUSION AND PERSPECTIVES

Conclusions and perspectives

As detailed in the introduction part, the skeletal muscle microvasculature possesses unexpected and newly identified roles. The idea that muscle microvasculature only provides the oxygen and nutrient supply is now largely outdated. It has become increasingly clear that the muscle vasculature plays an important role in myogenesis. In turn, muscle cells secrete angiogenic factors in response to changes in metabolic demand or stress. Expanding spectrum of the muscle-vessels interactions has been recently described in physiological situations (exercice, aging, development...) and during muscle repair after an injury. Skeletal muscle exhibits an exceptional capacity to recover from injury. This capacity is conferred by satellite cells located between the basal lamina and the sarcolema of mature myofibers. In addition, satellite cells reside in close proximity to capillaries and receive support from endothelial cells via various growth factors. The bulk of my work was to explore interrelations between vessel and muscle in some human myopathies.

At the tissue level:" capillaries and myofibers close proximity for better or worse…"

The knowledge of microvascular bed microanatomy is a prerequisite of studies of the vessel-muscle interactions at the tissue level. We have previously studied in details the microvascular anatomy in normal adult muscle. The adult normal muscle MVU, which is the smallest functional unit for control of blood flow highly conserved between human and mouse, is formed of 6–8 capillaries. Arcade arterioles located in the perimysium feed transverse arterioles, which penetrate into the endomysium, and divide asymmetrically to yield terminal arterioles which, in turn, resolve into capillaries. Once formed, capillaries run in parallel to the muscle fibers to collect in venules situated up or down the length of the fiber (Gitiaux et al., 2013). The understanding of the normal microvascular anatomy allowed the reassessment of the capillary loss in adult DM. The demonstration that early capillary loss

obeys a 6-by-6 rule, consistent with whole MVU drops out rather than random capillary damage, raised new pathophysiologic hypothesis in DM.

Furthermore, we have studied the age-related variations of the muscle microvasculature, and established the capillary density (CD) per fascicular area and capillary-to-fiber (C/F) ratio in normal deltoid muscle at various pediatric ages, showing that CD and C/F correlated significantly with age. On this basis, we confirmed in each age group a significant decrease of deltoid muscle capillarization in severe JDM patients. This provides the first conclusive documentation of capillary loss in severe JDM (article 1).

These studies of the microvascular network in human were obtained in the 2D space, not allowing the assessment of the vessel geometry. In our laboratory, using 3D reconstructions of the microvascular network in Flk1GFP/+ old *mdx* mice, significant capillary alterations were substantiated and were characterized by a marked increase in tortuosity and irregular scattering of capillaries characterized by a higher anastomose count (Claire Latroche, in review, Figure 13)

One perspective of this work could be to further analyse in 3D the microvascular human anatomy in normal or in pathologic conditions. Indeed, it is tempting to reproduce the study carried out in *mdx* mice using a multi-photon scanner resonant confocal microscope on 100 µm human muscle sections immunostained for CD31.

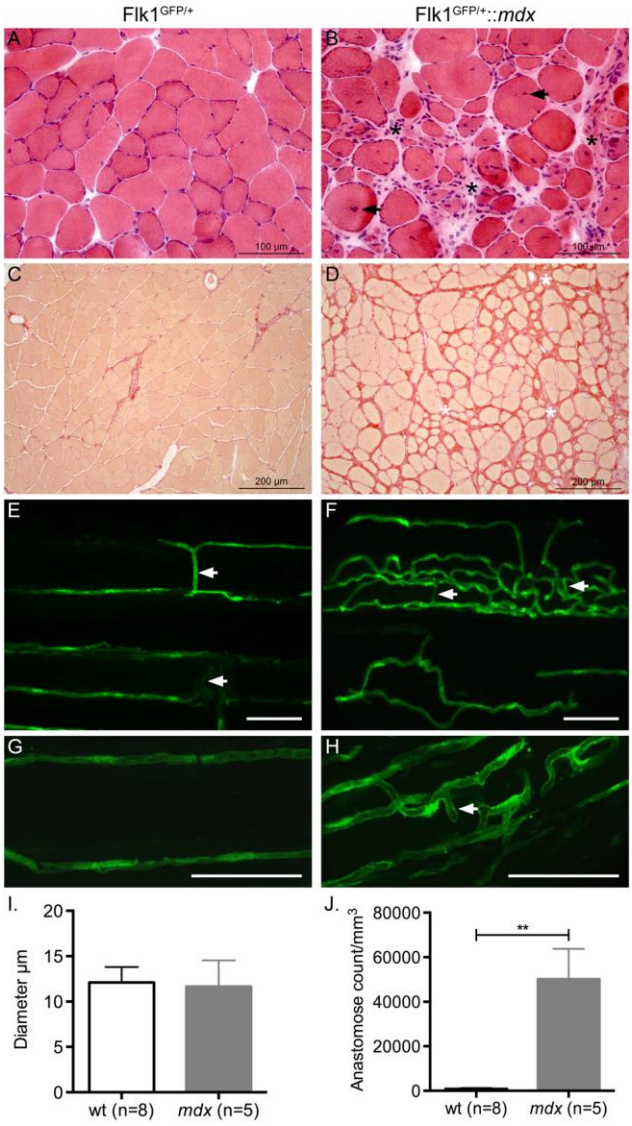

Figure 13. Alteration of microvascular network in 12 month-old *mdx* mice. (Claire Latroche in review Am J Pathol)

Twelve month-old wild-type mice display histologically normal muscles (A), with no fibrosis (C), and regularly scattered capillaries along myofibers, with few anastomoses (E,G,J). In contrast, 12 month-old *mdx* mice display chronic histological lesions (B), characterized by multifocal inflammatory infiltrates (mostly macrophages), included in endomysial collagen tissue (fibrosis; stars), associated with a marked variation in myofiber size and the presence of atrophic and regenerating myofibers displaying centrally-located nuclei (arrows). Sirius red staining and fluorescence microscopy reveal a moderate to marked endomysial fibrosis (D) and microvascular network alterations (F,H), characterized by irregularly scattered tortuous capillaries (Scale bars: 50µm). Even if capillary diameter is similar between *mdx* and wild-type mice (I), a clear increase in anastomose count/mm3 is detected for old *mdx* mice (J). A, B: HE staining. C, D: Sirius red staining (specific for collagen staining). **p<0,01.

A second perspective of this work would be the confirmation of clinical and histological predictive factors by a multicentric prospective study in JDM. Although we ensured the homogeneity of the dataset, the monocentric design of our study restricts the number of patients for some important aspects of the disease (eg, autoantibodies screening, muscle MRI assessment), calling for further research. Particularly, large series of JDM patients will be of particular interest to decipher the relative contributions of the autoantibodies screening correlated with biopsy features and to explore new applications of the muscle MRI, including assessment of the vasculopathy with Diffusion-weighted MR imaging (DWI) (Qi et al., 2008).

At the cellular and molecular level: MPCs and ECs interactions, the science of cohabitation…

Previous work of the laboratory showed the crucial role of endothelial cells during normal muscle regeneration (Abou-Khalil et al., 2009; Christov et al., 2007). Skeletal muscle regeneration following injury is regulated by a highly coordinated gene expression program that drives muscle precursor cells to be activated very rapidly, and then proliferate and differentiate (Bentzinger et al., 2013). Within the complexity of regenerating muscles, satellite cells are submitted to a variable environment determined by the spatial and temporal presence of cytokines, growth factors and other cell types including granulocytes, monocytes, macrophages, fibroblasts, endothelial and periendothelial cells. Vascular cells number peak is concomitant with the one of satellite cells/myoblasts, consistent with the role of vascular cells to promote myoblasts proliferation and self-renewal (Luque et al., 1995; Ochoa et al., 2007) (Figure 14). Reciproqually, MPCs are proangionenic and promote the formation of capillary-like structures in 3D models of angiogenesis (Christov et al., 2007; Latroche, personnal data). We demonstrated in human myopathies that MPC mediated-angiogenesis is modified depending on the pathologic context of regenerating muscles.

Figure 14: Participation of non-myogenic cell types in muscle regeneration. The relative presence of immune, fibrotic, vascular and myogenic cell types after muscle injury (adapted from Bentzinger et al., 2013).

In DMD, dysregulation of the angiogenesis/ myogenesis coupling:

MPCs mediated angiogenesis is altered. The coupling between angiogenesis and myogenesis that is observed during skeletal muscle regeneration is not operative in this context, likely due to strong defect in MPC homeostasis. Furthermore, loss of dystrophin in smooth muscle results in decreased capacity of vasculature to respond to shear stress induced endothelium-

dependant dilatation, probably related to NO production alteration (Loufrani et al., 2001). An original approach using *in vivo* nuclear magnetic resonance (NMR) in Flk1GFP/+ crossed with *mdx* mice, demonstrated *in vivo* functional modifications of muscle perfusion in the mouse model of DMD (Latroche et al; in review). In DMD we showed *in vitro* that the dysregulation of the muscle homeostasis is associated with an alteration of the MPCs capacities to promote a functionnal angiogenesis. ECs unbalanced homeotasis would in turn provoke an alteration of myofiber regeneration maintaining a vicious circle. Collectively, these results suggest that complex interactions between angiogenesis and myogenesis could be progressively affected in DMD, relevant for a progressive exhaustion of the muscle function, not-controlled by vessels.

Proposed model for JDM pathophysiology:

Increasing number of studies has been carried out to decipher the role of the mysterious combination of pathogenic features in JDM: specific vascular changes associated with muscle injury and inflammation. It has become widely understood that cytokines play a significant role in regulating immune responses in JDM. Particular attention has been drawn to a class of cytokines known as type 1 IFNs mostly consisting of α-IFN and β-IFN and their involvement in the pathogenesis (Arshanapalli et al., 2014).

Our study allows a better understanding of the interrelations at work between MPCs and ECs in JDM. Indeed, the description of MPCs effects on the ECs functions *in vitro* and the transcriptomic analysis of isolated MPCs and ECs from JDM muscles provide new cues for the JDM pathophysiology. We confirmed that the vessel pathology is a central feature of the JDM pathophysiology, ECs exhibiting an "antiangiogenic signature" including a strong upregulation of *CXCL10/IP10 CXCL11/I-TAC* and *MRP8/14*. We demonstrated that MPCs fully participate in vessel reconstruction, through response to inflammatory signal including

type1 IFNs leading to the expression of a specific "IFN signature". MPCs enhance their capacities to induce angiogenesis through the secretion of various factors including high levels of IFN regulated chemokines (MCP-1/CCL-2) and IL-6 triggering extensive gene reprogrammation in ECs, finally favorable to angiogenesis (Figure 15).

One perspective of this work could be to further explore *in vivo*, using an animal model, the ECs and MPCs interactions. However, currently no relevant animal model of dermatomyositis exists, so that *in vivo* exploration of these mechanisms will likely await future development of such a model. A second perspective could be to analyse the interactions between monocytes and endothelial cells in JDM to elucidate the involvement of this third partner in the vessel injury.

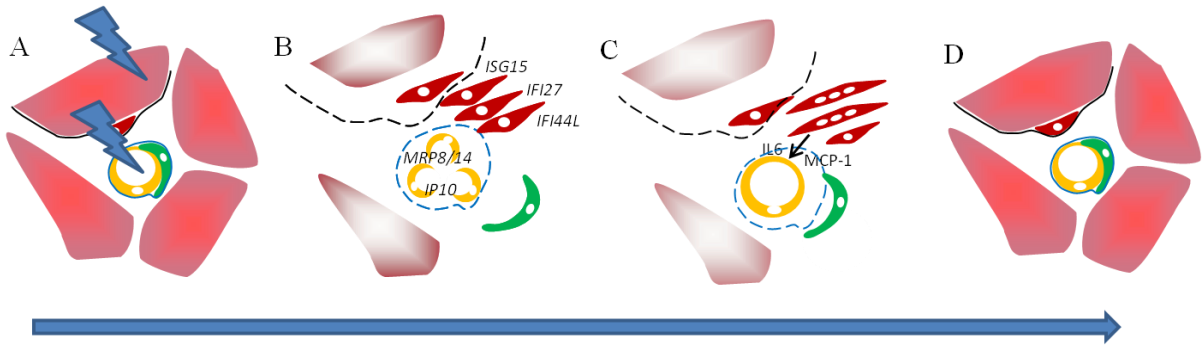

Figure 15: Proposed model for JDM pathophysiology: A) An initial non specific muscle injury with main vessel damages is associated with ECs and MPCs activation B) The subsequent inflammatory response is characterized by strong IFN upregulation (secreted by PDCs and others cells?), the transcriptomic analysis of MPCs showing an specific "type 1 IFNs signature" (upregulation of *IFI27, ISG15, IFI44L*…) and the transcriptomic analysis of ECs showing an "antiangiogenic signature" (upregulation of *IP10, MRP8/14,* dowregulation of genes involved in the vessel development) C) MPCs promote angiogenesis by secretion of various factors including high levels of IFN-regulated cytokines (MCP-1/CCL2) and IL-6 (via an MRP8/14-dependent pathway?) D) The coordinated deregulation of type1-IFN signaling and IL-6 production may further promote the neoangiogenesis and sustain the inflammatory response. In most cases, the angiogenesis/myogenenesis coupling is efficient and allows the restoration of a normal muscle function.

References

Abou-Khalil, R., Le Grand, F., Pallafacchina, G., Valable, S., Authier, F.-J., Rudnicki, M.A., Gherardi, R.K., Germain, S., Chretien, F., Sotiropoulos, A., et al. (2009). Autocrine and paracrine angiopoietin 1/Tie-2 signaling promotes muscle satellite cell self-renewal. Cell Stem Cell *5*, 298–309.

Abou-Khalil, R., Mounier, R., and Chazaud, B. (2010). Regulation of myogenic stem cell behavior by vessel cells: the "ménage à trois" of satellite cells, periendothelial cells and endothelial cells. Cell Cycle. *9*, 892–896.

Alvarez-Buylla, A., and Lim, D.A. (2004). For the long run: maintaining germinal niches in the adult brain. Neuron *41*, 683–686.

Arany, Z., Foo, S.-Y., Ma, Y., Ruas, J.L., Bommi-Reddy, A., Girnun, G., Cooper, M., Laznik, D., Chinsomboon, J., Rangwala, S.M., et al. (2008). HIF-independent regulation of VEGF and angiogenesis by the transcriptional coactivator PGC-1alpha. Nature *451*, 1008–1012.

Arshanapalli, A., Shah, M., Veerula, V., and Somani, A.-K. (2014). The role of type I interferons and other cytokines in dermatomyositis. Cytokine.

Arsic, N., Zacchigna, S., Zentilin, L., Ramirez-Correa, G., Pattarini, L., Salvi, A., Sinagra, G., and Giacca, M. (2004). Vascular endothelial growth factor stimulates skeletal muscle regeneration in vivo. Mol. Ther. J. Am. Soc. Gene Ther. *10*, 844–854.

Augustin, H.G., Young Koh, G., Thurston, G., and Alitalo, K. (2009). Control of vascular morphogenesis and homeostasis through the angiopoietin–Tie system. Nat. Rev. Mol. Cell Biol. *10*, 165–177.

Baar, K., Wende, A.R., Jones, T.E., Marison, M., Nolte, L.A., Chen, M.A.Y., Kelly, D.P., and Holloszy, J.O. (2002). Adaptations of skeletal muscle to exercise: rapid increase in the transcriptional coactivator PGC-1. FASEB J. *16*, 1879–1886.

Baechler, E.C., Bauer, J.W., Slattery, C.A., Ortmann, W.A., Espe, K.J., Novitzke, J., Ytterberg, S.R., Gregersen, P.K., Behrens, T.W., and Reed, A.M. (2007). An interferon signature in the peripheral blood of dermatomyositis patients is associated with disease activity. Mol. Med. *13*, 59.

Bai, Y., Cui, M., Meng, Z., Shen, L., He, Q., Zhang, X., Chen, F., and Xiao, J. (2009). Ectopic expression of angiopoietin-1 promotes neuronal differentiation in neural progenitor cells through the Akt pathway. Biochem. Biophys. Res. Commun. *378*, 296–301.

Bailey, A.M., O'Neill, T.J., Morris, C.E., and Peirce, S.M. (2008). Arteriolar Remodeling Following Ischemic Injury Extends from Capillary to Large Arteriole in the Microcirculation. Microcirc. N. Y. N 1994 *15*, 389–404.

Baraibar, M.A., Gueugneau, M., Duguez, S., Butler-Browne, G., Bechet, D., and Friguet, B. (2013). Expression and modification proteomics during skeletal muscle ageing. Biogerontology *14*, 339–352.

Batthish, M., and Feldman, B.M. (2011). Juvenile Dermatomyositis. Curr. Rheumatol. Rep. *13*, 216–224.

Bell, C.D., and Conen, P.E. (1968). Histopathological changes in Duchenne muscular dystrophy. J. Neurol. Sci. *7*, 529–544.

Bellamy, L.M., Johnston, A.P.W., De Lisio, M., and Parise, G. (2010). Skeletal muscle-endothelial cell cross talk through angiotensin II. Am. J. Physiol. Cell Physiol. *299*, C1402–C1408.

Bellutti Enders, F., van Wijk, F., Scholman, R., Hofer, M., Prakken, B.J., van Royen-Kerkhof, A., and de Jager, W. (2014). CXCL10, TNFR2 and Galectin-9 correlate with disease activity in Juvenile Dermatomyositis. Arthritis Rheumatol. Hoboken NJ.

Bentzinger, C.F., Wang, Y.X., Dumont, N.A., and Rudnicki, M.A. (2013). Cellular dynamics in the muscle satellite cell niche. EMBO Rep. *14*, 1062–1072.

Bernet, J.D., Doles, J.D., Hall, J.K., Kelly Tanaka, K., Carter, T.A., and Olwin, B.B. (2014). p38 MAPK signaling underlies a cell-autonomous loss of stem cell self-renewal in skeletal muscle of aged mice. Nat. Med. *20*, 265–271.

Bilgic, H., Ytterberg, S.R., Amin, S., McNallan, K.T., Wilson, J.C., Koeuth, T., Ellingson, S., Newman, B., Bauer, J.W., Peterson, E.J., et al. (2009). Interleukin-6 and type I interferon-regulated genes and chemokines mark disease activity in dermatomyositis. Arthritis Rheum. *60*, 3436–3446.

Biressi, S., Miyabara, E.H., Gopinath, S.D., M Carlig, P.M., and Rando, T.A. (2014). A Wnt-TGFβ2 axis induces a fibrogenic program in muscle stem cells from dystrophic mice. Sci. Transl. Med. *6*, 267ra176.

Bloch, E.H., and Iberall, A.S. (1982). Toward a concept of the functional unit of mammalian skeletal muscle. Am. J. Physiol.-Regul. Integr. Comp. Physiol. *242*, R411–R420.

Bloor, C.M. (2005). Angiogenesis during exercise and training. Angiogenesis *8*, 263–271.

Bobadilla, M., Sáinz, N., Rodriguez, J.A., Abizanda, G., Orbe, J., de Martino, A., García Verdugo, J.M., Páramo, J.A., Prósper, F., and Pérez-Ruiz, A. (2014). MMP-10 is required for efficient muscle regeneration in mouse models of injury and muscular dystrophy. Stem Cells Dayt. Ohio *32*, 447–461.

Bode, R.K., Klein-Gitelman, M.S., Miller, M.L., Lechman, T.S., and Pachman, L.M. (2003). Disease activity score for children with juvenile dermatomyositis: Reliability and validity evidence. Arthritis Rheum. *49*, 7–15.

Bohan, A., and Peter, J.B. (1975). Polymyositis and dermatomyositis (first of two parts). N. Engl. J. Med. *292*, 344–347.

Bonapace, L., Coissieux, M.-M., Wyckoff, J., Mertz, K.D., Varga, Z., Junt, T., and Bentires-Alj, M. (2014). Cessation of CCL2 inhibition accelerates breast cancer metastasis by promoting angiogenesis. Nature *515*, 130–133.

Borselli, C., Storrie, H., Benesch-Lee, F., Shvartsman, D., Cezar, C., Lichtman, J.W., Vandenburgh, H.H., and Mooney, D.J. (2010). Functional muscle regeneration with combined delivery of angiogenesis and myogenesis factors. Proc. Natl. Acad. Sci. *107*, 3287–3292.

Brack, A.S., Conboy, M.J., Roy, S., Lee, M., Kuo, C.J., Keller, C., and Rando, T.A. (2007). Increased Wnt signaling during aging alters muscle stem cell fate and increases fibrosis. Science *317*, 807–810.

Breen, E.C., Johnson, E.C., Wagner, H., Tseng, H.M., Sung, L.A., and Wagner, P.D. (1996). Angiogenic growth factor mRNA responses in muscle to a single bout of exercise. J. Appl. Physiol. Bethesda Md 1985 *81*, 355–361.

Brenman, J.E., Chao, D.S., Xia, H., Aldape, K., and Bredt, D.S. (1995). Nitric oxide synthase complexed with dystrophin and absent from skeletal muscle sarcolemma in Duchenne muscular dystrophy. Cell *82*, 743–752.

Brooke, M.H., Fenichel, G.M., Griggs, R.C., Mendell, J.R., Moxley, R., Florence, J., King, W.M., Pandya, S., Robison, J., and Schierbecker, J. (1989). Duchenne muscular dystrophy: patterns of clinical progression and effects of supportive therapy. Neurology *39*, 475–481.

Brooke MH, and Kaiser KK (1970). Muscle fiber types: How many and what kind? Arch. Neurol. *23*, 369–379.

Brown, M.D., Kent, J., Kelsall, C.J., Milkiewicz, M., and Hudlicka, O. (2003). Remodeling in the Microcirculation of Rat Skeletal Muscle During Chronic Ischemia. Microcirculation *10*, 179–191.

Brown, M.D., Kelsall, C.J., Milkiewicz, M., Anderson, S., and Hudlicka, O. (2005). A New Model of Peripheral Arterial Disease: Sustained Impairment of Nutritive Microcirculation and Its Recovery by Chronic Electrical Stimulation. Microcirculation *12*, 373–381.

Brown, V.E., Pilkington, C.A., Feldman, B.M., Davidson, J.E., and Network for Juvenile Dermatomyositis, Paediatric Rheumatology European Society (PReS) (2006). An international consensus survey of the diagnostic criteria for juvenile dermatomyositis (JDM). Rheumatol. Oxf. Engl. *45*, 990–993.

Bryan, B.A., Walshe, T.E., Mitchell, D.C., Havumaki, J.S., Saint-Geniez, M., Maharaj, A.S., Maldonado, A.E., and D'Amore, P.A. (2008). Coordinated vascular endothelial growth factor expression and signaling during skeletal myogenic differentiation. Mol. Biol. Cell *19*, 994–1006.

Buckingham, M., and Vincent, S.D. (2009). Distinct and dynamic myogenic populations in the vertebrate embryo. Curr. Opin. Genet. Dev. *19*, 444–453.

Buckley, A.F., and Bossen, E.H. (2013). Skeletal muscle microvasculature in the diagnosis of neuromuscular disease. J. Neuropathol. Exp. Neurol. *72*, 906–918.

Bulfield, G., Siller, W.G., Wight, P.A., and Moore, K.J. (1984). X chromosome-linked muscular dystrophy (mdx) in the mouse. Proc. Natl. Acad. Sci. U. S. A. *81*, 1189–1192.

Campbell, K.P., and Kahl, S.D. (1989). Association of dystrophin and an integral membrane glycoprotein. Nature *338*, 259–262.

Capela, A., and Temple, S. (2002). LeX/ssea-1 is expressed by adult mouse CNS stem cells, identifying them as nonependymal. Neuron *35*, 865–875.

Caproni, M., Torchia, D., Cardinali, C., Volpi, W., Del Bianco, E., D'Agata, A., and Fabbri, P. (2004). Infiltrating cells, related cytokines and chemokine receptors in lesional skin of patients with dermatomyositis. Br. J. Dermatol. *151*, 784–791.

Carmeliet, P., and Jain, R.K. (2011). Molecular mechanisms and clinical applications of angiogenesis. Nature *473*, 298–307.

Carpenter, S., Karpati, G., Rothman, S., and Watters, G. (1976). The childhood type of dermatomyositis. Neurology *26*, 952–962.

Casciola-Rosen, L., and Mammen, A.L. (2012). Myositis autoantibodies: Curr. Opin. Rheumatol. *24*, 602–608.

Chazaud, B. (2003). Satellite cells attract monocytes and use macrophages as a support to escape apoptosis and enhance muscle growth. J. Cell Biol. *163*, 1133–1143.

Cheung, L.K. (1996). The blood supply of the human temporalis muscle: a vascular corrosion cast study. J. Anat. *189*, 431.

Chilibeck, P.D., Paterson, D.H., Cunningham, D.A., Taylor, A.W., and Noble, E.G. (1997). Muscle capillarization, O2diffusion distance, and V˙ o 2kinetics in old and young individuals. J. Appl. Physiol. *82*, 63–69.

Chinsomboon, J., Ruas, J., Gupta, R.K., Thom, R., Shoag, J., Rowe, G.C., Sawada, N., Raghuram, S., and Arany, Z. (2009). The transcriptional coactivator PGC-1alpha mediates exercise-induced angiogenesis in skeletal muscle. Proc. Natl. Acad. Sci. U. S. A. *106*, 21401–21406.

Christov, C., Chrétien, F., Abou-Khalil, R., Bassez, G., Vallet, G., Authier, F.-J., Bassaglia, Y., Shinin, V., Tajbakhsh, S., Chazaud, B., et al. (2007). Muscle satellite cells and endothelial cells: close neighbors and privileged partners. Mol. Biol. Cell *18*, 1397–1409.

Colmone, A., and Sipkins, D.A. (2008). Beyond angiogenesis: the role of endothelium in the bone marrow vascular niche. Transl. Res. *151*, 1–9.

Conboy, I.M., and Rando, T.A. (2002). The regulation of Notch signaling controls satellite cell activation and cell fate determination in postnatal myogenesis. Dev. Cell *3*, 397–409.

Conboy, I.M., Conboy, M.J., Smythe, G.M., and Rando, T.A. (2003). Notch-mediated restoration of regenerative potential to aged muscle. Science *302*, 1575–1577.

Consolaro, A., Varnier, G.C., Martini, A., and Ravelli, A. (2014). Advances in biomarkers for paediatric rheumatic diseases. Nat. Rev. Rheumatol.

Cosgrove, B.D., Gilbert, P.M., Porpiglia, E., Mourkioti, F., Lee, S.P., Corbel, S.Y., Llewellyn, M.E., Delp, S.L., and Blau, H.M. (2014). Rejuvenation of the muscle stem cell population restores strength to injured aged muscles. Nat. Med. *20*, 255–264.

Crescioli, C., Sottili, M., Bonini, P., Cosmi, L., Chiarugi, P., Romagnani, P., Vannelli, G.B., Colletti, M., Isidori, A.M., Serio, M., et al. (2012). Inflammatory response in human skeletal muscle cells: CXCL10 as a potential therapeutic target. Eur. J. Cell Biol. *91*, 139–149.

Crowe, W.E., Bove, K.E., Levinson, J.E., and Hilton, P.K. (1982). Clinical and pathogenetic implications of histopathology in childhood polydermatomyositis. Arthritis Rheum. *25*, 126–139.

Davis, W.R., Halls, J.E., Offiah, A.C., Pilkington, C., Owens, C.M., and Rosendahl, K. (2011). Assessment of active inflammation in juvenile dermatomyositis: a novel magnetic resonance imaging-based scoring system. Rheumatology *50*, 2237–2244.

Day, K., Shefer, G., Shearer, A., and Yablonka-Reuveni, Z. (2010). The depletion of skeletal muscle satellite cells with age is concomitant with reduced capacity of single progenitors to produce reserve progeny. Dev. Biol. *340*, 330–343.

Deasy, B.M., Feduska, J.M., Payne, T.R., Li, Y., Ambrosio, F., and Huard, J. (2009). Effect of VEGF on the Regenerative Capacity of Muscle Stem Cells in Dystrophic Skeletal Muscle. Mol. Ther. *17*, 1788–1798.

Degens, H., Turek, Z., Hoofd, L.J., and Binkhorst, R.A. (1994). Capillary proliferation related to fibre types in hypertrophied aging rat M. plantaris. Adv. Exp. Med. Biol. *345*, 669–676.

Delavar, H., Nogueira, L., Wagner, P.D., Hogan, M.C., Metzger, D., and Breen, E.C. (2014). Skeletal myofiber VEGF is essential for the exercise training response in adult mice. Am. J. Physiol. Regul. Integr. Comp. Physiol. *306*, R586–R595.

Desguerre, I., Christov, C., Mayer, M., Zeller, R., Becane, H.-M., Bastuji-Garin, S., Leturcq, F., Chiron, C., Chelly, J., and Gherardi, R.K. (2009). Clinical Heterogeneity of Duchenne Muscular Dystrophy (DMD): Definition of Sub-Phenotypes and Predictive Criteria by Long-Term Follow-Up. PLoS ONE *4*, e4347.

Desplanches, D., Hoppeler, H., Tüscher, L., Mayet, M.H., Spielvogel, H., Ferretti, G., Kayser, B., Leuenberger, M., Grünenfelder, A., and Favier, R. (1996). Muscle tissue adaptations of high-altitude natives to training in chronic hypoxia or acute normoxia. J. Appl. Physiol. Bethesda Md 1985 *81*, 1946–1951.

Ding, L., Saunders, T.L., Enikolopov, G., and Morrison, S.J. (2012). Endothelial and perivascular cells maintain haematopoietic stem cells. Nature *481*, 457–462.

Dobaczewski, M., Akrivakis, S., Nasser, K., Michael, L.H., Entman, M.L., and Frangogiannis, N.G. (2004). Vascular mural cells in healing canine myocardial infarcts. J. Histochem. Cytochem. Off. J. Histochem. Soc. *52*, 1019–1029.

Doles, J.D., and Olwin, B.B. (2014). The impact of JAK-STAT signaling on muscle regeneration. Nat. Med. *20*, 1094–1095.

Egginton, S. (2009). Invited review: activity-induced angiogenesis. Pflüg. Arch. Eur. J. Physiol. *457*, 963–977.

Egginton, S. (2011). Physiological factors influencing capillary growth: Physiological angiogenesis. Acta Physiol. *202*, 225–239.

Egginton, S., Hudlicka, O., Brown, M.D., Graciotti, L., and Granata, A.L. (1996). In vivo pericyte-endothelial cell interaction during angiogenesis in adult cardiac and skeletal muscle. Microvasc. Res. *51*, 213–228.

Egginton, S., Zhou, A.-L., Brown, M.D., and Hudlicka, O. (2001). Unorthodox angiogenesis in skeletal muscle. Cardiovasc. Res. *49*, 634–646.

Eliason, G., Abdel-Halim, S.M., Piehl-Aulin, K., and Kadi, F. (2010). Alterations in the muscle-to-capillary interface in patients with different degrees of chronic obstructive pulmonary disease. Respir. Res. *11*, 97.

Ellis, S.L., Grassinger, J., Jones, A., Borg, J., Camenisch, T., Haylock, D., Bertoncello, I., and Nilsson, S.K. (2011). The relationship between bone, hemopoietic stem cells, and vasculature. Blood *118*, 1516–1524.

Emanueli, C., Salis, M.B., Pinna, A., Graiani, G., Manni, L., and Madeddu, P. (2002). Nerve growth factor promotes angiogenesis and arteriogenesis in ischemic hindlimbs. Circulation *106*, 2257–2262.

Emslie-Smith, A.M., and Engel, A.G. (1990). Microvascular changes in early and advanced dermatomyositis: a quantitative study. Ann. Neurol. *27*, 343–356.

Engel, A. G. and Franzini-Armstrong, C. (2004). Myology. McGraw-Hill Professional I, 1960.

Engelson, E.T., Skalak, T.C., and Schmid-Schönbein, G.W. (1985). The microvasculature in skeletal muscle. I. Arteriolar network in rat spinotrapezius muscle. Microvasc. Res. *30*, 29–44.

Engelson, E.T., Schmid-Schönbein, G.W., and Zweifach, B.W. (1986). The microvasculature in skeletal muscle: II. Arteriolar network anatomy in normotensive and spontaneously hypertensive rats. Microvasc. Res. *31*, 356–374.

Ennen, J.P., Verma, M., and Asakura, A. (2013). Vascular-targeted therapies for Duchenne muscular dystrophy. Skelet. Muscle *3*, 9.

Eriksson, E., and Myrhage, R. (1972). Microvascular Dimensions and Blood Flow in Skeletal Muscle. Acta Physiol. Scand. *86*, 211–222.

Fall, N., Bove, K.E., Stringer, K., Lovell, D.J., Brunner, H.I., Weiss, J., Higgins, G.C., Bowyer, S.L., Graham, T.B., Thornton, S., et al. (2005). Association between lack of angiogenic response in muscle tissue and high expression of angiostatic ELR-negative CXC chemokines in patients with juvenile dermatomyositis: possible link to vasculopathy. Arthritis Rheum. *52*, 3175–3180.

Feldman, B.M., Rider, L.G., Reed, A.M., and Pachman, L.M. (2008). Juvenile dermatomyositis and other idiopathic inflammatory myopathies of childhood. The Lancet *371*, 2201–2212.

Flamme, I., Frölich, T., and Risau, W. (1997). Molecular mechanisms of vasculogenesis and embryonic angiogenesis. J. Cell. Physiol. *173*, 206–210.

Flann, K.L., Rathbone, C.R., Cole, L.C., Liu, X., Allen, R.E., and Rhoads, R.P. (2014). Hypoxia Simultaneously Alters Satellite Cell-Mediated Angiogenesis and Hepatocyte Growth Factor Expression: SATELLITE CELL ANGIOGENESIS DURING HYPOXIA. J. Cell. Physiol. *229*, 572–579.

Forsythe, J.A., Jiang, B.H., Iyer, N.V., Agani, F., Leung, S.W., Koos, R.D., and Semenza, G.L. (1996). Activation of vascular endothelial growth factor gene transcription by hypoxia-inducible factor 1. Mol. Cell. Biol. *16*, 4604–4613.

Franzi, S., Salajegheh, M., Nazareno, R., and Greenberg, S.A. (2013). Type 1 interferons inhibit myotube formation independently of upregulation of interferon-stimulated gene 15. PLoS.One. *8*, e65362.

Froehner, S.C., Reed, S.M., Anderson, K.N., Huang, P.L., and Percival, J.M. (2015). Loss of nNOS inhibits compensatory muscle hypertrophy and exacerbates inflammation and eccentric contraction-induced damage in mdx mice. Hum. Mol. Genet. *24*, 492–505.

Fry, C.S., Lee, J.D., Mula, J., Kirby, T.J., Jackson, J.R., Liu, F., Yang, L., Mendias, C.L., Dupont-Versteegden, E.E., McCarthy, J.J., et al. (2015). Inducible depletion of satellite cells in adult, sedentary mice impairs muscle regenerative capacity without affecting sarcopenia. Nat. Med. *21*, 76–80.

Germani, A., Di, C.A., Mangoni, A., Straino, S., Giacinti, C., Turrini, P., Biglioli, P., and Capogrossi, M.C. (2003). Vascular endothelial growth factor modulates skeletal myoblast function. Am.J.Pathol. *163*, 1417–1428.

Gianni-Barrera R, Trani M, Reginato S, Banfi A (2011). To sprout or to split? VEGF, Notch and vascular morphogenesis. Biochem Soc Trans.*39*, 1644-1648.

Gianni-Barrera, R., Trani, M., Fontanellaz, C., Heberer, M., Djonov, V., Hlushchuk, R., and Banfi, A. (2013). VEGF over-expression in skeletal muscle induces angiogenesis by intussusception rather than sprouting. Angiogenesis *16*, 123–136.

Gianni-Barrera, R., Bartolomeo, M., Vollmar, B., Djonov, V., and Banfi, A. (2014). Split for the cure: VEGF, PDGF-BB and intussusception in therapeutic angiogenesis. Biochem. Soc. Trans. *42*, 1637–1642.

Gillies, A.R., and Lieber, R.L. (2011). Structure and function of the skeletal muscle extracellular matrix. Muscle Nerve *44*, 318–331.

Gitiaux, C., Kostallari, E., Lafuste, P., Authier, F.-J., Christov, C., and Gherardi, R.K. (2012). Whole microvascular unit deletions in dermatomyositis. Ann. Rheum. Dis. *72*, 445–452.

Gouspillou, G., Sgarioto, N., Norris, B., Barbat-Artigas, S., Aubertin-Leheudre, M., Morais, J.A., Burelle, Y., Taivassalo, T., and Hepple, R.T. (2014). The relationship between muscle fiber type-specific PGC-1α content and mitochondrial content varies between rodent models and humans. PloS One *9*, e103044.

Greenberg, S.A., and Amato, A.A. (2004). Uncertainties in the pathogenesis of adult dermatomyositis. Curr. Opin. Neurol. *17*, 359–364.

Greenberg, S.A., Higgs, B.W., Morehouse, C., Walsh, R.J., Kong, S.W., Brohawn, P., Zhu, W., Amato, A., Salajegheh, M., White, B., et al. (2012). Relationship between disease activity and type 1 interferon- and other cytokine-inducible gene expression in blood in dermatomyositis and polymyositis. Genes Immun. *13*, 207–213.

Gridley, T. (2010). Notch signaling in the vasculature. Curr. Top. Dev. Biol. *92*, 277–309.

Guerrouahen, B.S., Al-Hijji, I., and Tabrizi, A.R. (2011). Osteoblastic and Vascular Endothelial Niches, Their Control on Normal Hematopoietic Stem Cells, and Their Consequences on the Development of Leukemia. Stem Cells Int. *2011*, 1–8.

Handschin, C., and Spiegelman, B.M. (2011). PGC-1 coactivators and the regulation of skeletal muscle fiber-type determination. Cell Metab. *13*, 351; author reply 352.

Hansen-Smith, F.M., Hudlicka, O., and Egginton, S. (1996). In vivo angiogenesis in adult rat skeletal muscle: early changes in capillary network architecture and ultrastructure. Cell Tissue Res. *286*, 123–136.

Harris, B.A. (2005). The influence of endurance and resistance exercise on muscle capillarization in the elderly: a review. Acta Physiol. Scand. *185*, 89–97.

Hathaway, P.W., Engel, W.K., and Zellweger, H. (1970). Experimental myopathy after microarterial embolization; comparison with childhood x-linked pseudohypertrophic muscular dystrophy. Arch. Neurol. *22*, 365–378.

Hepple, R.T., and Mathieu-Costello, O. (2001). Estimating the size of the capillary-to-fiber interface in skeletal muscle: a comparison of methods. J. Appl. Physiol. *91*, 2150–2156.

Hepple, R.T., Mackinnon, S.L.M., Goodman, J.M., Thomas, S.G., and Plyley, M.J. (1997). Resistance and aerobic training in older men: effects onV˙o 2 peak and the capillary supply to skeletal muscle. J. Appl. Physiol. *82*, 1305–1310.

Herbert, S.P., and Stainier, D.Y.R. (2011). Molecular control of endothelial cell behaviour during blood vessel morphogenesis. Nat. Rev. Mol. Cell Biol. *12*, 551–564.

Herrera, M.D., Mingorance, C., Rodríguez-Rodríguez, R., and Alvarez de Sotomayor, M. (2010). Endothelial dysfunction and aging: An update. Ageing Res. Rev. *9*, 142–152.

Hoier, B., and Hellsten, Y. (2014). Exercise-Induced Capillary Growth in Human Skeletal Muscle and the Dynamics of VEGF. Microcirculation *21*, 301–314.

Høier, B., Olsen, K., Nyberg, M., Bangsbo, J., and Hellsten, Y. (2010a). Contraction-induced secretion of VEGF from skeletal muscle cells is mediated by adenosine. Am. J. Physiol. Heart Circ. Physiol. *299*, H857–H862.

Høier, B., Rufener, N., Bojsen-Møller, J., Bangsbo, J., and Hellsten, Y. (2010b). The effect of passive movement training on angiogenic factors and capillary growth in human skeletal muscle: Angiogenic factors and capillary growth in skeletal muscle. J. Physiol. *588*, 3833–3845.

Hoier, B., Prats, C., Qvortrup, K., Pilegaard, H., Bangsbo, J., and Hellsten, Y. (2013). Subcellular localization and mechanism of secretion of vascular endothelial growth factor in human skeletal muscle. FASEB J. *27*, 3496–3504.

Huber, A., and Feldman, B.M. (2013). An update on inflammatory myositis in children: Curr. Opin. Rheumatol. *25*, 630–635.

Huber, A.M., Lang, B., LeBlanc, C.M., Birdi, N., Bolaria, R.K., Malleson, P., MacNeil, I., Momy, J.A., Avery, G., and Feldman, B.M. (2000). Medium- and long-term functional outcomes in a multicenter cohort of children with juvenile dermatomyositis. Arthritis Rheum. *43*, 541–549.

Huber, A.M., Feldman, B.M., Rennebohm, R.M., Hicks, J.E., Lindsley, C.B., Perez, M.D., Zemel, L.S., Wallace, C.A., Ballinger, S.H., Passo, M.H., et al. (2004). Validation and clinical significance of the Childhood Myositis Assessment Scale for assessment of muscle function in the juvenile idiopathic inflammatory myopathies. Arthritis Rheum. *50*, 1595–1603.

Hudlicka, O. (1998). Is physiological angiogenesis in skeletal muscle regulated by changes in microcirculation? Microcirc. N. Y. N 1994 *5*, 7–23.

Hudlicka, O. (2011). Microcirculation in skeletal muscle. Muscles Ligaments Tendons J. *1*, 3.

Hudlicka, O., and Brown, M.D. (2009). Adaptation of Skeletal Muscle Microvasculature to Increased or Decreased Blood Flow: Role of Shear Stress, Nitric Oxide and Vascular Endothelial Growth Factor. J. Vasc. Res. *46*, 504–512.

Iademarco, M.F., McQuillan, J.J., and Dean, D.C. (1993). Vascular cell adhesion molecule 1: contrasting transcriptional control mechanisms in muscle and endothelium. Proc. Natl. Acad. Sci. U. S. A. *90*, 3943–3947.

Ito, K. (2006). Smooth muscle-specific dystrophin expression improves aberrant vasoregulation in mdx mice. Hum. Mol. Genet. *15*, 2266–2275.

Jaakkola, P., Mole, D.R., Tian, Y.M., Wilson, M.I., Gielbert, J., Gaskell, S.J., von Kriegsheim, A., Hebestreit, H.F., Mukherji, M., Schofield, C.J., et al. (2001). Targeting of HIF-alpha to the von Hippel-Lindau ubiquitylation complex by O2-regulated prolyl hydroxylation. Science *292*, 468–472.

Jain, M., Smith, M., Cintas, H., Koziol, D., Wesley, R., Harris-Love, M., Lovell, D., Rider, L.G., and Hicks, J. (2006). Intra-rater and inter-rater reliability of the 10-point Manual Muscle Test (MMT) of strength in children with juvenile idiopathic inflammatory myopathies (JIIM). Phys. Occup. Ther. Pediatr. *26*, 5–17.

Jerusalem, F., Engel, A.G., and Gomez, M.R. (1974). Duchenne dystrophy. I. Morphometric study of the muscle microvasculature. Brain J. Neurol. *97*, 115–122.

Jewell, U.R., Kvietikova, I., Scheid, A., Bauer, C., Wenger, R.H., and Gassmann, M. (2001). Induction of HIF-1alpha in response to hypoxia is instantaneous. FASEB J. Off. Publ. Fed. Am. Soc. Exp. Biol. *15*, 1312–1314.

Karvinen, H., Pasanen, E., Rissanen, T.T., Korpisalo, P., Vähäkangas, E., Jazwa, A., Giacca, M., and Ylä-Herttuala, S. (2011). Long-term VEGF-A expression promotes aberrant angiogenesis and fibrosis in skeletal muscle. Gene Ther. *18*, 1166–1172.

Kim, E., Cook-Mills, J., Morgan, G., Sredni, S.T., and Pachman, L.M. (2012). Increased expression of vascular cell adhesion molecule 1 in muscle biopsy samples from juvenile dermatomyositis patients with short duration of untreated disease is regulated by miR-126. Arthritis Rheum. *64*, 3809–3817.

Kim, K., Cho, H.-J., Hahn, J.-Y., Kim, T.-Y., Park, K.-W., Koo, B.-K., Shin, C.S., Kim, C.-H., Oh, B.-H., Lee, M.-M., et al. (2006). Beta-catenin overexpression augments angiogenesis and skeletal muscle regeneration through dual mechanism of vascular endothelial growth factor-mediated endothelial cell proliferation and progenitor cell mobilization. Arterioscler. Thromb. Vasc. Biol. *26*, 91–98.

Kissel, J.T., Mendell, J.R., and Rammohan, K.W. (1986). Microvascular deposition of complement membrane attack complex in dermatomyositis. N. Engl. J. Med. *314*, 329–334.

Kobayashi, N., Takezaki, S., Kobayashi, I., Iwata, N., Mori, M., Nagai, K., Nakano, N., Miyoshi, M., Kinjo, N., Murata, T., et al. (2014). Clinical and laboratory features of fatal rapidly progressive interstitial lung disease associated with juvenile dermatomyositis. Rheumatology.

Koehler, J. (1977). Blood vessel structure in Duchenne muscular dystrophy. I. Light and electron microscopic observations in resting muscle. Neurology *27*, 861–868.

Koenig, M., Hoffman, E.P., Bertelson, C.J., Monaco, A.P., Feener, C., and Kunkel, L.M. (1987). Complete cloning of the Duchenne muscular dystrophy (DMD) cDNA and preliminary genomic organization of the DMD gene in normal and affected individuals. Cell *50*, 509–517.

Kopp, H.-G., Hooper, A.T., Avecilla, S.T., and Rafii, S. (2009). Functional Heterogeneity of the Bone Marrow Vascular Niche. Ann. N. Y. Acad. Sci. *1176*, 47–54.

Kottlors, M., and Kirschner, J. (2010). Elevated satellite cell number in Duchenne muscular dystrophy. Cell Tissue Res. *340*, 541–548.

Krogh, A. (1919). The rate of diffusion of gases through animal tissues, with some remarks on the coefficient of invasion. J. Physiol. *52*, 391–408.

Kuhn, H.G., Dickinson-Anson, H., and Gage, F.H. (1996). Neurogenesis in the dentate gyrus of the adult rat: age-related decrease of neuronal progenitor proliferation. J. Neurosci. Off. J. Soc. Neurosci. *16*, 2027–2033.

Kunisaki, Y., Bruns, I., Scheiermann, C., Ahmed, J., Pinho, S., Zhang, D., Mizoguchi, T., Wei, Q., Lucas, D., Ito, K., et al. (2013). Arteriolar niches maintain haematopoietic stem cell quiescence. Nature *502*, 637–643.

Lagha, M., Brunelli, S., Messina, G., Cumano, A., Kume, T., Relaix, F., and Buckingham, M.E. (2009). Pax3:Foxc2 Reciprocal Repression in the Somite Modulates Muscular versus Vascular Cell Fate Choice in Multipotent Progenitors. Dev. Cell *17*, 892–899.

Latil, M., Rocheteau, P., Châtre, L., Sanulli, S., Mémet, S., Ricchetti, M., Tajbakhsh, S., and Chrétien, F. (2012). Skeletal muscle stem cells adopt a dormant cell state post mortem and retain regenerative capacity. Nat. Commun. *3*, 903.

Lazarevic, D., Pistorio, A., Palmisani, E., Miettunen, P., Ravelli, A., Pilkington, C., Wulffraat, N.M., Malattia, C., Garay, S.M., Hofer, M., et al. (2012). The PRINTO criteria for clinically inactive disease in juvenile dermatomyositis. Ann. Rheum. Dis. *72*, 686–693.

Leick, L., Hellsten, Y., Fentz, J., Lyngby, S.S., Wojtaszewski, J.F.P., Hidalgo, J., and Pilegaard, H. (2009). PGC-1 mediates exercise-induced skeletal muscle VEGF expression in mice. AJP Endocrinol. Metab. *297*, E92–E103.

Lindahl, P., Johansson, B.R., Levéen, P., and Betsholtz, C. (1997). Pericyte loss and microaneurysm formation in PDGF-B-deficient mice. Science *277*, 242–245.

Lo, A., Fuglevand, A.J., and Secomb, T.W. (2003). Oxygen delivery to skeletal muscle fibers: effects of microvascular unit structure and control mechanisms. Am. J. Physiol. Heart Circ. Physiol. *285*, H955–H963.

López de Padilla, C.M., Vallejo, A.N., McNallan, K.T., Vehe, R., Smith, S.A., Dietz, A.B., Vuk-Pavlovic, S., and Reed, A.M. (2007). Plasmacytoid dendritic cells in inflamed muscle of patients with juvenile dermatomyositis. Arthritis Rheum. *56*, 1658–1668.

Lopez-Vales, R., Navarro, X., Shimizu, T., Baskakis, C., Kokotos, G., Constantinou-Kokotou, V., Stephens, D., Dennis, E.A., and David, S. (2008). Intracellular phospholipase A2 group IVA and group VIA play important roles in Wallerian degeneration and axon regeneration after peripheral nerve injury. Brain *131*, 2620–2631.

Loufrani, L. (2004). Absence of Dystrophin in Mice Reduces NO-Dependent Vascular Function and Vascular Density: Total Recovery After a Treatment with the Aminoglycoside Gentamicin. Arterioscler. Thromb. Vasc. Biol. *24*, 671–676.

Loufrani, L., Matrougui, K., Gorny, D., Duriez, M., Blanc, I., Lévy, B.I., and Henrion, D. (2001). Flow (shear stress)–induced endothelium-dependent dilation is altered in mice lacking the gene encoding for dystrophin. Circulation *103*, 864–870.

Loufrani, L., Levy, B.I., and Henrion, D. (2002). Defect in Microvascular Adaptation to Chronic Changes in Blood Flow in Mice Lacking the Gene Encoding for Dystrophin. Circ. Res. *91*, 1183–1189.

Lundby, C., Calbet, J.A.L., and Robach, P. (2009). The response of human skeletal muscle tissue to hypoxia. Cell. Mol. Life Sci. CMLS *66*, 3615–3623.

Luque, E., Peña, J., Martin, P., Jimena, I., and Vaamonde, R. (1995). Capillary supply during development of individual regenerating muscle fibers. Anat. Histol. Embryol. *24*, 87–89.

Lynch, G.S., Hinkle, R.T., Chamberlain, J.S., Brooks, S.V., and Faulkner, J.A. (2001). Force and power output of fast and slow skeletal muscles from mdx mice 6-28 months old. J. Physiol. *535*, 591–600.

Malattia, C., Damasio, M.B., Madeo, A., Pistorio, A., Providenti, A., Pederzoli, S., Viola, S., Buoncompagni, A., Mattiuz, C., Beltramo, A., et al. (2013). Whole-body MRI in the assessment of disease activity in juvenile dermatomyositis. Ann. Rheum. Dis.

Malek, M.H., Olfert, I.M., and Esposito, F. (2009). Detraining losses of skeletal muscle capillarization are associated with vascular endothelial growth factor protein expression in rats. Exp. Physiol. *95*, 359–368.

Mamyrova, G., Kleiner, D.E., James-Newton, L., Shaham, B., Miller, F.W., and Rider, L.G. (2007). Late-onset gastrointestinal pain in juvenile dermatomyositis as a manifestation of ischemic ulceration from chronic endarteropathy. Arthritis Care Res. *57*, 881–884.

Marhaug, G., Shah, V., Shroff, R., Varsani, H., Wedderburn, L.R., Pilkington, C.A., and Brogan, P.A. (2008). Age-dependent inhibition of ectopic calcification: a possible role for fetuin-A and osteopontin in patients with juvenile dermatomyositis with calcinosis. Rheumatol. Oxf. Engl. *47*, 1031–1037.

Mason, S., and Johnson, R.S. (2007). The role of HIF-1 in hypoxic response in the skeletal muscle. Adv. Exp. Med. Biol. *618*, 229–244.

Mason, S.D., Howlett, R.A., Kim, M.J., Olfert, I.M., Hogan, M.C., McNulty, W., Hickey, R.P., Wagner, P.D., Kahn, C.R., Giordano, F.J., et al. (2004). Loss of skeletal muscle HIF-1alpha results in altered exercise endurance. PLoS Biol. *2*, e288.

Mathiesen, P., Hegaard, H., Herlin, T., Zak, M., Pedersen, F., and Nielsen, S. (2012). Long-term outcome in patients with juvenile dermatomyositis: a cross-sectional follow-up study. Scand. J. Rheumatol. *41*, 50–58.

Mathieu-Costello, O. (2005). Greater capillary-fiber interface per fiber mitochondrial volume in skeletal muscles of old rats. J. Appl. Physiol. *99*, 281–289.

Mathieu-Costello, O., Ellis, C.G., Potter, R.F., MacDonald, I.C., and Groom, A.C. (1991). Muscle capillary-to-fiber perimeter ratio: morphometry. Am. J. Physiol. *261*, H1617–H1625.

Mayeuf-Louchart, A., Lagha, M., Danckaert, A., Rocancourt, D., Relaix, F., Vincent, S.D., and Buckingham, M. (2014). Notch regulation of myogenic versus endothelial fates of cells that migrate from the somite to the limb. Proc. Natl. Acad. Sci. *111*, 8844–8849.

McCall, G.E., Byrnes, W.C., Dickinson, A., Pattany, P.M., and Fleck, S.J. (1996). Muscle fiber hypertrophy, hyperplasia, and capillary density in college men after resistance training. J. Appl. Physiol. Bethesda Md 1985 *81*, 2004–2012.

McCann, L.J., Juggins, A.D., Maillard, S.M., Wedderburn, L.R., Davidson, J.E., Murray, K.J., Pilkington, C.A., and Juvenile Dermatomyositis Research Group (2006). The Juvenile Dermatomyositis National Registry and Repository (UK and Ireland)--clinical characteristics of children recruited within the first 5 yr. Rheumatol. Oxf. Engl. *45*, 1255–1260.

Mendell, J.R., Engel, W.K., and Derrer, E.C. (1971). Duchenne muscular dystrophy: functional ischemia reproduces its characteristic lesions. Science *172*, 1143–1145.

Mendelson, A., and Frenette, P.S. (2014). Hematopoietic stem cell niche maintenance during homeostasis and regeneration. Nat. Med. *20*, 833–846.

Messina, S., Mazzeo, A., Bitto, A., Aguennouz, M., Migliorato, A., De Pasquale, M.G., Minutoli, L., Altavilla, D., Zentilin, L., Giacca, M., et al. (2007). VEGF overexpression via adeno-associated virus gene transfer promotes skeletal muscle regeneration and enhances muscle function in mdx mice. FASEB J. *21*, 3737–3746.

Miles, L., Bove, K.E., Lovell, D., Wargula, J.C., Bukulmez, H., Shao, M., Salisbury, S., and Bean, J.A. (2007). Predictability of the clinical course of juvenile dermatomyositis based on initial muscle biopsy: A retrospective study of 72 patients. Arthritis Rheum. *57*, 1183–1191.

Milisenda, J.C., Doti, P.I., Prieto-González, S., and Grau, J.M. (2014). Dermatomyositis presenting with severe subcutaneous edema: Five additional cases and review of the literature. Semin. Arthritis Rheum. *44*, 228–233.

Mitchell, J.P., Dennis, G.J., and Rider, L.G. (2001). Juvenile dermatomyositis presenting with anasarca: A possible indicator of severe disease activity. J. Pediatr. *138*, 942–945.

Miura, S., Kai, Y., Kamei, Y., and Ezaki, O. (2008). Isoform-specific increases in murine skeletal muscle peroxisome proliferator-activated receptor-gamma coactivator-1alpha (PGC-1alpha) mRNA in response to beta2-adrenergic receptor activation and exercise. Endocrinology *149*, 4527–4533.

Miyazaki, D., Nakamura, A., Fukushima, K., Yoshida, K., Takeda, S., and Ikeda, S. -i. (2011). Matrix metalloproteinase-2 ablation in dystrophin-deficient mdx muscles reduces angiogenesis resulting in impaired growth of regenerated muscle fibers. Hum. Mol. Genet. *20*, 1787–1799.

Mohassel, P., Rosen, P., Casciola-Rosen, L., Pak, K., and Mammen, A.L. (2014). Expression of the Dermatomyositis Autoantigen TIF1γ in Regenerating Muscle. Arthritis Rheumatol. n/a – n/a.

Morrison, S.J., and Scadden, D.T. (2014). The bone marrow niche for haematopoietic stem cells. Nature *505*, 327–334.

Mounier, R., Pialoux, V., Roels, B., Thomas, C., Millet, G., Mercier, J., Coudert, J., Fellmann, N., and Clottes, E. (2009). Effect of intermittent hypoxic training on HIF gene expression in human skeletal muscle and leukocytes. Eur. J. Appl. Physiol. *105*, 515–524.

Mounier, R., Chrétien, F., and Chazaud, B. (2011). Blood Vessels and the Satellite Cell Niche. In Current Topics in Developmental Biology, (Elsevier), pp. 121–138.

Muñoz-Cánoves, P., Scheele, C., Pedersen, B.K., and Serrano, A.L. (2013). Interleukin-6 myokine signaling in skeletal muscle: a double-edged sword? FEBS J. *280*, 4131–4148.

Muntoni, F., Torelli, S., and Ferlini, A. (2003). Dystrophin and mutations: one gene, several proteins, multiple phenotypes. Lancet Neurol. *2*, 731–740.

MURRAY, B., and Wilson, D.J. (1997). Muscle patterning, differentiation and vascularisation in the chick wing bud. J. Anat. *190*, 261–273.

Musch, B.C., Papapetropoulos, T.A., McQueen, D.A., Hudgson, P., and Weightman, D. (1975). A comparison of the structure of small blood vessels in normal, denervated and dystrophic human muscle. J. Neurol. Sci. *26*, 221–234.

Myrhage, R., and Eriksson, E. (1980). Vascular arrangements in hind limb muscles of the cat. J. Anat. *131*, 1.

Nagaraju, K., Raben, N., Loeffler, L., Parker, T., Rochon, P.J., Lee, E., Danning, C., Wada, R., Thompson, C., Bahtiyar, G., et al. (2000). Conditional up-regulation of MHC class I in skeletal muscle leads to self-sustaining autoimmune myositis and myositis-specific autoantibodies. Proc. Natl. Acad. Sci. U. S. A. *97*, 9209–9214.

Nakagomi, N., Nakagomi, T., Kubo, S., Nakano-Doi, A., Saino, O., Takata, M., Yoshikawa, H., Stern, D.M., Matsuyama, T., and Taguchi, A. (2009). Endothelial Cells Support Survival, Proliferation, and Neuronal Differentiation of Transplanted Adult Ischemia-Induced Neural Stem/Progenitor Cells After Cerebral Infarction. Stem Cells *27*, 2185–2195.

Naylor, A.J., McGettrick, H.M., Maynard, W.D., May, P., Barone, F., Croft, A.P., Egginton, S., and Buckley, C.D. (2014). A Differential Role for CD248 (Endosialin) in PDGF-Mediated Skeletal Muscle Angiogenesis. PLoS ONE *9*, e107146.

Nguyen, F., Guigand, L., Goubault-Leroux, I., Wyers, M., and Cherel, Y. (2005). Microvessel density in muscles of dogs with golden retriever muscular dystrophy. Neuromuscul. Disord. *15*, 154–163.

Niewold, T.B., Wu, S.C., Smith, M., Morgan, G.A., and Pachman, L.M. (2011). Familial aggregation of autoimmune disease in juvenile dermatomyositis. Pediatrics *127*, e1239–e1246.

Nistala, K., Varsani, H., Wittkowski, H., Vogl, T., Krol, P., Shah, V., Mamchaoui, K., Brogan, P.A., Roth, J., and Wedderburn, L.R. (2013). Myeloid related protein induces muscle derived inflammatory mediators in juvenile dermatomyositis. Arthritis Res. Ther. *15*, R131.

Ochoa, O., Sun, D., Reyes-Reyna, S.M., Waite, L.L., Michalek, J.E., McManus, L.M., and Shireman, P.K. (2007). Delayed angiogenesis and VEGF production in CCR2-/- mice during impaired skeletal muscle regeneration. Am. J. Physiol. Regul. Integr. Comp. Physiol. *293*, R651–R661.

O'Connor, K.A., Abbott, K.A., Sabin, B., Kuroda, M., and Pachman, L.M. (2006). MxA gene expression in juvenile dermatomyositis peripheral blood mononuclear cells: association with muscle involvement. Clin. Immunol. Orlando Fla *120*, 319–325.

Oertel, G. (1988). Morphometric analysis of normal skeletal muscles in infancy, childhood and adolescence. An autopsy study. J. Neurol. Sci. *88*, 303–313.

Ohab, J.J., Fleming, S., Blesch, A., and Carmichael, S.T. (2006). A Neurovascular Niche for Neurogenesis after Stroke. J. Neurosci. *26*, 13007–13016.

O'Hagan, K.A., Cocchiglia, S., Zhdanov, A.V., Tambuwala, M.M., Tambawala, M.M., Cummins, E.P., Monfared, M., Agbor, T.A., Garvey, J.F., Papkovsky, D.B., et al. (2009). PGC-1alpha is coupled to HIF-1alpha-dependent gene expression by increasing mitochondrial oxygen consumption in skeletal muscle cells. Proc. Natl. Acad. Sci. U. S. A. *106*, 2188–2193.

Olenich, S.A., Gutierrez-Reed, N., Audet, G.N., and Olfert, I.M. (2013). Temporal response of positive and negative regulators in response to acute and chronic exercise training in mice. J. Physiol. *591*, 5157–5169.

Olfert, I.M., and Birot, O. (2011). Importance of anti-angiogenic factors in the regulation of skeletal muscle angiogenesis. Microcirc. N. Y. N 1994 *18*, 316–330.

Olfert, I.M., Breen, E.C., Mathieu-Costello, O., and Wagner, P.D. (2001). Skeletal muscle capillarity and angiogenic mRNA levels after exercise training in normoxia and chronic hypoxia. J. Appl. Physiol. *91*, 1176–1184.

Olfert, I.M., Howlett, R.A., Tang, K., Dalton, N.D., Gu, Y., Peterson, K.L., Wagner, P.D., and Breen, E.C. (2009). Muscle-specific VEGF deficiency greatly reduces exercise endurance in mice: VEGF-deficiency reduces exercise capacity. J. Physiol. *587*, 1755–1767.

Olfert, I.M., Howlett, R.A., Wagner, P.D., and Breen, E.C. (2010). Myocyte vascular endothelial growth factor is required for exercise-induced skeletal muscle angiogenesis. Am. J. Physiol. Regul. Integr. Comp. Physiol. *299*, R1059–R1067.

Ontell, M., and Dunn, R.F. (1978). Neonatal muscle growth: a quantitative study. Am. J. Anat. *152*, 539–555.

Ontell, M., and Kozeka, K. (1984). The organogenesis of murine striated muscle: a cytoarchitectural study. Am. J. Anat. *171*, 133–148.

Ou, L.C., Cai, Y.N., and Tenney, S.M. (1985). Responses of blood volume and red cell mass in two strains of rats acclimatized to high altitude. Respir. Physiol. *62*, 85–94.

Pachman, L.M., Liotta-Davis, M.R., Hong, D.K., Kinsella, T.R., Mendez, E.P., Kinder, J.M., and Chen, E.H. (2000). TNFalpha-308A allele in juvenile dermatomyositis: association with increased production of tumor necrosis factor alpha, disease duration, and pathologic calcifications. Arthritis Rheum. *43*, 2368–2377.

Pachman, L.M., Lipton, R., Ramsey-Goldman, R., Shamiyeh, E., Abbott, K., Mendez, E.P., Dyer, A., Curdy, D.M., Vogler, L., Reed, A., et al. (2005). History of infection before the onset of juvenile dermatomyositis: Results from the National Institute of Arthritis and Musculoskeletal and Skin Diseases Research Registry. Arthritis Care Res. *53*, 166–172.

Palladino, M., Gatto, I., Neri, V., Straino, S., Smith, R.C., Silver, M., Gaetani, E., Marcantoni, M., Giarretta, I., Stigliano, E., et al. (2013). Angiogenic Impairment of the Vascular Endothelium A Novel Mechanism and Potential Therapeutic Target in Muscular Dystrophy. Arterioscler. Thromb. Vasc. Biol. *33*, 2867–2876.

Palmer, T.D., Willhoite, A.R., and Gage, F.H. (2000). Vascular niche for adult hippocampal neurogenesis. J. Comp. Neurol. *425*, 479–494.

Pastoret, C., and Sebille, A. (1995). mdx mice show progressive weakness and muscle deterioration with age. J. Neurol. Sci. *129*, 97–105.

Piccioni, A., Gaetani, E., Palladino, M., Gatto, I., Smith, R.C., Neri, V., Marcantoni, M., Giarretta, I., Silver, M., Straino, S., et al. (2014). Sonic hedgehog gene therapy increases the ability of the dystrophic skeletal muscle to regenerate after injury. Gene Ther. *21*, 413–421.

Piec, I., Listrat, A., Alliot, J., Chambon, C., Taylor, R.G., and Bechet, D. (2005). Differential proteome analysis of aging in rat skeletal muscle. FASEB J. Off. Publ. Fed. Am. Soc. Exp. Biol. *19*, 1143–1145.

Pisani, D.F. (2005). Skeletal Muscle HIF-1 Expression Is Dependent on Muscle Fiber Type. J. Gen. Physiol. *126*, 173–178.

Pittman, R.N. (2011). Oxygen gradients in the microcirculation. Acta Physiol. *202*, 311–322.

Pola, R., Ling, L.E., Silver, M., Corbley, M.J., Kearney, M., Blake Pepinsky, R., Shapiro, R., Taylor, F.R., Baker, D.P., Asahara, T., et al. (2001). The morphogen Sonic hedgehog is an indirect angiogenic agent upregulating two families of angiogenic growth factors. Nat. Med. *7*, 706–711.

Pola, R., Ling, L.E., Aprahamian, T.R., Barban, E., Bosch-Marce, M., Curry, C., Corbley, M., Kearney, M., Isner, J.M., and Losordo, D.W. (2003). Postnatal recapitulation of embryonic hedgehog pathway in response to skeletal muscle ischemia. Circulation *108*, 479–485.

Porter, M.M., Stuart, S., Boij, M., and Lexell, J. (2002a). Capillary supply of the tibialis anterior muscle in young, healthy, and moderately active men and women. J. Appl. Physiol. *92*, 1451–1457.

Porter, M.M., Koolage, C.W., and Lexell, J. (2002b). Biopsy sampling requirements for the estimation of muscle capillarization. Muscle Nerve *26*, 546–548.

Price, R.J., and Skalak, T.C. (1998). Arteriolar remodeling in skeletal muscle of rats exposed to chronic hypoxia. J. Vasc. Res. *35*, 238–244.

Price, F.D., von Maltzahn, J., Bentzinger, C.F., Dumont, N.A., Yin, H., Chang, N.C., Wilson, D.H., Frenette, J., and Rudnicki, M.A. (2014). Inhibition of JAK-STAT signaling stimulates adult satellite cell function. Nat. Med. *20*, 1174–1181.

Qi, J., Olsen, N.J., Price, R.R., Winston, J.A., and Park, J.H. (2008). Diffusion-weighted imaging of inflammatory myopathies: Polymyositis and dermatomyositis. J. Magn. Reson. Imaging *27*, 212–217.

Qian, H.S., de Resende, M.M., Beausejour, C., Huw, L.-Y., Liu, P., Rubanyi, G.M., and Kauser, K. (2006). Age-dependent acceleration of ischemic injury in endothelial nitric oxide synthase-deficient mice: potential role of impaired VEGF receptor 2 expression. J. Cardiovasc. Pharmacol. *47*, 587–593.

Qu, Z., Andersen, J.L., and Zhou, S. (1997). Visualisation of capillaries in human skeletal muscle. Histochem. Cell Biol. *107*, 169–174.

Quartier P, Gherardi R.K. Juvenile dermatomyositis. In Handbook of Clinical Neurology Volume 113, Pages 2-1987 (2013). Edited by Olivier Dulac, Maryse Lassonde and Harvey B. Sarnat.

Ravelli, A., Trail, L., Ferrari, C., Ruperto, N., Pistorio, A., Pilkington, C., Maillard, S., Oliveira, S.K., Sztajnbok, F., Cuttica, R., et al. (2010). Long-term outcome and prognostic factors of juvenile dermatomyositis: A multinational, multicenter study of 490 patients. Arthritis Care Res. *62*, 63–72.

Reed, A.M., Peterson, E., Bilgic, H., Ytterberg, S.R., Amin, S., Hein, M.S., Crowson, C.S., Ernste, F., and Gillespie, E.B. (2012). Changes in novel biomarkers of disease activity in juvenile and adult dermatomyositis are sensitive biomarkers of disease course. Arthritis Rheum. *64*, 4078–4086.

Rehn, M., Olsson, A., Reckzeh, K., Diffner, E., Carmeliet, P., Landberg, G., and Cammenga, J. (2011). Hypoxic induction of vascular endothelial growth factor regulates murine hematopoietic stem cell function in the low-oxygenic niche. Blood *118*, 1534–1543.

Renault, M.-A., Robbesyn, F., Chapouly, C., Yao, Q., Vandierdonck, S., Reynaud, A., Belloc, I., Traiffort, E., Ruat, M., Desgranges, C., et al. (2013a). Hedgehog-dependent regulation of angiogenesis and myogenesis is impaired in aged mice. Arterioscler. Thromb. Vasc. Biol. *33*, 2858–2866.

Renault, M.-A., Vandierdonck, S., Chapouly, C., Yu, Y., Qin, G., Metras, A., Couffinhal, T., Losordo, D.W., Yao, Q., Reynaud, A., et al. (2013b). Gli3 Regulation of Myogenesis Is Necessary for Ischemia-Induced Angiogenesis. Circ. Res. *113*, 1148–1158.

Rezza, A., Sennett, R., and Rendl, M. (2014). Adult stem cell niches: cellular and molecular components. Curr. Top. Dev. Biol. *107*, 333–372.

Rhoads, R.P., Johnson, R.M., Rathbone, C.R., Liu, X., Temm-Grove, C., Sheehan, S.M., Hoying, J.B., and Allen, R.E. (2009). Satellite cell-mediated angiogenesis in vitro coincides with a functional hypoxia-inducible factor pathway. AJP Cell Physiol. *296*, C1321–C1328.

Rhoads, R.P., Flann, K.L., Cardinal, T.R., Rathbone, C.R., Liu, X., and Allen, R.E. (2013). Satellite cells isolated from aged or dystrophic muscle exhibit a reduced capacity to promote angiogenesis in vitro. Biochem. Biophys. Res. Commun. *440*, 399–404.

Ribatti, D., Nico, B., and Crivellato, E. (2011). The role of pericytes in angiogenesis. Int. J. Dev. Biol. *55*, 261–268.

Richardson, R.S., Wagner, H., Mudaliar, S.R.D., Henry, R., Noyszewski, E.A., and Wagner, P.D. (1999). Human VEGF gene expression in skeletal muscle: effect of acute normoxic and hypoxic exercise. Am. J. Physiol.-Heart Circ. Physiol. *277*, H2247–H2252.

Rider, L.G., Feldman, B.M., Perez, M.D., Rennebohm, R.M., Lindsley, C.B., Zemel, L.S., Wallace, C.A., Ballinger, S.H., Bowyer, S.L., Reed, A.M., et al. (1997). Development of validated disease activity and damage indices for the juvenile idiopathic inflammatory myopathies: I. Physician, parent, and patient global assessments. Juvenile Dermatomyositis Disease Activity Collaborative Study Group. Arthritis Rheum. *40*, 1976–1983.

Rissanen, T.T., Vajanto, I., Hiltunen, M.O., Rutanen, J., Kettunen, M.I., Niemi, M., Leppänen, P., Turunen, M.P., Markkanen, J.E., Arve, K., et al. (2002a). Expression of vascular endothelial growth factor and vascular endothelial growth factor receptor-2 (KDR/Flk-1) in ischemic skeletal muscle and its regeneration. Am. J. Pathol. *160*, 1393–1403.

Rivard, A., Silver, M., Chen, D., Kearney, M., Magner, M., Annex, B., Peters, K., and Isner, J.M. (1999). Rescue of diabetes-related impairment of angiogenesis by intramuscular gene therapy with adeno-VEGF. Am. J. Pathol. *154*, 355–363.

Robinson, A.B., and Reed, A.M. (2011). Clinical features, pathogenesis and treatment of juvenile and adult dermatomyositis. Nat. Rev. Rheumatol. *7*, 664–675.

Robinson, A.B., Hoeltzel, M.F., Wahezi, D.M., Becker, M.L., Kessler, E., Schmeling, H., Carrasco, R., Huber, A.M., Feldman, B.M., Reed, A.M., et al. (2013). Clinical characteristics of children with juvenile dermatomyositis - the children's arthritis and rheumatology research alliance (CARRA) registry. Arthritis Care Res. n/a – n/a.

Ross, E.A., Freeman, S., Zhao, Y., Dhanjal, T.S., Ross, E.J., Lax, S., Ahmed, Z., Hou, T.Z., Kalia, N., Egginton, S., et al. (2008). A Novel Role for PECAM-1 (CD31) in Regulating Haematopoietic Progenitor Cell Compartmentalization between the Peripheral Blood and Bone Marrow. PLoS ONE *3*, e2338.

Rowe, G.C., Raghuram, S., Jang, C., Nagy, J.A., Patten, I.S., Goyal, A., Chan, M.C., Liu, L.X., Jiang, A., Spokes, K.C., et al. (2014). PGC-1α induces SPP1 to activate macrophages and orchestrate functional angiogenesis in skeletal muscle. Circ. Res. *115*, 504–517.

Ruperto, N., Ravelli, A., Murray, K.J., Lovell, D.J., Andersson-Gare, B., Feldman, B.M., Garay, S., Kuis, W., Machado, C., Pachman, L., et al. (2003). Preliminary core sets of measures for disease activity and damage assessment in juvenile systemic lupus erythematosus and juvenile dermatomyositis. Rheumatol. Oxf. Engl. *42*, 1452–1459.

Saito, T., Yamamoto, Y., Matsumura, T., Fujimura, H., and Shinno, S. (2009). Serum levels of vascular endothelial growth factor elevated in patients with muscular dystrophy. Brain Dev. *31*, 612–617.

Salajegheh, M., Kong, S.W., Pinkus, J.L., Walsh, R.J., Liao, A., Nazareno, R., Amato, A.A., Krastins, B., Morehouse, C., Higgs, B.W., et al. (2010). Interferon-stimulated gene 15 (ISG15) conjugates proteins in dermatomyositis muscle with perifascicular atrophy. Ann. Neurol. *67*, 53–63.

Sallum, A.M., Varsani, H., Holton, J.L., Marie, S.K., and Wedderburn, L.R. (2013). Morphometric analyses of normal pediatric brachial biceps and quadriceps muscle tissue. Histol. Histopathol. *28*, 525.

Sallum, A.M.E., Kiss, M.H.B., Silva, C.A.A., Wakamatsu, A., Vianna, M.A.A.G., Sachetti, S., and Marie, S.K.N. (2006). Difference in adhesion molecule expression (ICAM-1 and VCAM-1) in juvenile and adult dermatomyositis, polymyositis and inclusion body myositis. Autoimmun. Rev. *5*, 93–100.

Saltzman, D., DeLano, F.A., and Schmid-Schönbein, G.W. (1992). The microvasculature in skeletal muscle: VI. Adrenergic innervation of arterioles in normotensive and spontaneously hypertensive rats. Microvasc. Res. *44*, 263–273.

Sander, M., Chavoshan, B., Harris, S.A., Iannaccone, S.T., Stull, J.T., Thomas, G.D., and Victor, R.G. (2000). Functional muscle ischemia in neuronal nitric oxide synthase-deficient skeletal muscle of children with Duchenne muscular dystrophy. Proc. Natl. Acad. Sci. *97*, 13818–13823.

Sanner, H., Kirkhus, E., Merckoll, E., Tollisen, A., Røisland, M., Lie, B.A., Taraldsrud, E., Gran, J.T., and Flatø, B. (2010). Long-term muscular outcome and predisposing and prognostic factors in juvenile dermatomyositis: A case–control study. Arthritis Care Res. *62*, 1103–1111.

Sanner, H., Schwartz, T., Flatø, B., Vistnes, M., Christensen, G., and Sjaastad, I. (2014). Increased levels of eotaxin and MCP-1 in juvenile dermatomyositis median 16.8 years after disease onset; associations with disease activity, duration and organ damage. PloS One *9*, e92171.

Scadden, D.T. (2014). Nice neighborhood: emerging concepts of the stem cell niche. Cell *157*, 41–50.

Schade van Westrum, S.M., Hoogerwaard, E.M., Dekker, L., Standaar, T.S., Bakker, E., Ippel, P.F., Oosterwijk, J.C., Majoor-Krakauer, D.F., van Essen, A.J., Leschot, N.J., et al.

(2011). Cardiac abnormalities in a follow-up study on carriers of Duchenne and Becker muscular dystrophy. Neurology *77*, 62–66.

Schirmer, S.H., Bot, P.T., Fledderus, J.O., van der Laan, A.M., Volger, O.L., Laufs, U., Böhm, M., de Vries, C.J.M., Horrevoets, A.J.G., Piek, J.J., et al. (2010). Blocking interferon {beta} stimulates vascular smooth muscle cell proliferation and arteriogenesis. J. Biol. Chem. *285*, 34677–34685.

Schmeling, H., Stephens, S., Goia, C., Manlhiot, C., Schneider, R., Luthra, S., Stringer, E., and Feldman, B.M. (2010). Nailfold capillary density is importantly associated over time with muscle and skin disease activity in juvenile dermatomyositis. Rheumatology *50*, 885–893.

Schmid-Schönbein, G.W., Skalak, T.C., and Firestone, G. (1987). The microvasculature in skeletal muscle V. The microvascular arcades in normotensive and hypertensive rats. Microvasc. Res. *34*, 385–393.

Schmidt, N.O., Koeder, D., Messing, M., Mueller, F.-J., Aboody, K.S., Kim, S.U., Black, P.M., Carroll, R.S., Westphal, M., and Lamszus, K. (2009). Vascular endothelial growth factor-stimulated cerebral microvascular endothelial cells mediate the recruitment of neural stem cells to the neurovascular niche. Brain Res. *1268*, 24–37.

Scholz, D., Thomas, S., Sass, S., and Podzuweit, T. (2003). Angiogenesis and myogenesis as two facets of inflammatory post-ischemic tissue regeneration. Mol. Cell. Biochem. *246*, 57–67.

Schroeder, K.L., Rosser, B.W., and Kim, S.Y. (2014). Fiber type composition of the human quadratus plantae muscle: a comparison of the lateral and medial heads. J. Foot Ankle Res. *7*, 54.

Schroeter, S., and Tosney, K.W. (1991). Ultrastructural and morphometric analysis of the separation of two thigh muscles in the chick. Am. J. Anat. *191*, 351–368.

Scuderi, F., Mannella, F., Marino, M., Provenzano, C., and Bartoccioni, E. (2006). IL-6-deficient mice show impaired inflammatory response in a model of myosin-induced experimental myositis. J. Neuroimmunol. *176*, 9–15.

Semenza, G.L. (2003). Targeting HIF-1 for cancer therapy. Nat. Rev. Cancer *3*, 721–732.

Semenza, G.L. (2011). Oxygen sensing, homeostasis, and disease. N. Engl. J. Med. *365*, 537–547.

Shen, Q. (2004). Endothelial Cells Stimulate Self-Renewal and Expand Neurogenesis of Neural Stem Cells. Science *304*, 1338–1340.

Shen, Q., Wang, Y., Kokovay, E., Lin, G., Chuang, S.-M., Goderie, S.K., Roysam, B., and Temple, S. (2008). Adult SVZ Stem Cells Lie in a Vascular Niche: A Quantitative Analysis of Niche Cell-Cell Interactions. Cell Stem Cell *3*, 289–300.

Shimizu-Motohashi, Y., and Asakura, A. (2014). Angiogenesis as a novel therapeutic strategy for Duchenne muscular dystrophy through decreased ischemia and increased satellite cells. Front. Physiol. *5*.

Shin, Y., Yang, K., Han, S., Park, H.-J., Seok Heo, Y., Cho, S.-W., and Chung, S. (2014). Reconstituting vascular microenvironment of neural stem cell niche in three-dimensional extracellular matrix. Adv. Healthc. Mater. *3*, 1457–1464.

Shuai, K., and Liu, B. (2003). Regulation of JAK-STAT signalling in the immune system. Nat. Rev. Immunol. *3*, 900–911.

Silvestre, J.-S., Smadja, D.M., and Levy, B.I. (2013). Postischemic Revascularization: From Cellular and Molecular Mechanisms to Clinical Applications. Physiol. Rev. *93*, 1743–1802.

Sjøgaard, G. (1982). Capillary supply and cross-sectional area of slow and fast twitch muscle fibres in man. Histochemistry *76*, 547–555.

Skalak, T.C., and Schmid-Schönbein, G.W. (1986). The microvasculature in skeletal muscle. IV. A model of the capillary network. Microvasc. Res. *32*, 333–347.

De Smet, F., Segura, I., De Bock, K., Hohensinner, P.J., and Carmeliet, P. (2009). Mechanisms of vessel branching: filopodia on endothelial tip cells lead the way. Arterioscler. Thromb. Vasc. Biol. *29*, 639–649.

Smith, K., and Marshall, J.M. (1999). Physiological adjustments and arteriolar remodelling within skeletal muscle during acclimation to chronic hypoxia in the rat. J. Physiol. *521 Pt 1*, 261–272.

Smith, D., Green, H., Thomson, J., and Sharratt, M. (1989). Capillary and size interrelationships in developing rat diaphragm, EDL, and soleus muscle fiber types. Am. J. Physiol. *256*, C50–C58.

Snyder, G.K. (1988). Anatomical organisation of the microvasculature in the anterior and posterior latissimus dorsi muscles of the chicken. J. Anat. *156*, 97.

Snyder, G.K., and Coelho, J.R. (1989). Microvascular development in chick anterior latissimus dorsi following hypertrophy. J. Anat. *162*, 215.

Somani, A.-K., Swick, A.R., Cooper, K.D., and McCormick, T.S. (2008). Severe dermatomyositis triggered by interferon beta-1a therapy and associated with enhanced type I interferon signaling. Arch. Dermatol. *144*, 1341–1349.

Sousa-Victor, P., Gutarra, S., García-Prat, L., Rodriguez-Ubreva, J., Ortet, L., Ruiz-Bonilla, V., Jardí, M., Ballestar, E., González, S., Serrano, A.L., et al. (2014). Geriatric muscle stem cells switch reversible quiescence into senescence. Nature *506*, 316–321.

Spencer, C.H., Hanson, V., Singsen, B.H., Bernstein, B.H., Kornreich, H.K., and King, K.K. (1984). Course of treated juvenile dermatomyositis. J. Pediatr. *105*, 399–408.

Spencer, J.A., Ferraro, F., Roussakis, E., Klein, A., Wu, J., Runnels, J.M., Zaher, W., Mortensen, L.J., Alt, C., Turcotte, R., et al. (2014). Direct measurement of local oxygen concentration in the bone marrow of live animals. Nature *508*, 269–273.

Speth, J.M., Hoggatt, J., Singh, P., and Pelus, L.M. (2014). Pharmacologic increase in HIF1α enhances hematopoietic stem and progenitor homing and engraftment. Blood *123*, 203–207.

Stingl, J., and Rhodin, J.A. (1994). Early postnatal growth of skeletal muscle blood vessels of the rat. Cell Tissue Res. *275*, 419–434.

Straino, S. (2004). Enhanced Arteriogenesis and Wound Repair in Dystrophin-Deficient mdx Mice. Circulation *110*, 3341–3348.

Suda, T., Takubo, K., and Semenza, G.L. (2011). Metabolic regulation of hematopoietic stem cells in the hypoxic niche. Cell Stem Cell *9*, 298–310.

Sugiura, T., Kawaguchi, Y., Harigai, M., Takagi, K., Ohta, S., Fukasawa, C., Hara, M., and Kamatani, N. (2000). Increased CD40 expression on muscle cells of polymyositis and dermatomyositis: role of CD40-CD40 ligand interaction in IL-6, IL-8, IL-15, and monocyte chemoattractant protein-1 production. J.Immunol. *164*, 6593–6600.

Symmons, D.P., Sills, J.A., and Davis, S.M. (1995). The incidence of juvenile dermatomyositis: results from a nation-wide study. Br. J. Rheumatol. *34*, 732–736.

Tangsrud, S., Petersen, I.L., Lødrup Carlsen, K.C., and Carlsen, K.H. (2001). Lung function in children with Duchenne's muscular dystrophy. Respir. Med. *95*, 898–903.

Tansley, S.L., and McHugh, N.J. (2014). Myositis Specific and Associated Autoantibodies in the Diagnosis and Management of Juvenile and Adult Idiopathic Inflammatory Myopathies. Curr. Rheumatol. Rep. *16*, 1–7.

Tansley, S.L., Betteridge, Z.E., and McHugh, N.J. (2013). The diagnostic utility of autoantibodies in adult and juvenile myositis: Curr. Opin. Rheumatol. *25*, 772–777.

Tansley, S.L., Betteridge, Z.E., Gunawardena, H., Jacques, T.S., Owens, C.M., Pilkington, C., Arnold, K., Yasin, S., Moraitis, E., Wedderburn, L.R., et al. (2014a). Anti-MDA5 autoantibodies in juvenile dermatomyositis identify a distinct clinical phenotype: a prospective cohort study. Arthritis Res. Ther. *16*, R138.

Tansley, S.L., Betteridge, Z.E., Shaddick, G., Gunawardena, H., Arnold, K., Wedderburn, L.R., McHugh, N.J., and on behalf of the Juvenile Dermatomyositis Research Group (2014b). Calcinosis in juvenile dermatomyositis is influenced by both anti-NXP2 autoantibody status and age at disease onset. Rheumatology *53*, 2204–2208.

Tidball, J.G., Albrecht, D.E., Lokensgard, B.E., and Spencer, M.J. (1995). Apoptosis precedes necrosis of dystrophin-deficient muscle. J. Cell Sci. *108 (Pt 6)*, 2197–2204.

Tierney, M.T., Aydogdu, T., Sala, D., Malecova, B., Gatto, S., Puri, P.L., Latella, L., and Sacco, A. (2014). STAT3 signaling controls satellite cell expansion and skeletal muscle repair. Nat. Med. *20*, 1182–1186.

Tozer, S., Bonnin, M.-A., Relaix, F., Di Savino, S., Garcia-Villalba, P., Coumailleau, P., and Duprez, D. (2007). Involvement of vessels and PDGFB in muscle splitting during chick limb development. Development *134*, 2579–2591.

Tuomisto, T.T., Rissanen, T.T., Vajanto, I., Korkeela, A., Rutanen, J., and Ylä-Herttuala, S. (2004). HIF-VEGF-VEGFR-2, TNF-alpha and IGF pathways are upregulated in critical human skeletal muscle ischemia as studied with DNA array. Atherosclerosis *174*, 111–120.

Valentine, B.A., Cooper, B.J., de Lahunta, A., O'Quinn, R., and Blue, J.T. (1988). Canine X-linked muscular dystrophy. An animal model of Duchenne muscular dystrophy: clinical studies. J. Neurol. Sci. *88*, 69–81.

Verdijk, L.B., Snijders, T., Drost, M., Delhaas, T., Kadi, F., and Loon, L.J.C. van (2014). Satellite cells in human skeletal muscle; from birth to old. AGE *36*, 545–557.

Verma, M., Asakura, Y., Hirai, H., Watanabe, S., Tastad, C., Fong, G.-H., Ema, M., Call, J.A., Lowe, D.A., and Asakura, A. (2010). Flt-1 haploinsufficiency ameliorates muscular dystrophy phenotype by developmentally increased vasculature in mdx mice. Hum. Mol. Genet. *19*, 4145–4159.

Verney, J., Kadi, F., Charifi, N., Féasson, L., Saafi, M.A., Castells, J., Piehl-Aulin, K., and Denis, C. (2008). Effects of combined lower body endurance and upper body resistance training on the satellite cell pool in elderly subjects. Muscle Nerve *38*, 1147–1154.

Vogt, M., Puntschart, A., Geiser, J., Zuleger, C., Billeter, R., and Hoppeler, H. (2001). Molecular adaptations in human skeletal muscle to endurance training under simulated hypoxic conditions. J. Appl. Physiol. Bethesda Md 1985 *91*, 173–182.

Wagatsuma, A. (2007). Endogenous expression of angiogenesis-related factors in response to muscle injury. Mol. Cell. Biochem. *298*, 151–159.

Wang, H., Listrat, A., Meunier, B., Gueugneau, M., Coudy-Gandilhon, C., Combaret, L., Taillandier, D., Polge, C., Attaix, D., Lethias, C., et al. (2014). Apoptosis in capillary endothelial cells in ageing skeletal muscle. Aging Cell *13*, 254–262.

Wende, A.R., Schaeffer, P.J., Parker, G.J., Zechner, C., Han, D.-H., Chen, M.M., Hancock, C.R., Lehman, J.J., Huss, J.M., McClain, D.A., et al. (2007). A role for the transcriptional coactivator PGC-1alpha in muscle refueling. J. Biol. Chem. *282*, 36642–36651.

White, R.B., Biérinx, A.-S., Gnocchi, V.F., and Zammit, P.S. (2010). Dynamics of muscle fibre growth during postnatal mouse development. BMC Dev. Biol. *10*, 21.

Wilson, A., and Trumpp, A. (2006). Bone-marrow haematopoietic-stem-cell niches. Nat. Rev. Immunol. *6*, 93–106.

Xiao, H.-B., Zhou, W.-Y., Chen, X.-F., Mei, J., Lv, Z.-W., Ding, F.-B., Li, G.-Q., Zhong, H., and Bao, C.-R. (2012). Interferon-β efficiently inhibited endothelial progenitor cell-induced tumor angiogenesis. Gene Ther. *19*, 1030–1034.

Zhao, Y., Fedczyna, T.O., McVicker, V., Caliendo, J., Li, H., and Pachman, L.M. (2007). Apoptosis in the skeletal muscle of untreated children with juvenile dermatomyositis: impact of duration of untreated disease. Clin. Immunol. Orlando Fla *125*, 165–172.

Role of vascular plasticity in muscle remodeling in the child

Skeletal muscle is highly vascularised. Beyond oxygen and nutriment supply, new functions for vessels have been recently identified, through the interactions that vessel cells (endothelial cells) establish with muscle cells, particularly with muscle stem cells (satellite cells). These latter closely interact with endothelial cells for their expansion and their differentiation, then with periendothelial cells for their self-renewal and return to quiescence. During skeletal muscle regeneration endothelial cells reciprocally interact with myogenic cells by direct contact or by releasing soluble factors to promote both myogenesis and angiogenesis processes. Skeletal muscle regeneration typically occurs as a result of a trauma or disease,

such as congenital or acquired myopathies. To better understand the role of vessel plasticity in tissue remodeling, we took advantage of two muscular disorders that could be considered as paradigmatic situations of regenerating skeletal muscle in the child: Juvenile Dermatomyositis (JDM), the most frequent inflammatory myopathy and Duchenne Muscular Dystrophy (DMD), the most common type of muscular dystrophy. Although these two muscular disorders share, at the tissue level, similar mechanisms of necrosis-inflammation, they differ regarding the vessel domain. In JDM patients, microvascular changes consist in a destruction of endothelial cells assessed by focal capillary loss. This capillary bed destruction is transient. The tissue remodeling is efficient and muscle may progressively recover its function. By contrast, in DMD, despite an increase of vessels density in an attempt to improve the muscle perfusion, the muscle function progressively alters with age.

Here, we identified clinical and pathological markers of severity and predictive factors for poor clinical outcome in JDM by computing a comprehensive initial and follow-up clinical data set with deltoid muscle biopsy alterations controlled by age-based analysis of the deltoid muscle capillarization. We demonstrated that JDM can be divided into two distinctive clinical subgroups. The severe clinical presentation and outcome are linked to vasculopathy. Furthermore, a set of simple predictors (CMAS<34, gastrointestinal involvement, muscle endomysial fibrosis at disease onset) allow early recognition of patients needing rapid therapeutic escalation with more potent drugs.

We studied *in vitro* the specific cell interactions between myogenic cells issued from JDM and DMD patients and normal endothelial cells to explore whether myogenic cells participate to the vessel remodeling observed in the two pathologies. We demonstrated that MPCs possessed angiogenic properties depending on the pathological environment. In DMD, MPCs promoted the development of establishment of an anarchic, although strong, EC stimulation, leading to the formation of weakly functional vessels. In JDM, MPCs enhanced the vessel reconstruction *via* the secretion of proangiogenic factors. This functional analysis was supported by the transcriptomic analysis consistent with a central vasculopathy in JDM including a strong and specific response to an inflammatory environment. On the contrary, DMD cells presented an unbalanced homeostasis with deregulation of several processes including muscle and vessel development with attempts to recover neuromuscular system by MPCs.

To summarize, our data should allow the definition of new functions of vessel cells in skeletal muscle remodelling during muscle pathologies of the child that will open the way to explore new therapeutic options and to gain further insights in the pathogenesis of these diseases.